LOAD ANALYSIS OF AN AIRCRAFT USING SIMPLIFIED AERODYNAMIC AND STRUCTURAL MODELS

A THESIS SUBMITTED TO
THE GRADUATE SCHOOL OF NATURAL AND APPLIED SCIENCES
OF
MIDDLE EAST TECHNICAL UNIVERSITY

BY

EMRE ÜNAY

IN PARTIAL FULLFILLMENT OF THE REQUIREMENTS
FOR
THE DEGREE OF MASTER OF SCIENCE
IN
AEROSPACE ENGINEERING

FEBRUARY 2015

Approval of the thesis:

LOAD ANALYSIS OF AN AIRCRAFT USING SIMPLIFIED AERODYNAMIC AND STRUCTURAL MODELS

submitted by **EMRE ÜNAY** in partial fulfillment of the requirements for the degree of **Master of Science in Aerospace Engineering Department, Middle East Technical University** by,

Prof. Dr. M. Gülbin Dural Ünver
Dean, Graduate School of **Natural and Applied Sciences** _____

Prof. Dr. Ozan Tekinalp
Head of Department, **Aerospace Engineering** _____

Prof. Dr. Altan Kayran
Supervisor, **Aerospace Engineering Dept., METU** _____

Examining Committee Members

Prof. Dr. D. Serkan Özgen
Aerospace Engineering Department, METU _____

Prof. Dr. Altan Kayran
Aerospace Engineering Department, METU _____

Assoc. Prof. Dr. D. Funda Kurtuluş
Aerospace Engineering Department, METU _____

Prof. Dr. Yusuf Özyörük
Aerospace Engineering Department, METU _____

Derya Gürak, M.Sc.
Turkish Aerospace Industries, Inc. _____

Date: 04.02.2015

I hereby declare that all information in this document has been obtained and presented in accordance with academic rules and ethical conduct. I also declare that, as required by these rules and conduct, I have fully cited and referenced all material and results that are not original to this work.

Name, Last name : Emre Ünay

Signature :

ABSTRACT

LOAD ANALYSIS OF AN AIRCRAFT USING SIMPLIFIED AERODYNAMIC AND STRUCTURAL MODELS

Ünay, Emre

M.S., Department of Aerospace Engineering

Supervisor: Prof. Dr. Altan Kayran

February 2015, 120 pages

Aircraft must be light enough to fly but also strong enough to endure the loads they experience during flight. Designing such a structure is one of the most demanding works in an aircraft design project. In order to design such a structure, accurate evaluation of loads is important. Once the loads applied to the structure are calculated precisely, then the deflections and stresses can be calculated and sizing of the structures can be performed accordingly.

Therefore, in aircraft design projects, loads group lies at the heart of the design cycle. It receives inputs from various design groups such as aerodynamics group,

structures group, weight and balance group, systems groups, airworthiness group, and so on. Not only receiving these inputs, but load group also provides outputs to various groups, mainly structural design and analysis. Those interactions make aircraft loads one of the most multidisciplinary subjects in aircraft design and analysis. On the other hand, because of those interactions with all disciplines of the design cycle, load analyses are also quite complex, requires systematic work, ability to process massive amounts of data, adequate insight of both aerodynamic and structural issues and communication with not only within the company but also with certification authorities.

The objective of this study is provide a comprehensive overview of load analysis process, to develop methods for simplification of aircraft structural and aerodynamic models to make it possible to perform the load analysis in a fast and integrated way during conceptual and preliminary design phases, then to perform a load analysis of an ultralight aircraft as a case study for the demonstration of the load analysis process.

Keywords: aircraft loads, static load analysis, structural analysis, static aeroelasticity

ÖZ

BİR UÇAĞIN SADELEŞTİRİLMİŞ AERODİNAMİK VE YAPISAL MODELLERİNİ KULLANARAK YÜK ANALİZİ

Ünay, Emre

Yüksek Lisans, Havacılık ve Uzay Mühendisliği Bölümü

Tez Yöneticisi: Prof. Dr. Altan Kayran

Şubat 2015, 120 sayfa

Uçaklar uçabilmek için yeteri kadar hafif olmak, fakat aynı zamanda üzerilerine etki eden yüklere dayanabilecek kadar da sağlam olmak zorundadırlar. Bu koşulları sağlayabilecek bir yapıyı tasarlamak uçak tasarım projelerindeki en emek isteyen işlerden biridir. Böylesine bir yapıyı tasarlamak için yükleri hassas bir şekilde hesaplayabilmek önemlidir. Yapıya etki eden yükler hesaplandığında, yapıdaki bükülmeler ve gerinimler de hesaplanabilir ve yapısal elemanlar boyutlandırılabilir.

Bu sebeplerden dolayı, uçak tasarım projelerinde, uçak yükleri tasarım döngüsünün kalbinde yer alır. Aerodinamik grubu, yapısal tasarım ve analiz grubu, ağırlık ve denge grubu, sistem grupları, uçuşa elverişlilik ve sertifikasyon grubu gibi tasarım gruplarından girdiler alır. Sadece girdiler almak değil, aynı zamanda yapısal grubu başta olmak üzere birçok gruba da çıktı sağlar. Bütün bu etkileşimler, uçak yükleri konusunu uçak tasarımının en çoklu-disiplinli konularından birisi yapmaktadır. Öte taraftan, uçak tasarım döngüsündeki tüm bu etkileşimleri sebebiyle, yük analizleri gayet karmaşık olmakta; sistematik çalışma, büyük verileri işleme kabiliyeti ve aerodinamik ve yapısal konularda geniş bilgi birikimi gerektirmektedir. Ayrıca analizler esnasında sadece şirket içi değil sertifikasyon ve uçuşa elverişlilik otoriteleriyle de iletişim içinde olunması gerekmektedir.

Bu tez çalışmasının amacı, yük analizi sürecinin geniş bir derlemesini ve tanıtımını yapmak, yük analizini özellikle kavramsal ve ön tasarım aşamalarında bütünleşik ve hızlı bir şekilde yapabilmek için gereken uçak aerodinamik ve yapısal modellerini sadeleştirme yöntemleri geliştirmek ve yük analizi sürecini örneklendirmek adına bir ultralight tipi uçağın yük analizini gerçekleştirmektir.

Anahtar Kelimeler: uçak yükleri, statik yük analizi, yapısal analiz, statik aeroelastisite,

To Ahmet Emin Ünay and Şerife Ünay

ACKNOWLEDGEMENTS

I would like to thank my supervisor, Prof. Dr. Altan Kayran, who always helped me not only in this thesis work, but also in all aspects of my both academic and professional career. His endless patience is appreciated. I also want to thank the chair of the department, Prof. Dr. Ozan Tekinalp, whose tolerant and helpful attitude made it possible to complete this thesis work.

I could not thank enough the people who made me who I am, my former coworkers and superiors from Turkish Aerospace Industries. Among them are Hüseyin Yağcı, Varlık Özerciyes, Yavuz Güleç, Akif Çetintaş, Ömer Onur, Umut Susuz, Evren Sakarya, Özlem Işıkdoğan, Dilek Ünalmış, Engin Kahraman, Abdülkadir Çekiç, Tuğçe Kiper, Göknur Aydoğan, Muvaffak Hasan, Hakan Taşkaya, Mustafa Açıkgöz, Muhittin Nami Altuğ, Can Kurgan, Alper Uzunoğlu, Davut Çıkrıkcı, Hakan Kestek, Mustafa Bahtiyar, Kıvanç Ülker, Murat Çetinel, Kağan Çakır, Ertan Zaferoğlu, Benan Aylangan and many others that I could not write here due to space constraints, but I wish I could.

If I have something to write anything about aircraft loads, I owe it to my former leader and mentor, Derya Gürak. As my first leader, she was there to tolerate the crude and reckless behaviors of a young, inexperienced engineer. I was lucky to have such visionary leader who always encouraged innovation, and who contributed not only to my thesis work, but also to the company and to the literature about aircraft loads.

I want to thank specially Dr. Gürsel Erarslanoğlu, the man who was behind the engineering work in aircraft projects in my former workplace and who endured the

difficulties of those projects. He was the one who believed me most and I have never shown my gratitude.

I do not have an elder brother, but Fatih Mutlu Karadal was the closest person to one. He has an outstanding technical background, loving heart, rational mind, and is the most capable engineer I have ever met. I not only thank him, but also wish the best for him.

I would like to thank Arda Kandemir and Yiğit Anıl Yücesan, my fellow coworkers and comrades, who endure the worst of me.

There exists proportionality between countries' achievements in aerospace technologies and national aviation culture; as seen in Germany of 1930's, Germany of today, USA, United Kingdom, etc. I believe Turkey will join among them soon. I am grateful to Directorate General of Civil Aviation (SHGM) for paving the way for the development of light aircraft, general aviation aircraft, etc. via preparation of certification specifications for such aircraft.

I want to thank the Ministry of Science, Industry and Technology, for their support that helped my dreams come true.

Special thanks to my parents, Ahmet Emin Ünay and Şerife Ünay whom I dedicated this study to. I cannot find any words to thank them enough for their support.

Finally, I would like to mention Vecihi Hürkuş, Nuri Demirağ, Selahattin Reşit Alan and other heroes of Turkish aviation history. But, most importantly, I want to express my eternal gratitude to Mustafa Kemal Atatürk, whose ideas shall always enlighten my path.

TABLE OF CONTENTS

ABSTRACT ..... **v**

ÖZ ..... **vii**

ACKNOWLEDGEMENTS ..... **x**

TABLE OF CONTENTS ..... **xiii**

LIST OF TABLES ..... **xvi**

LIST OF FIGURES ..... **xviii**

LIST OF ABBREVıATIONS ..... **xxii**

CHAPTER 1 INTRODUCTION **1**

1.1 Structural Loads in Aircraft Design Cycle 1

1.2 Analysis of Aircraft Loads 6

1.2.1 Input for Load Analysis 6

1.2.2 Load Cases 13

1.2.3 Calculation of Loads 23

1.2.4 Output of Load Analysis 23

1.3 Effects of Static Aeroelasticity in Load Analysis 26

1.3.1 Deflection and Pressure Redistribution 26

1.3.2 Divergence Instability 28

1.3.3 Flight Mechanics Coupling 28

1.4 Aim of the Study 29

CHAPTER 2 AERODYNAMIC, INERTIAL AND STRUCTURAL MODELLING OF THE AIRCRAFT 31

2.1 Description and Details of the Aircraft 31

2.2 Modeling Philosophy 36

2.3 Aircraft Aerodynamic Model 36

2.3.1 Simplification of the Aerodynamic Model 39

2.3.2 Verification of the Model 42

2.4 Aircraft Mass Model 47

2.5 Aircraft Structural Model 55

CHAPTER 3 LOAD CASES 61

3.1 Requirements 61

3.2 Configurations and Mass States 61

3.3 Airspeeds and Altitudes 64

3.4 Load Factors 65

3.5 Flight Conditions and Maneuvers 68

3.5.1 Symmetrical Maneuvers 68

3.5.2 Unsymmetrical Maneuvers 69

3.6 Ground Conditions 71

3.7 Load Cases Table 71

CHAPTER 4 AIRCRAFT LOADS CALCULATIONS 73

CHAPTER 5 LOADS POST-PROCESSING AND RESULTS 79

5.1 Loads and Critical Cases for the Wing 80

5.2 Loads and Critical Cases for the Horizontal Tail 85

5.3 Loads and Critical Cases for the Vertical Tail 87

5.4 Loads and Critical Cases for the Fuselage 89

5.5 Deflection of the Wing under Critical Loads 91

5.6 Loads Redistribution 92

5.7 Divergence Analysis of the Wing 93

CHAPTER 6 CONCLUSIONS 97

6.1 Recommendations of Future Work 99

REFERENCES 101

APPENDIX A CODE FOR INTEGRATION OF CFD RESULTS 107

APPENDIX B COMPLETE LIST OF LOAD CASES 113

APPENDIX C WING LOADS CALCULATION FLOWCHART 119

LIST OF TABLES

Table 2-1: Limbach L550 E Engine Specifications [40].....33

Table 2-2: Aircraft Design Specifications 34

Table 2-3: Aircraft Performance Specifications 35

Table 2-4: Comparison of Aerodynamic Coefficients 38

Table 2-5: Weight Breakdown of the Aircraft 48

Table 2-6: Structure and System Mass Distribution at Station Points 52

Table 2-7: Moment of Inertia Calculation of the Wing Section.....57

Table 2-8: Sectional Moment of Inertia Values.....58

Table 3-1: Aircraft Weights.....62

Table 3-2: Mass States.....62

Table 3-3: Aircraft Design Airspeeds.....65

Table 3-4: Symmetrical Design Conditions for the Ultralight Aircraft 69

Table 3-5: Unsymmetrical Flight Conditions for the Ultralight Aircraft 70

Table 3-6: A Portion of Load Case Table 71

Table 5-1: Critical Load Cases for the Wing 82

Table 5-2: Critical Cases for the Wing Torsion.....83

Table 5-3: Critical Cases for the Horizontal Tail.....87

Table 5-4: Critical Cases for the Vertical Tail 89

Table 5-5: Comparison of Gust and Yawing Cases 89

LIST OF FIGURES

Figure 1-1: Collar Aeroelastic Triangle [4] 3

Figure 1-2: Loads Triangle [4]....4

Figure 1-3: Interactions of Loads Group in Aircraft Design Organization [8] 5

Figure 1-4: Input for Load Analysis 6

Figure 1-5: Schrenk's Method [12] 9

Figure 1-6: Application of Strain Gauge Bridges on Structure for Flight Loads Measurement [19]..11

Figure 1-7: A Sample Mass Distribution along Wing [4]....12

Figure 1-8: A Sample Aircraft Beam Model [24]....13

Figure 1-9: Sample Load Case Definition Chart....14

Figure 1-10: An Example of a typical V-A Diagram [4]....16

Figure 1-11: V-n Diagram, or Flight Envelope, as defined by CS-23 [30]....17

Figure 1-12: A Typical Weight - CG Envelope [3] 18

Figure 1-13: Phases of Roll Maneuver [10]....20

Figure 1-14: Phases of Yaw Maneuver [10] 21

Figure 1-15: Landing Conditions according to CS-25....22

Figure 1-16: 1D Loads Envelope with a Reduced Number of Load Cases....24

Figure 1-17: 2-D Loads Envelope [32]....24

Figure 1-18: Altair UAV of NASA. (Photo from NASA) 26

Figure 1-19: Deflection of F/A-18 wing during pull-up maneuver [36] 27

Figure 1-20: Comparison of lift distributions on rigid wing and elastic wing [5] 27

Figure 1-21: Jig shape [37] 28

Figure 1-22: Pitching Moment Derivative for Rigid and Elastic Aircraft [37] 29

Figure 2-1: The aircraft in isometric view 31

Figure 2-2: The aircraft in three-view 32

Figure 2-3: Limbach L550 E 33

Figure 2-4:Structured Aerodynamic Mesh of the Aircraft 36

Figure 2-5: Unstructured Aerodynamic Mesh of the Aircraft 37

Figure 2-6: CFD Solutions of Structured and Unstructured Meshes at AoA=5 37

Figure 2-7: Comparison of Structured and Unstructured Grid Results 39

Figure 2-8: Comparison of Schrenk Method, Modified Analytical Method and CFD Results, Wing Twist=0, AoA=5 deg. 43

Figure 2-9: Comparison of Schrenk Method, Modified Analytical Method and CFD Results, Wing Twist=6 deg, AoA=10 deg 44

Figure 2-10: CFD results of the Aircraft with 10 degrees Aileron Deflection 45

Figure 2-11: Comparison of Schrenk Method, Modified Analytical Method and CFD Results, Aileron Deflection=10 deg, AoA=10 deg 45

Figure 2-12: Location of Center of Pressure obtained from CFD and Analytical Methods. 47

Figure 2-13: Structural and System Layout of the Aircraft 48

Figure 2-14: Lumped Mass Points on the Aircraft Structure 52

Figure 2-15: Front Fuselage Mass Distribution 54

Figure 2-16: Wing Mass Distribution 55

Figure 2-17: Beam Model Representation of the Aircraft Structural Model 56

Figure 2-18: Wing Structural Layout 56

Figure 3-1: Aircraft Weight - CG Envelope with Mass States 63

Figure 3-2: V-n Diagram of the Aircraft with Gust Lines at Sea Level 67

Figure 3-3: V-n Diagram of the Aircraft with Gust Lines at 4000 m Altitude 67

Figure 4-1: Load Calculation Process of Aerodynamic and Inertial Loads 73

Figure 4-2: Integration of Airloads and Inertial Loads along the Aircraft [12] 74

Figure 4-3: Loads Distributions along the Wing for LC79 75

Figure 4-4: Shear Diagram along the Wing for LC79 75

Figure 4-5: Bending Moment Diagram along the Wing for LC79 76

Figure 4-6: Static Aeroelastic Analysis as Coupled Aero-Structural Calculations 77

Figure 4-7: Static Aeroelastic Analysis with Simplified Models 77

Figure 5-1: Load Case Colour Map for Loads Envelopes 80

Figure 5-2: Wing Load Distribution 81

Figure 5-3: Wing Shear Force Distributiom 81

Figure 5-4: Wing Bending Moment 82

Figure 5-5: Wing Torsional Moment Distribution 83

Figure 5-6: Wing Bending and Torsional Moment at Wing Root 84

Figure 5-7: Comparison of Wind Bending Moment for Flexible and Rigid Analyses 85

Figure 5-8: Horizontal Tail Load Distribution 85

Figure 5-9: Horizontal Tail Shear Force Distribution 86

Figure 5-10: Horizontal Tail Bending Moment Distribution 86

Figure 5-11: Vertical Tail Load Distribution 87

Figure 5-12: Vertical Tail Shear Force Distribution 88

Figure 5-13: Vertical Tail Bending Moment Distribution..... 88

Figure 5-14: Fuselage Vertical Shear Force Distribution..... 90

Figure 5-15: Fuselage Lateral Shear Force Distribution 90

Figure 5-16: Bending Deflection of the Wing Under Critical Load Case 91

Figure 5-17: Torsional Deflection of the Wing Under Critical Load Case 92

Figure 5-18: Comparison of Load Distributions over Flexible and Rigid Wing..... 93

Figure 5-19: Torsional Deflection of the Wing at Various Airspeeds..... 94

Figure 5-20: Torsional Deflection and Divergence Speed Comparison at Wing Root 95

Figure 5-21: Torsional Deflection and Divergence Speed Comparison at Different Sections 95

Figure C-1: Flowchart of Wing Loads Calculation 119

LIST OF ABBREVIATIONS

a	Lift curve slope
AoA	Angle of attack
b	Wing reference span
c	Wing chord
CX, CY, CZ	Aerodynamic force coefficients along body x, y and z axes
CL, CM, CN	Aerodynamic rolling, pitching and yawing moment coefficients
C_P	Pressure coefficient
c_l, c_L	Lift coefficient
$c_{l\alpha}$	Lift curve slope, or derivative of lift coefficient w.r.t. angle of attack
CFD	Computational Fluid Dynamics
CS	Certification Specifications (European Aviation Safety Agency)
DLM	Doublet Lattice Method
e	Oswald efficiency coefficient, or chordwise location of elastic axis
E	Young's Modulus
EASA	European Aviation Safety Agency
EW	Empty Weight
FAA	Federal Aviation Administration
FAR	Federal Aviation Regulations
F_X, F_Y, F_Z	Forces in x, y, z direction
g	Gravitational acceleration

G	Shear Modulus
HT	Horizontal tail
I_{XX}, I_{YY}, I_{ZZ}	Inertia in body axes x, y, z
J	Polar moment of inertia
k	Gust alleviation factor
L, M, N	Rolling, pitching, yawing moments
LC	Load Case
m	Mass
M_X, M_Y, M_Z	Moments around x, y, z axes
MLW	Maximum Landing Weight
MTOW	Maximum Take-off Weight
MTW	Maximum Take-off Weight
MZFW	Maximum Zero Fuel Weight
n	Load factor
OEW	Operational Empty Weight
q	Dynamic pressure
S	Wing area
SFC	Specific Fuel Consumption
T	Torsion
TR-UL	Turkish Ultralight Certification Specifications
UL	Ultralight
V_A, VA	Design Maneuvering Speed
V_B, VB	Design Gust Speed
V_C, VC	Cruise Speed

V_D, VD	Dive Speed
V_H, VH	Maximum Speed for Level Flight at Continuous Power
V_S, VS	Stall Speed
VLM	Vortex Lattice Method
VT	Vertical Tail
α	Angle of Attack
β	Sideslip Angle
$\Delta\alpha$	Angle of attack increment due to sectional twist, or gust condition
λ	Taper Ratio
ρ	Air density

CHAPTER 1

INTRODUCTION

There exists a motto, which is quoted to famous aircraft designer William Bushnell Stout: “Simplicate and Add Lightness” [1]. This motto was also used extensively by Ed Heinemann, another legendary aircraft designer. It represents the design philosophy, which implies simplification of design leads to reduction of aircraft weight, which in turn makes avoidance of complex design solutions more possible, hence allowing more simple design and more weight reduction.

This thesis work is prepared by the same notion of simplification and weight reduction. However, what essentially being simplified in this study is the aerodynamic and structural model of the aircraft and the methods for load analysis. The ultimate objective, on the other hand, is quite the same: design of a lighter structure for more efficient aircraft.

1.1 Structural Loads in Aircraft Design Cycle

Aircraft are designed to satisfy certain design requirements, just like any other vehicles, or any other machines. Among those design requirements, some of the most important ones are performance requirements, such as range, endurance, maximum speed, stall speed, take-off distance, landing distance, maximum sustained load factor, maximum load factor and payload capacity and so on [2].

Those performance specifications depend on various parameters based on aircraft geometry, aerodynamic coefficients and aircraft weight. Among these, aircraft weight is the most critical parameter that affects the performance of the aircraft in every aspect. Weight related terms such as wing loading or thrust-to-weight ratio appears in most of the equations in performance analysis [2].

The term "aircraft weight", however, does not represent a single particular value. Technically, there are terms such as Empty Weight, Operational Empty Weight, Minimum Flying Weight, Maximum Take-off Weight, etc. The definition of those terms are done in following chapters, but it must be noted that it is the empty weight, or more precisely, the structural weight that can be minimized by comprehensive engineering work; since the weights of systems, crew, fuel and payload are generally pre-defined from the start of project. In this thesis work, the weight reduction is used in conjunction with structural weight reduction.

Therefore, it is clear that, designing the aircraft structure as light as possible is a critical objective for aircraft designers, in order to meet performance parameters set by the project requirements. In other words, the aircraft structure must be light enough to meet design objectives, yet strong enough to endure the forces it experiences during its lifetime. Determination of those forces acting on the aircraft during maneuvers, turbulence, landing and ground operations is defined as load analysis [3].

Maneuver, turbulence, landing and ground loads arise from the interaction between elastic, inertial and aerodynamic forces, acting on the aircraft structure. This interaction of aerodynamic, elastic and inertial forces is defined as aeroelasticity [4]. The Figure 1-1 is called the famous Collar aeroelastic triangle [4].

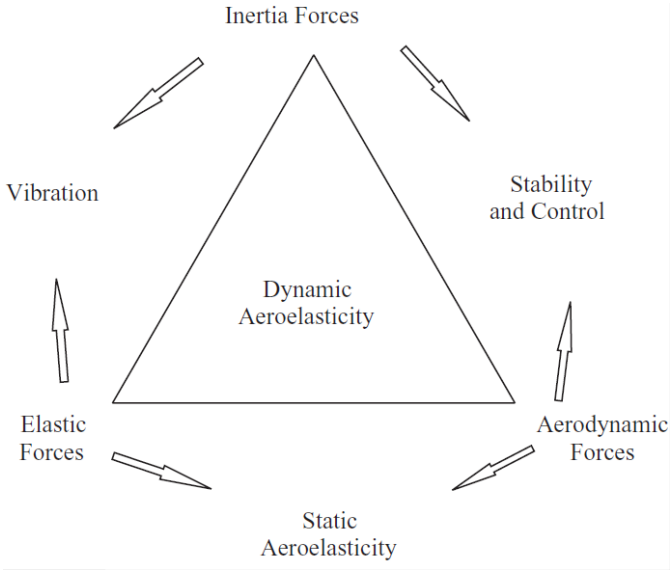

Figure 1-1: Collar Aeroelastic Triangle [4]

Aeroelasticity is a phenomenon which has been observed since the very years of the history of aviation; in fact, it was the aeroelastic divergence which caused Samuel Langley's aircraft crash in Potomac River earlier in 1903, even before Wright Brothers [5]. The history of aeroelasticity itself is quite interesting subject worth exploring.

Aeroelasticity, likewise, is a huge topic itself, which is impossible to be covered in this study. Static aeroelasticity, which deals with non-oscillatory interaction of aerodynamic and elastic forces on the aircraft structure, however, is generally used in conjunction with static load analysis [3, 4]. The topics of static aeroelasticity such as structural deflection and pressure redistribution are required to be taken into account according to airworthiness and certification standards such as CS-25 and FAR-25 [6, 7].

With the definition of loads is given in previous paragraph as the aerodynamic, inertial and elastic forces acting on aircraft structure, the aeroelastic triangle can be

modified for further definition and classification of aircraft loads, as given in Figure 1-2.

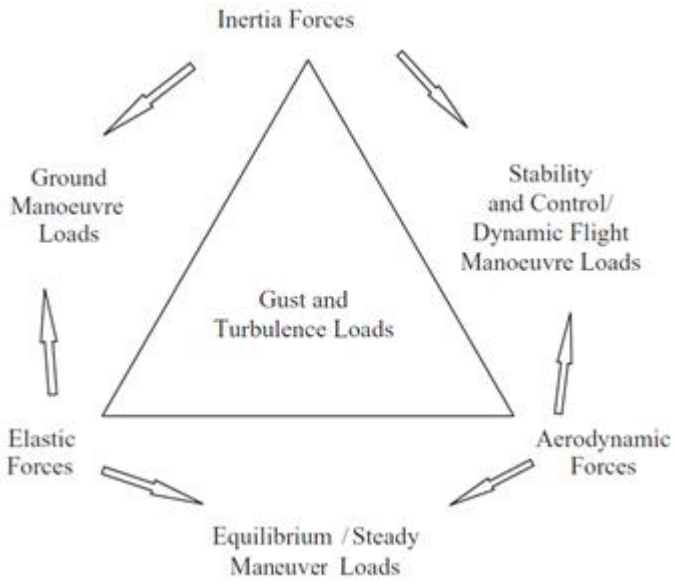

Figure 1-2: Loads Triangle [4]

In this thesis work, the term "load analysis" refers to static load analysis whereas dynamic load analysis, which deals with flutter, limit cycle oscillations, structural dynamics, etc. is beyond the scope of this study. The inertial forces are non-oscillatory and arise from the steady state gravitational acceleration acting on aircraft mass.

In conceptual design phase, estimation of structural weight to meet design objectives requires the estimation of structural loads. Also, in preliminary analysis, load analyses are performed for selection of basic structural layout. Finally, in detailed and certification phase, load analyses are performed with maximum detail with all latest aerodynamic, inertia and stiffness properties obtained from other groups [4].

The input and output of loads activities and its interactions with other design groups are detailed in following sections. The interaction of load analysis with other design activities is given in Figure 1-3.

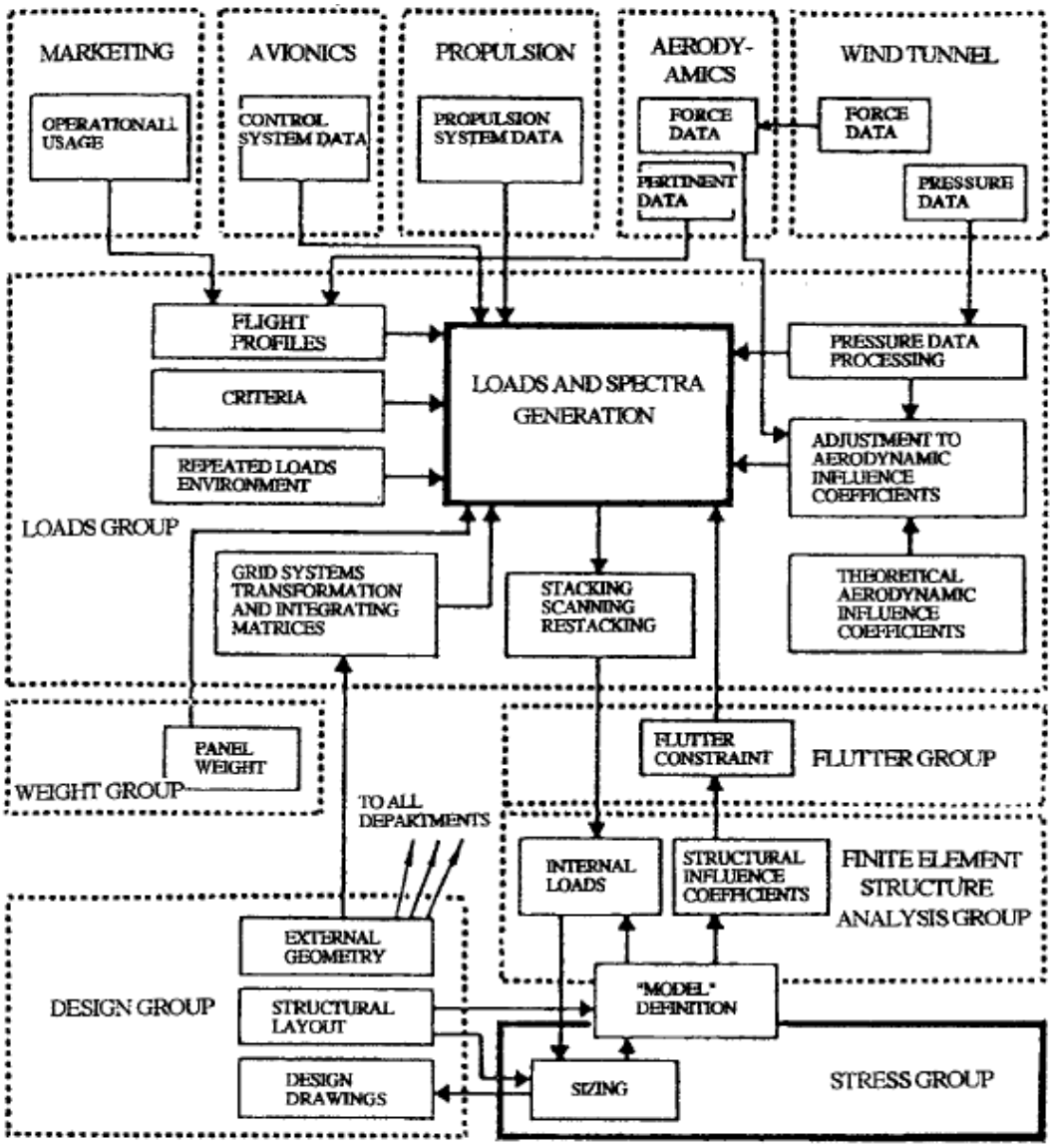

Figure 1-3: Interactions of Loads Group in Aircraft Design Organization [8]

1.2 Analysis of Aircraft Loads

This thesis work aims to detail load analysis in aircraft preliminary design phase with the broadest scope possible.

1.2.1 Input for Load Analysis

As stated before, load analysis is a multi-disciplinary process, receiving inputs from various groups and providing output to other groups as well. Input can be listed as distributed aerodynamic forces, mass and inertia distribution, stiffness distribution and system data such as flight control system and actuators [9, 10]. The inputs for load analysis can be summarized as given in Figure 1-4.

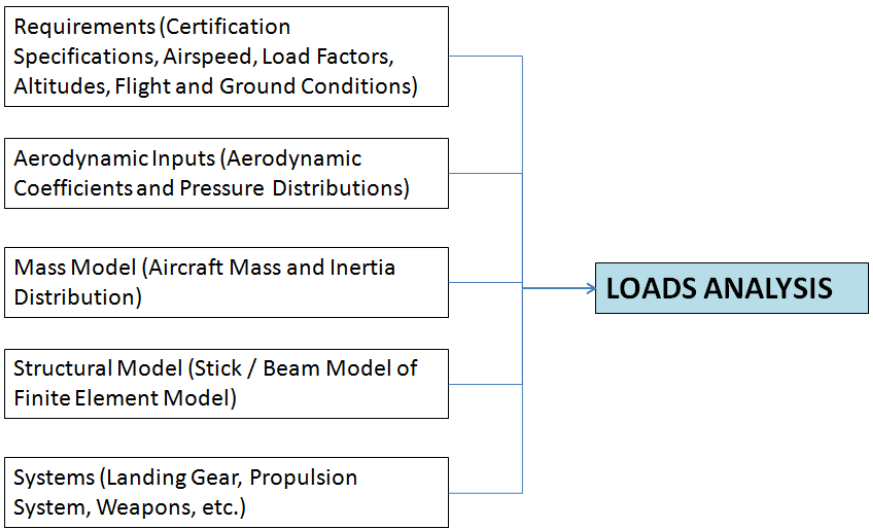

Figure 1-4: Input for Load Analysis

1.2.1.1 Requirements

Load analysis of an aircraft is performed at different load cases. The load cases are essentially the combinations of airspeeds, altitudes, temperatures and flight and ground conditions. Those conditions are generally dictated by airworthiness

specifications and project requirements. Generation of load cases is detailed in the following sections.

Beginning from 1907, the airworthiness requirements have been established for the design of aircraft structures [10]. Today, there exist military and civilian airworthiness specifications. These airworthiness specifications cover the requirements for performance, handling, structure and loads, operating procedures, systems and installations, etc.

Certification specifications, such as the specifications prepared by Federal Aviation Agency (FAA) and European Aviation Safety Agency (EASA), play important role on the definition of load conditions for civilian aircraft [6, 7]. For military aircraft, there are also specifications such as MIL-A-8861B, which define the maneuvers for aircraft load analysis [11].

1.2.1.2 Aerodynamic Input

With the definition of aircraft loads having been made as the aerodynamic, inertial and elastic forces acting on the aircraft structure; the calculation of these forces requires their corresponding input.

1.2.1.2.1 Analytical and Empirical Approaches

Especially during the conceptual and preliminary design phases, where design flexibility is needed to optimize the aircraft geometry and layout, the use of empirical and analytical formulas provides fast results for aerodynamic force distributions without comprehensive CFD analyses.

Since aerodynamic loads are more significant on lifting surfaces such as wings, some empirical and analytical methods have been developed to estimate the spanwise and chordwise distribution of such forces [12].

One of the most widely used approximation methods for spanwise airload distribution along wing is the Schrenk method, which was developed by Oskar Schrenk in 1940 [13]. It is generally used in conceptual analysis and proved to provide good results for unswept and untwisted wings as demonstrated in both in this thesis study and literature [10, 12]. Schrenk method implies that the airload distribution along the wing can be approximated as the arithmetic mean of the elliptic distribution and geometric distribution [13].

$$C_{sch}(y) = \frac{1}{2}\left(C(y) + C_{ell}(y)\right) \tag{1. 1}$$

where C(y) is the geometric chord distribution and C_ell is elliptic chord distribution.

The elliptic chord distribution can be formulated as follows:

$$C_{ell}(y) = \frac{4S}{\pi b}\sqrt{1 - \left(\frac{2y}{b}\right)^2} \tag{1. 2}$$

where S is the wing area and b is the wingspan.

If the wing shape is trapezoidal, then the chord distribution can be formulated as:

$$C(y) = C_r\left(1 - \frac{2y}{b}(1 - \lambda)\right) \tag{1. 3}$$

where λ is the taper ratio and C_r is the root chord. The wing area for such wing shape than would be:

$$S = \frac{b}{2} C_r(1 + \lambda) \tag{1. 4}$$

The graphical representation of the Schrenk Method is given in Figure 1-5.

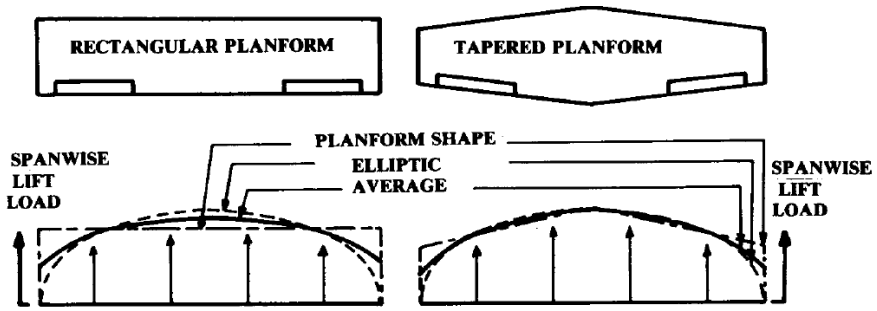

Figure 1-5: Schrenk's Method [12]

Unfortunately, Schrenk Method does not take sweep and twist effects of airload distribution into account. Several additions and modifications have been made on Schrenk method to include those effects [10, 14]. In addition to these methods, there are methods using lifting surface theory for spanwise lift distribution [15, 16].

Chordwise lift distribution, similarly can be approximated for airload estimations in early design phases. The center of pressure, which is chordwise position of the resultant lift force on the airfoil generally moves with angle of attack, however is generally accepted to be located in 25 - 28 percent of the chord for symmetric airfoil [10] and around 34 percent of the chord for cambered airfoil [12] for subsonic flow and typical angles of attack. This center can move to 0.5 of the chord for supersonic flows. It is also possible to use airfoil data (i.e. airfoil moment coefficient), to estimate the position of lift force resultant [10, 12].

1.2.1.2.2 CFD Applications for Load Analysis

Aerodynamic force distribution can be obtained from Computational Fluid Dynamic (CFD) methods such as Vortex Lattice Method (VLM), Doublet Lattice Method (DLM), Panel Method or Navier Stokes Method. 3-D aerodynamic model consisting of thousands or millions of meshes is often used in load analysis in the detail design phase of the aircraft. Also, for aeroelastic analysis, the certification requirements for large aircraft dictated the use of unsteady DLM of Panel Method for the calculation of aerodynamic forces [4, 6].

1.2.1.2.3 Wind Tunnel Practices for Loads Distribution

Apart from CFD, one of the sources for airload distribution of the aircraft surface is the pressure measurements from wind tunnel tests. It is a common industrial practice to obtain wind tunnel pressure data and interpolate the pressure distribution over the loads model of the aircraft [17, 18].

1.2.1.2.4 Flight Test Data

Similar to the wind tunnel tests, flight test also provide pressure measurements, which can be interpolated on the aircraft loads model.

However, more common and important practice for loads measurements in aircraft flight testing is performed by application of strain gauges on structures. Strain gauges are applied as Wheatstone bridges so that they can directly measure shear and bending moment on the structure [19]. A typical application of strain gauge bridge on a spar is shown in Figure 1-6.

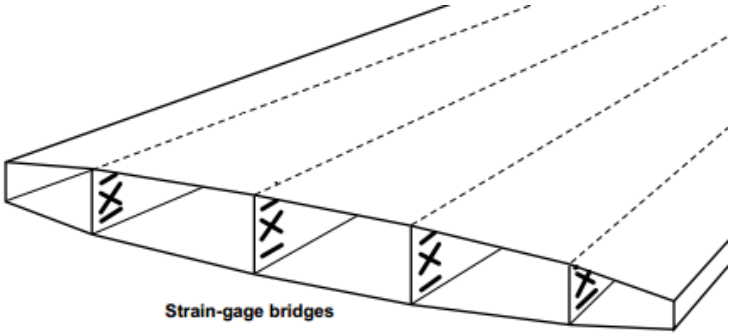

Figure 1-6: Application of Strain Gauge Bridges on Structure for Flight Loads Measurement [19]

The strain gauges bridges are calibrated by applying known loads to the structure. Therefore, in flight, the measurements taken from bridges can be transformed into loads and can be monitored [20, 21]. During flight loads tests, also known as flight loads survey, the measured loads can be used for the verification of load analysis.

1.2.1.3 Mass and Inertia Inputs

Although static load analysis does not involve the inertial forces arising from the oscillatory motion of the structure, the forces arising from the mass distribution of aircraft play important role on the summation of forces acting on the structure.

The mass and inertia distribution of the aircraft is generally modeled as lumped mass points along the axes of main components such as fuselage, wing and tails [4]. A sample mass distribution is represented in the Figure 1-7.

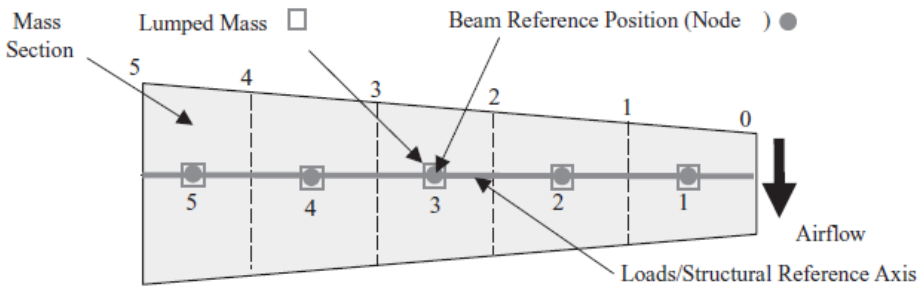

Figure 1-7: A Sample Mass Distribution along Wing [4]

Mass and inertia values on the lumped mass points are calculated by "slicing" the structure, system and payload into slices and summing the mass and inertia values for each section [22]. This can be performed by either idealizing the mass distribution of structural parts, systems and payload, or using advanced CAD software.

1.2.1.4 Stiffness Input

Static load analysis of rigid aircraft does not usually require stiffness input, however, when the deformations are significant, structural model must be provided to calculate static aeroelastic effects.

The structural model for the aircraft is generally finite element model. However, since finite element model for the aircraft is usually prepared in detail design phase and has many degrees of freedom, which makes quick calculations improbable, some idealization can be made in preliminary design. The aircraft structure is reduced to a simple beam model along main components [4, 23, 24, 25, 26, 27]. An example to an aircraft beam model is shown in Figure 1-8.

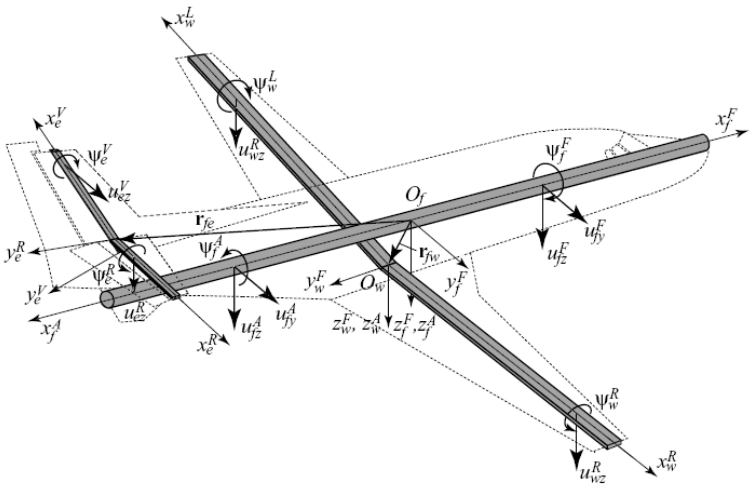

Figure 1-8: A Sample Aircraft Beam Model [24]

The beam model is prepared by structural idealizations with some assumptions [28]. Sectional bending and torsion stiffness values are calculated using major structural parts to obtain 3-D beam representation of the aircraft components.

1.2.1.5 Loads from Miscellaneous Systems

Apart from aerodynamic and inertial loads, there are forces exerted of aircraft structure from landing gears, actuators, propulsion systems, etc [29]. During load analysis, these forces must also be taken into account along with aerodynamic and inertial forces.

1.2.2 Load Cases

As mentioned briefly in the requirements sub-section of input for load analyses section, load cases are generated by the airworthiness and project requirements. The

airworthiness specifications usually define the flight and ground conditions at which the load analysis needs to be performed and structural integrity must be shown.

Although the load cases are mostly defined by the military and civilian regulations, projects requirements are also used for defining load cases. Therefore it is possible to divide the load analysis into two approaches. The bookcase approach utilizes the load cases defined by the certification specifications whereas the rational approach mostly defines flight and ground conditions via simulations and mission profile analysis [4].

The load cases are generated by combining those conditions either specified by airworthiness specs or project requirements, so that it can cover all possible in the aircraft flight regime or the operational envelope. An example to this combination is listed in Figure 1-9.

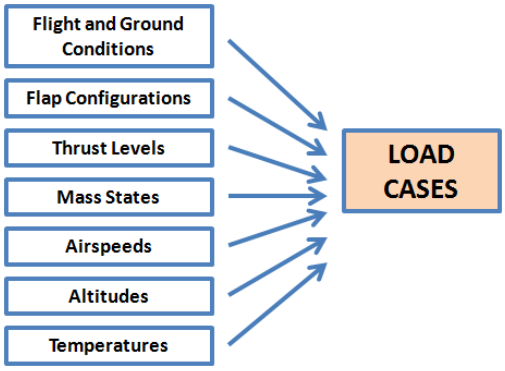

Figure 1-9: Sample Load Case Definition Chart

1.2.2.1 Airspeeds, Altitudes and V-A Placards

The design airspeeds are universally defined in aviation industry worldwide. They are sometimes are referred as “V-Speeds”. These airspeed are used extensively in load analysis since most of the flight and ground conditions are defined with them [3, 10]. Design airspeeds are briefly listed below.

Stall Speed, V_S: It is defined as the minimum speed that an airplane can be maintained. V_{S1} is the stall speed at 1-g flight with all high lift devices retracted [6, 7].

Maneuver Speed, V_A: Design maneuvering speed is the minimum speed for the airplane to fly with maximum load factor. It is related to stall speed such that $V_A = V_{S1}*(n)^{1/2}$ where n is the maximum load factor.

Gust Speed, V_B: It is the airspeed for maximum gust intensity. Its detailed calculation is given in certification specifications such as FAR 23, FAR 25, CS 23 and CS 25.

Cruise Speed, V_C: Definition of the cruise speed is different for each kind of aircraft according to certification regulations. For CS-23 utility aircraft for instance, it is defined as the speed which should not be less than $33*(W/S)^{1/2}$ and should not be more than V_H [30], which is maximum speed at level flight with continuous power. For large aircraft, however, it depends of the gust speed [6].

Dive Speed, V_D: Design dive speed is also defined differently in various certification specifications. But, in general, it was historically considered as the maximum speed that an airplane should attain in a dive [10].

Maximum Speed for Level Flight with Continuous Power, V_H: It is the air

Together with the airspeeds, the altitudes are defined to establish the flight regime of the aircraft. The airspeed altitude plots are called V-A diagrams, as in Figure 1-10.

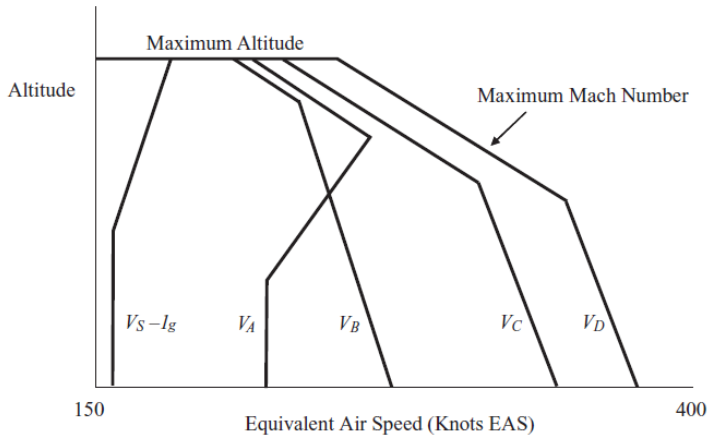

Figure 1-10: An Example of a typical V-A Diagram [4]

1.2.2.2 Load Factors and V-n Diagrams

Load factors are defined as the ratio of lift of an aircraft to its weight. Limit load factor of an aircraft is an important design parameter, which varies from 2.5 g of general aviation planes to 9 g for fighters. Negative limits for the load factors are also defined for the aircraft, but they are usually much lower in magnitude than positive limits [12].

The load factors can arise from maneuver of gust. The load factor increment due to a vertical gust is calculated according to the formulae given in military and civilian certification specifications [6, 7].

The load factor limits, along with the airspeed limits, can be plotted as an envelope, as shown in Figure 1-11, which is called the flight envelope, maneuvering envelope or the V-n diagram [3].

The load factor increment is linearly dependent of airspeed, therefore, they can be plotted as lines, which are called gust lines [12].

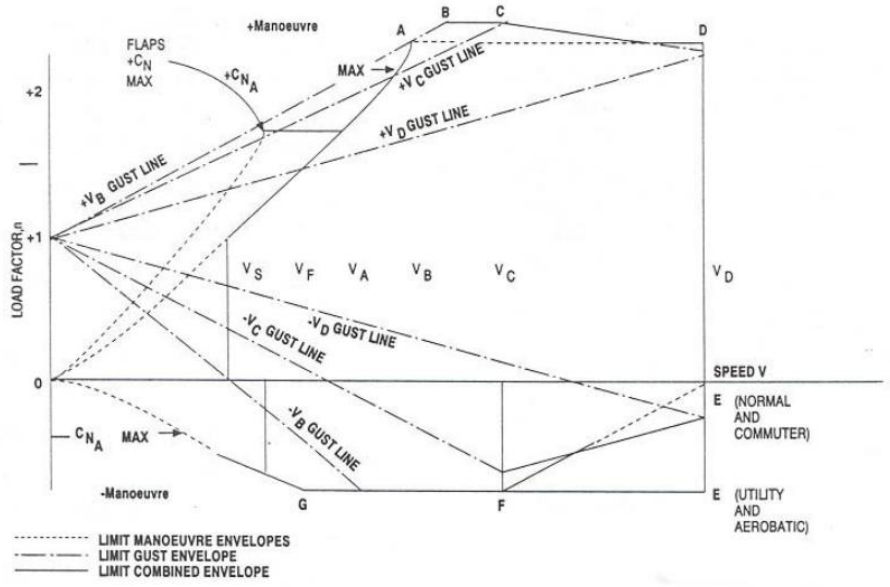

Figure 1-11: V-n Diagram, or Flight Envelope, as defined by CS-23 [30]

1.2.2.3 Mass States and Weight Envelopes

Load analyses are performed for each possible combination of aircraft fuel, payload, and passenger configurations. These sets of combinations are called mass states.

Some of those mass state combinations represent certain special weights of the aircraft, such as Maximum Take-off Weight (MTW), Maximum Landing Weight (MLW), Maximum Zero Fuel Weight (MZFW), Operational Empty Weight (OEW), Empty Weight (EW), etc.

The weight envelope is a plot of aircraft weight and center of gravity. A typical example is given in Figure 1-12.

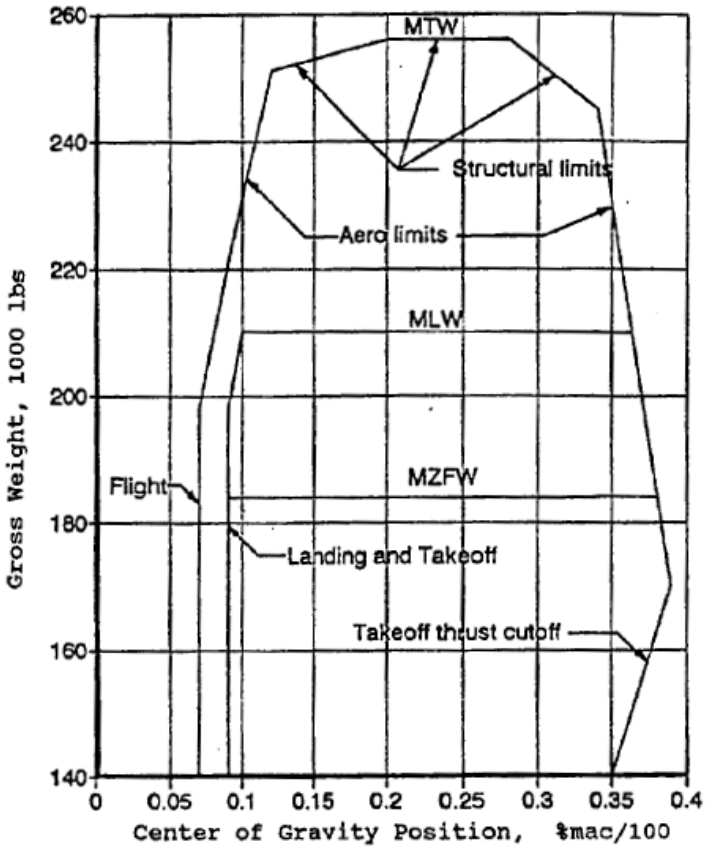

Figure 1-12: A Typical Weight - CG Envelope [3]

1.2.2.4 Flight Conditions

Flight conditions are generally dictated by civilian and military airworthiness specifications, but depending on the project requirements, additional maneuvers can also be analyzed, especially in military aircraft design projects.

1.2.2.4.1 Symmetric Maneuvers

Symmetric maneuvers are basically steady pull-up / push-down maneuvers and pitching maneuvers [3, 10]. The difference between pull-up / push-down maneuvers and pitching maneuvers is the pitching cases are abrupt maneuvers involving pitch velocity or acceleration whereas pull-up and push-down cases are steady state at a constant load factor.

1.2.2.4.2 Rolling Maneuvers

Rolling maneuvers involve aileron action, hence giving aircraft angular speed and acceleration along its longitudinal axis [3]. CS and FAR specifications dictate the roll maneuvers to be analyzed at maximum two thirds of maximum limit load factor and minimum 0 load factor [3, 6, 7].

Roll maneuvers can be divided into four phases, which are steady level flight, roll initiation, steady roll rate and roll arresting or reverse roll [10]. These phases are illustrated in Figure 1-13.

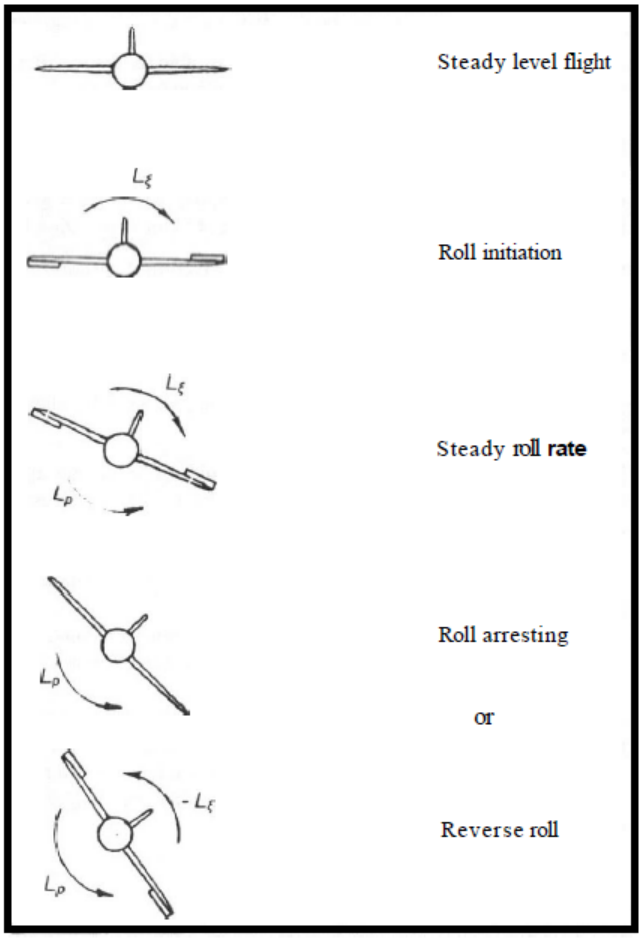

Figure 1-13: Phases of Roll Maneuver [10]

1.2.2.4.3 Yawing Maneuvers

Yawing maneuvers arise from rudder application, sideslip conditions or unsymmetrical engine conditions [3].

There are basically four phases of yawing maneuvers which can also be analyzed in a quasi steady sense: yaw initiation, over-swing, equilibrium sideslip angle and yaw arresting [10]. There phases are illustrated in Figure 1-14.

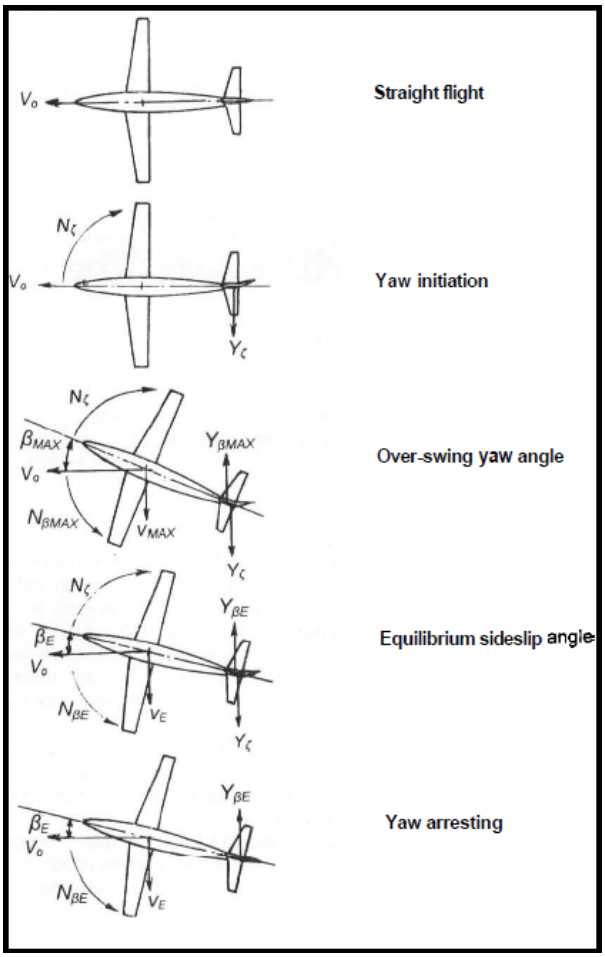

Figure 1-14: Phases of Yaw Maneuver [10]

1.2.2.5 Ground Conditions

Especially for the fuselage components and local structures around landing gear, ground conditions are usually the most critical load cases. These ground conditions are divided into three groups: landing, taxi and ground handling [3, 6, 7].

1.2.2.5.1 Landing

Landing conditions are specified with great detail in airworthiness specifications such as FAR-25 and CS-25. Figure 1-15 gives the ground conditions specified by CS-25.

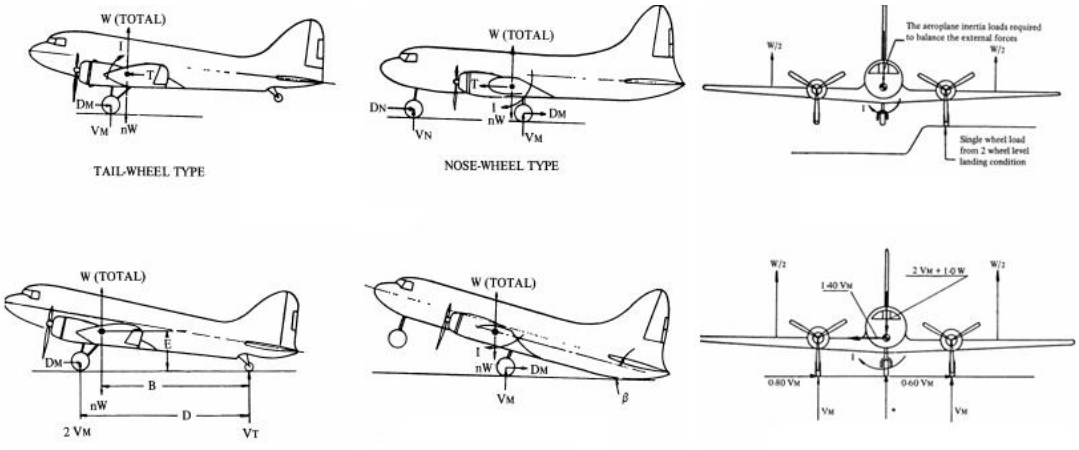

Figure 1-15: Landing Conditions according to CS-25

1.2.2.5.2 Taxiing

Similar to landing conditions, taxiing cases are also detailed in specifications and analyzed in a bookcase approach. These conditions include braking, ground turning, pivoting, etc. [3, 6, 7].

1.2.2.5.3 Ground Handling Loads

Ground handling loads are divided into three groups: jacking, towing and mooring (tethering) [3, 6, 7].

1.2.3 Calculation of Loads

Calculation of loads can be performed by a steady maneuver analysis at a trim point or by maneuver simulation with time history in a quasi steady manner [3, 23]. Civilian and military certification specifications sometimes require a time history maneuver simulation depending on the flight condition or the type of the aircraft. For this kind of load cases, a 6 DOF trim analysis is needed.

1.2.4 Output of Load Analysis

In the aircraft design cycle, load analysis provides output mainly to structures group as critical load cases and critical structural loads [31].

1.2.4.1 Loads Envelopes

Loads envelopes are generated in order to visualize the load distribution. Load envelopes can be classified into 1-D Loads Envelopes, 2-D Loads Envelopes and Load – Flight Parameter Envelopes.

1-D loads envelopes are the distribution of loads along the aircraft components. These are merely the shear, torsion and bending moment diagrams [3, 10]. A typical example is given in Figure 1-16.

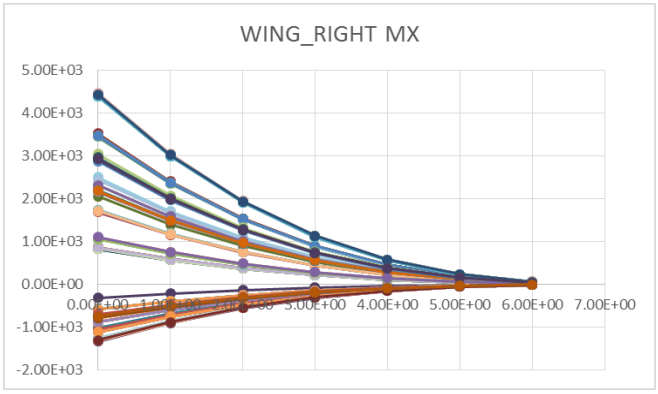

Figure 1-16: 1D Loads Envelope with a Reduced Number of Load Cases

On the other hand, 2-D loads envelopes are prepared to visualize two force components on a single section [29, 32]. An example to a 2-D loads envelope is given in Figure 1-17:

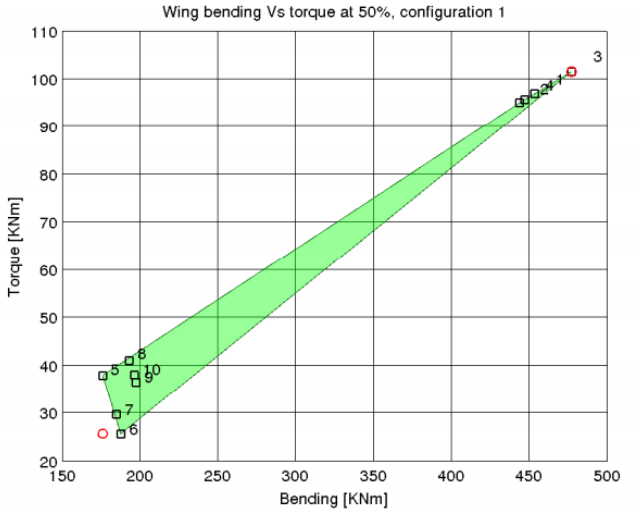

Figure 1-17: 2-D Loads Envelope [32]

Load – Flight Parameter Envelopes are similar to 2D Loads Envelopes, but they are plots of load component versus flight parameters. Flight parameters can be mass, airspeed, angle of attack, load factors, angular accelerations, or combination of these.

They is also a common output of load analysis and gives useful insight especially regarding maneuver loads and flight mechanics [Neubacher, 33, 34].

1.2.4.2 Selection of Critical Load Cases from Loads Envelopes

In aircraft design projects, a typical load analysis for a certified aircraft involves hundreds of thousands of load cases. However, only a few hundreds of these load cases are selected to be critical cases and used for the structural analysis. Therefore, it is important to carefully select the critical load cases using 1D load envelopes, 2D load envelopes, and load – flight parameter envelopes. The load selection criteria is generally decided by loads and structural analysis engineers and according to these criteria, critical load cases are selected from the envelopes [35].

1.2.4.3 Evaluation of Critical Structural Loads and Structural Analysis

After the critical load cases are decided, it becomes possible to evaluate the critical structural loads acting on the aircraft. Therefore, finally, the maximum forces acting on the aircraft structure during its entire lifetime can be decided which the structure can be analyzed accordingly. Critical loads are submitted to structural analyses engineers as the main output of load analysis [8].

Obtaining moment, axial, shear and torsion forces along the components from loads envelopes and calculating internal structural loads is a practice performed in early detail design phases. As the level of detail increases in analysis of structural parts, the critical load cases will be used for further 3D finite element analysis [4].

1.3 Effects of Static Aeroelasticity in Load Analysis

As mentioned in previous sections, the terms “static aeroelasticity” and “static load analysis” are sometimes used in conjunction, but the main difference is that the load analysis is involved in the calculation of maximum structural forces whereas static aeroelasticity is a phenomenon involving aero-structural coupling and its effects such as structural deformations, pressure re-distribution, divergence, control reversals, etc [3, 4]. However, these phenomena can have significant effect, either positive of negative, on aircraft loads [10].

1.3.1 Deflection and Pressure Redistribution

It is unavoidable that wings, like all structures, deform under loads. The magnitude of those deformations may be small for stiff and low aspect ratio wings and high for wings with high aspect ratio. Figure 1-18 shows the deflection of the wing of NASA Altair UAV.

Figure 1-18: Altair UAV of NASA. (Photo from NASA)

However, even low aspect ratio fighter wing can deflect significantly under critical loads. For instance the wing of an F-18 fighter may deform up to 0.5 meters during flight, as shown in Figure 1-19 [36].

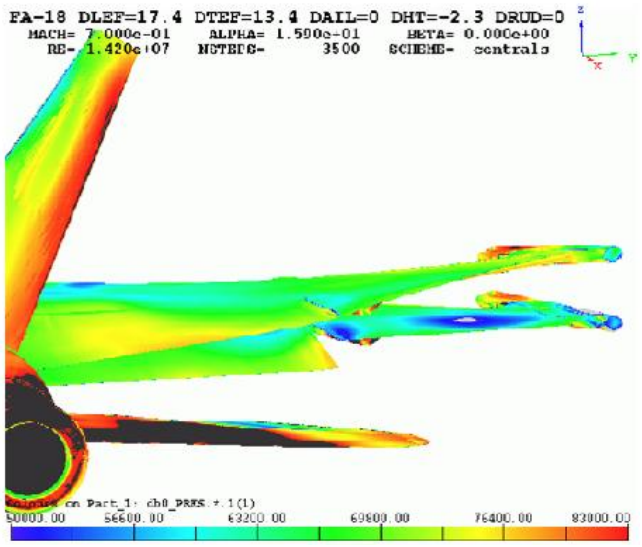

Figure 1-19: Deflection of F/A-18 wing during pull-up maneuver [36]

The deflections of lifting surfaces results in aerodynamic pressure redistribution. This affects the spanwise lift distribution along wings and tails. When analyzing the change in lift distribution, either the total lift of the aircraft or the initial angle of attack is kept constant, depending on how the load case is defined.

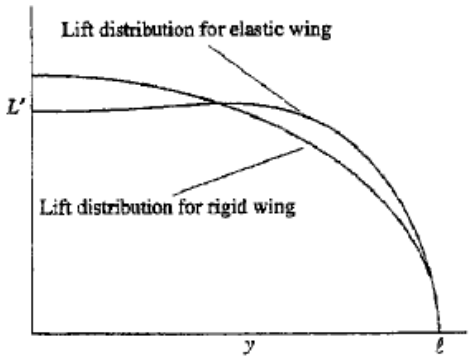

Figure 1-20: Comparison of lift distributions on rigid wing and elastic wing [5]

Although the pressure redistributions generally arises from torsional deflections mainly due to local angle of attack changes, bending deflections also affects the pressure distribution on swept wings [5].

1.3.2 Divergence Instability

Divergence can simply be defined as the case where the torsional deflection of wing results in higher angle of attack, which in turn leads more torsional deflection beyond the point above structural limit [3, 4, 5, 10].

1.3.3 Flight Mechanics Coupling

With the aircraft deforming under static aeroelastic effects, stability and control coefficients and derivatives also change along with the geometry.

The aircraft geometry can significantly differ from its manufactured shape and its shape in cruise, which it is optimized for. Hence, the term “jig shape” is used to define its geometry for its undeformed state. Jig shape is illustrated in Figure 1-20.

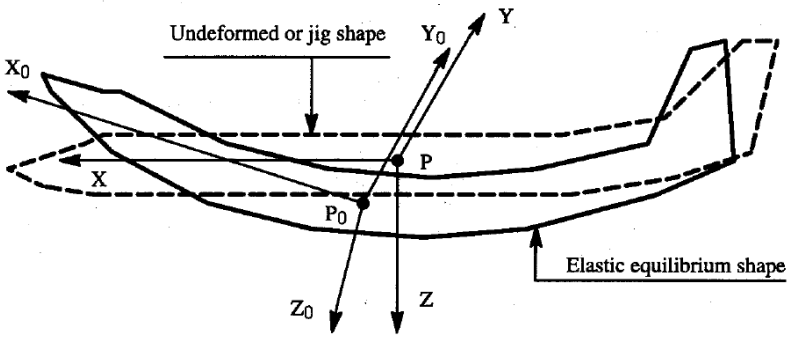

Figure 1-21: Jig shape [37]

Deflections on the fuselage, for instance, may have great effects on longitudinal stability and control derivatives [37]. Figure 1-21 gives the moment coefficient values of Boeing 707-320B for a rigid and elastic airplane.

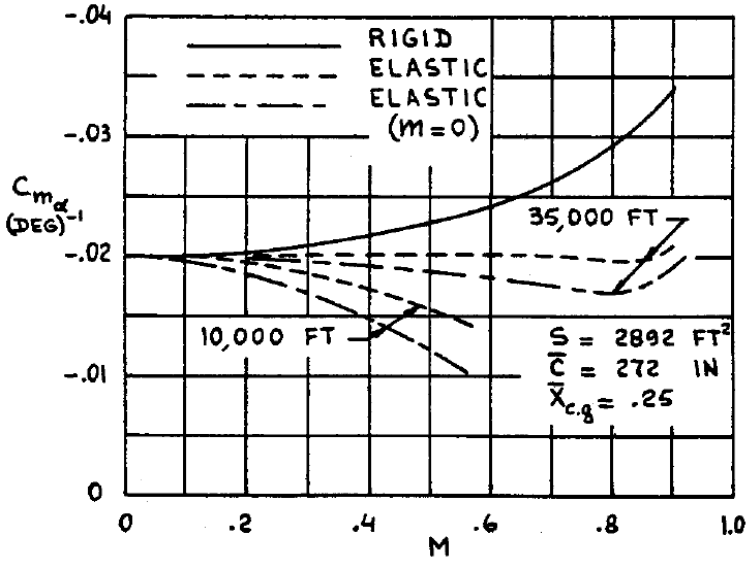

Figure 1-22: Pitching Moment Derivative for Rigid and Elastic Aircraft [37]

Not only fuselage deflection, but also wing deflections result in serious flight mechanics and control coupling. One phenomenon is called the control reversal, which is the loss of control surface effectiveness, such as ailerons, to a point at which the application of aileron results in a wing torsional deformation such that the resultant force is opposite to the desired force [10].

1.4 Aim of the Study

The scope of this study is to detail the load analysis process in generical and from an industrial point of view in the first chapter. One of the major motivations of this

thesis work is to provide a compact reference for those who wish to study aircraft loads. Although loads, in general, is a highly comprehensive subject and lies at the hearth of aircraft design cycle, there are few references which cover aircraft loads from an industrial point of view. Therefore, the first chapter aims to detail the load analysis in general to give reader the basics. The following chapters are intended to provide a case study for the concepts introduced in this chapter. In the second chapter, an ultralight class simple aircraft is introduced and its simplified aerodynamic and structural models are generated. Chapter 3 deals with the generation of load cases according to the airworthiness and certification specifications. The fourth chapter outlines the loads calculation process briefly whereas the results of load analyses are provided in Chapter 5. Finally, conclusions and discussions are made in the last chapter, Chapter 6.

CHAPTER 2

AERODYNAMIC, INERTIAL AND STRUCTURAL MODELLING OF THE AIRCRAFT

2.1 Description and Details of the Aircraft

The aircraft to be analyzed in this thesis work is selected to be a conventional airplane so that all aspects of load analysis can be covered. The airplane is decided to be a single-seat ultralight class aircraft with pusher configuration and short take-off and landing capability. It has a high wing and conventional tail. Its crude geometry is given in Figure 2-1.

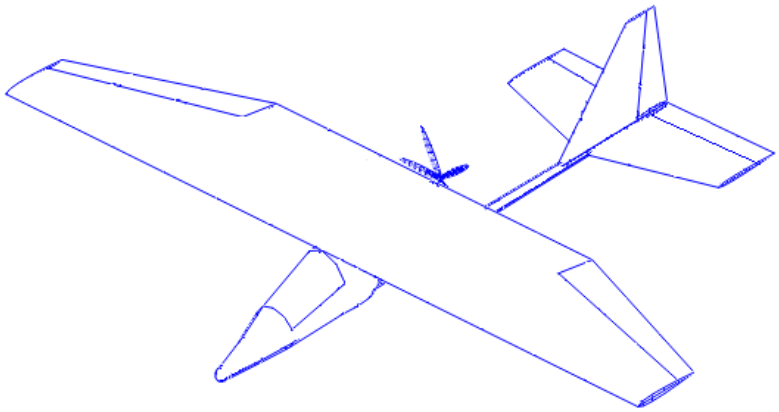

Figure 2-1: The aircraft in isometric view

A three-view illustration and the axis system used in the models and analyses are given in Figure 2-2.

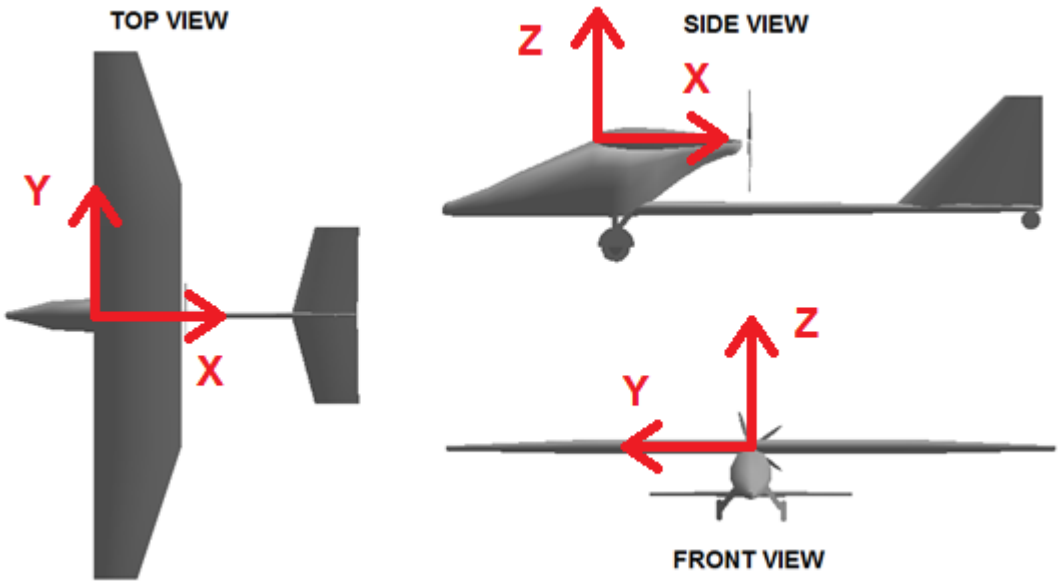

Figure 2-2: The aircraft in three-view

The aircraft is powered by a single Limbach L-550E. L-550E is a four cylinder, horizontally opposed, air-cooled, two cycle engine with a maximum power of 50 horsepower. The engine is shown in Figure 2-3 and engine specifications are given in Table 2-1.

Figure 2-3: Limbach L550 E

Table 2-1: Limbach L550 E Engine Specifications [40]

Dry Weight	16 kg
Length	300 mm
Width	410 mm
Height	302 mm
Maximum Power	50 hp
Average SFC	340 g/hph @ 50 hp

The Limbach L550 E engine is mounted on the fuselage, behind the wing trailing edge. The cooling is performed by air intakes on the sides of fuselage. The propeller

is a 5 blade constant pitch propeller. The propeller is selected to be constant pitch for the sake of simplicity.

As mentioned above, geometry of the aircraft is optimized for short take-off and landing. Design and technical specifications of the aircraft are given in Table 2-2.

Table 2-2: Aircraft Design Specifications

Crew:	1 pilot
Wing Area:	21 m^2
Wing Span:	12 m
Length:	8 m
Height:	1.8 m
Wing Airfoil	NACA 23015 -
Horizontal Tail Airfoil	NACA 0008
Vertical Tail Airfoil	NACA 0006
Powerplant:	Limbach L550 E (50 hp)
Propeller:	1.4 m (5 Blade, C.P.)
Landing Gear:	Fixed, Tail Dragger
Empty Weight:	124 kg (114 kg w/o BRS)
Fuel Capacity:	50 kg
Payload Capacity:	20 kg
Maximum Take-off Weight:	294 kg

From certification point of view, the aircraft has an empty weight of 114 kg, (without Ballistic Rescue System) which is below 115 kg empty weight limit of FAR Part-103, therefore the aircraft complies with ultralight vehicle definition in United States [38]. In Turkey, it also complies with the ultralight specification with its maximum take-off weight being less than 300 kg [39].

Based on the performance calculations, which are beyond the scope of this study, the performance specifications of the aircraft is given in Table 2-3.

Table 2-3: Aircraft Performance Specifications

Maximum Speed:	150 km/h, 82 knots
Cruise Speed:	126 km/h, 68 knots
Stall Speed:	43 km/h, 23 knots
Range:	760 km
Rate of Climb:	7 m/s
Service Ceiling:	4000 m, 13,000 ft
Take off Distance:	Less than 40 m
Landing Distance:	Less than 50 m
Limit Load Factors:	4 g / -2 g

2.2 Modeling Philosophy

In this study, the aircraft aerodynamic, inertial and structural models are prepared to allow simple load calculations, while these models are also prepared in detail for verification.

2.3 Aircraft Aerodynamic Model

Aircraft aerodynamic mesh is generated using geometry and surface data for CFD analyses. However, some simplifications to the aerodynamic model is done such as omitting the propeller, landing gear, gaps between control surfaces and platforms, hinges, etc.

Two kinds of meshes are prepared and the results of test runs with those meshes are compared. VSP (Vehicle Sketch Pad), open-source software developed by NASA, is used for the generation of aerodynamic meshes. First mesh is the structured grid. The structured grid of the aircraft is given in Figure 2-4.

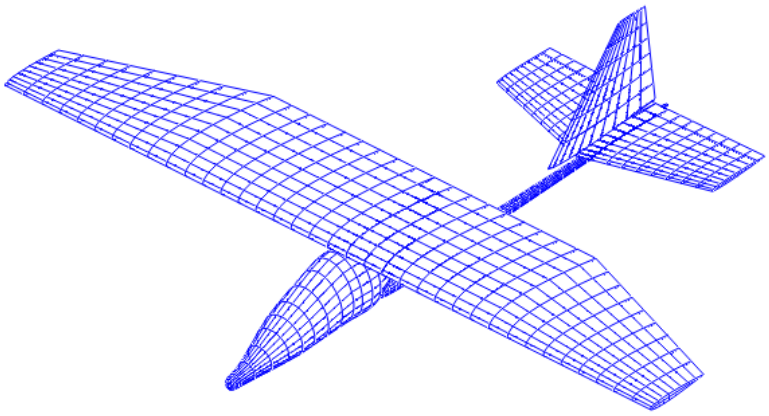

Figure 2-4:Structured Aerodynamic Mesh of the Aircraft

The unstructured grid is also prepared using aircraft geometry, and it is given in Figure 2-5.

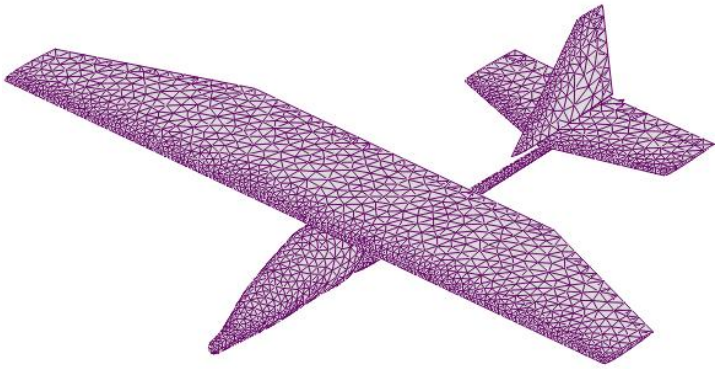

Figure 2-5: Unstructured Aerodynamic Mesh of the Aircraft

The CFD code used here is a 3D panel method code developed in University of Zagreb by Daniel Filkovic and is presented as open source code called “Apame”.

A simple test run, using the panel method code, at 5 degrees angle of attack and zero sideslip without mach effects is prepared and performed with two meshes. Pressure coefficient distribution results are given in Figure 2-6.

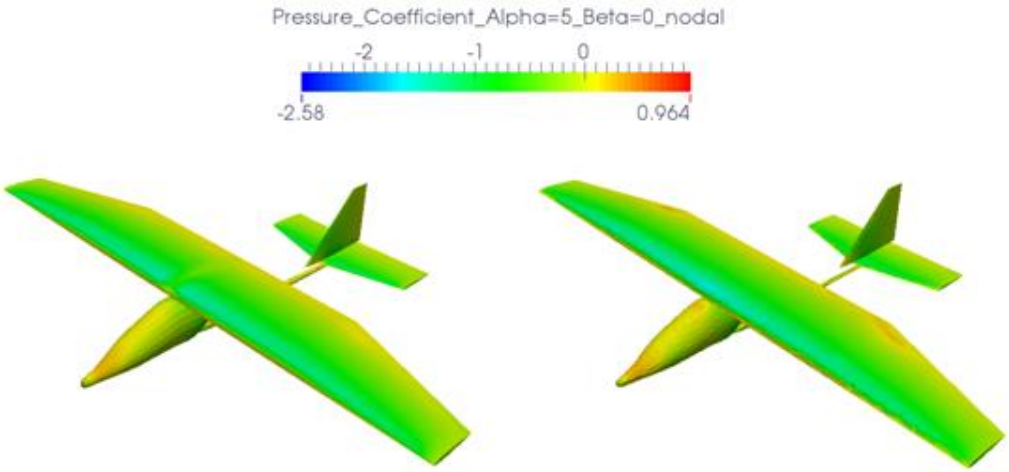

Figure 2-6: CFD Solutions of Structured and Unstructured Meshes at AoA=5

For comparison, the aerodynamic coefficients generated by these CFD runs are tabulated in Table 2-4.

Table 2-4: Comparison of Aerodynamic Coefficients

Mesh Type	CX	CY	CZ	CL	CM	CN
Structured Mesh	-0.0267	0.0001	0.3936	0.0001	-0.276	0.0004
Unstructured Mesh	-0.0269	0.0023	0.3902	0.002	-0.269	0.0013

As seen from Table 2-4, the structured and unstructured meshes produce similar results in symmetrical aerodynamic coefficients. Although non-symmetrical aerodynamic coefficients (CY – sideslip coefficient, CL – roll moment coefficient, and CN – yaw moment coefficient) are supposed to be zero, structural and unstructured meshes have some negligible positive values, mainly because of meshing and truncation errors.

The lift distribution along the wing is obtained by a simple integration code, which uses the center points of the elements and integrates from wing tip to wing root. The code is given in Appendix A. The code uses the output file of a commercial CFD code. The output of the CFD code consists of the mesh points and Cp distribution.

The spanwise lift distribution for the case above (at 5 degrees angle of attack and zero sideslip) is plotted along the wing span in Figure 2-7.

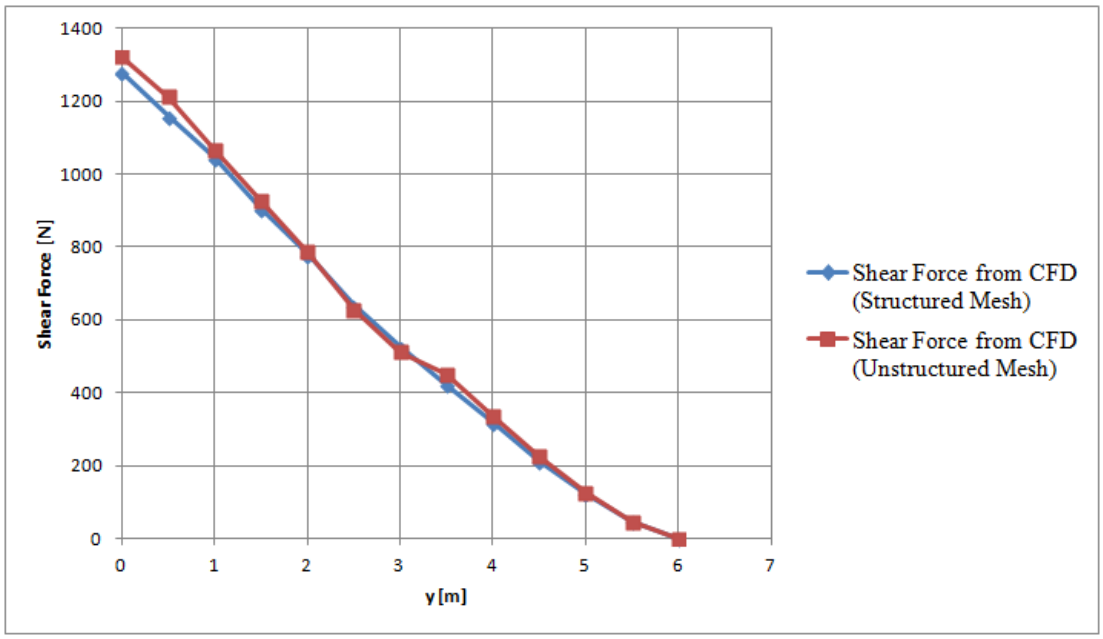

Figure 2-7: Comparison of Structured and Unstructured Grid Results

Shear force diagram obtained from CFD analyses of two kinds of meshes shows that the difference between structured and unstructured grids is negligible.

2.3.1 Simplification of the Aerodynamic Model

In order to develop a simple analytical model for the calculation of aircraft aerodynamic loads, it is decided to use a modified analytical approach based on both airfoil data and empirical method.

As mentioned in Chapter 1, the Schrenk method uses arithmetic mean of an elliptical distribution and geometrical chord distribution, therefore it is fully analytical formula with no discrete numerical calculations such as Multhopp Method. However, Schrenk Method does not take wing twist into account, which becomes important especially when static aeroelastic effects are also studied.

Moreover, although the chordwise lift distribution of a plain airfoil can be approximated, in case of a control surface, more approximations are required.

Hence, in this study, the Schrenk method is modified to take twist and control surface deflections into account. The sectional lift coefficient for a lifting surface can be decomposed with respect to Schrenk lift distribution as follows:

$$c_{l,section} = c_{l,basic} + c_{l,additional} \tag{2. 1}$$

where $c_{l,basic}$ is the sectional lift coefficient without and twist of control surface deflection effects and $c_{l,additional}$ is the additional sectional lift coefficient at the section due to twist and control surface deflection. Assuming linear lift curve slope, with is valid for the linear flight regime, the additional sectional lift coefficient

$$c_{l,additional} = c_{l_\propto} \Delta\propto \tag{2. 2}$$

where $\Delta\propto$ is the additional angle of attack increment at the section. This incremental angle of attack can be a result of either sectional twist or control surface deflection. The effect control surface deflection on the sectional angle of attack increment can be approximated as the linear camber line with passing through the leading edge of the lifting surface and trailing edge of the control surface . However, since the airfoil shape is altered, the chordwise lift distribution must be approximated utilizing the methods given by Howe [10].

Since the linear lift curve slope is assumed, the sectional lift coefficient is;

$$c_{l,basic} = c_{l_0} + c_{l_\propto} \propto \tag{2. 3}$$

Hence, substituting Equation 2-2 and Equation 2-3 into Equation 2-1, the sectional lift coefficient becomes;

$$c_{l,section} = c_{l_0} + c_{l_\propto} \propto + c_{l_\propto} \Delta\propto \tag{2. 4}$$

Dividing both sides of equation with $c_{l,basic}$ gives;

$$\frac{c_{l,section}}{c_{l,basic}} = \frac{c_{l_0} + c_{l_\propto} \propto + c_{l_\propto} \Delta\propto}{c_{l_0} + c_{l_\propto} \propto} \tag{2. 5}$$

The equation then becomes;

$$\frac{c_{l,section}}{c_{l,basic}} = 1 + \frac{c_{l_\propto} \Delta\propto}{c_{l_0} + c_{l_\propto} \propto} \tag{2. 6}$$

Therefore the ratio of sectional lift coefficient and basic lift coefficient becomes a linear function of sectional angle of attack increment;

$$\frac{c_{l,section}}{c_{l,basic}} = 1 + \left(\frac{1}{\frac{c_{l_0}}{c_{l_\propto}} + \propto} \right) \Delta\propto \tag{2. 7}$$

Finally, the sectional lift coefficient is directly proportional to the basic lift coefficient distribution.

$$c_{l,section} = \left(1 + \left(\frac{1}{\frac{c_{l_0}}{c_{l_\alpha}} + \alpha}\right)\Delta\alpha\right) c_{l,basic} \tag{2. 8}$$

If the basic lift coefficient distribution is assumed to be the Schrenk lift distribution, the aircraft spanwise lift distribution can be approximated to be;

$$c_{l,section} = \left(1 + \left(\frac{1}{\frac{c_{l_0}}{c_{l_\alpha}} + \alpha}\right)\Delta\alpha\right) c_{l,Schrenk} \tag{2. 9}$$

So the modified analytical method presented here uses Schrenk distribution, airfoil parameters, and angle of attack.

2.3.2 Verification of the Model

Using the detailed aerodynamic models and CFD, the method to simplify the aerodynamic data in this study can be verified. Two main output of the simplified method are the lift distribution along the wing and lift distribution along the chord. Those are verified separately by different cases.

The spanwise lift distribution is verified for three different cases: wing with no twist, wing with 6 degrees of twist and wing with aileron deflection. The results are compared in Figure 2-8.

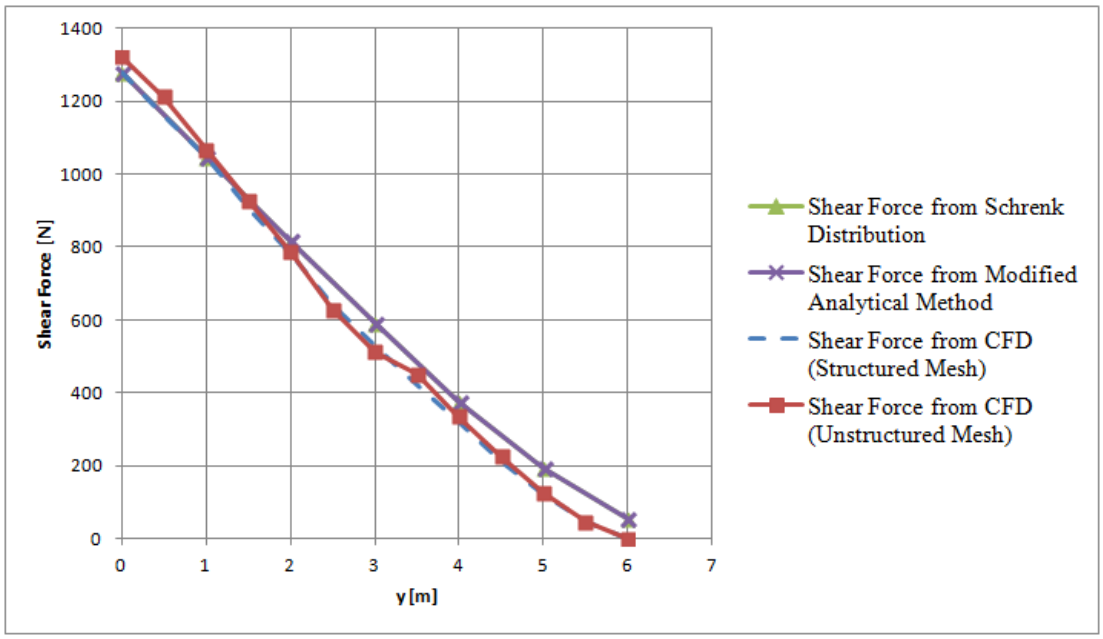

Figure 2-8: Comparison of Schrenk Method, Modified Analytical Method and CFD Results, Wing Twist=0, AoA=5 deg.

As shown in Figure 2-8, Schrenk method and the modified analytical method produced exact results and they are quite accurate for the approximation of the lift distribution over the untwisted wing.

The verification of the modified analytical method for airload distribution is also performed with a wing twisted by 6 degrees from root to the tip (downward twist, there the angle of incidence of the sections decrease from root to tip). The results are compared in Figure 2-9.

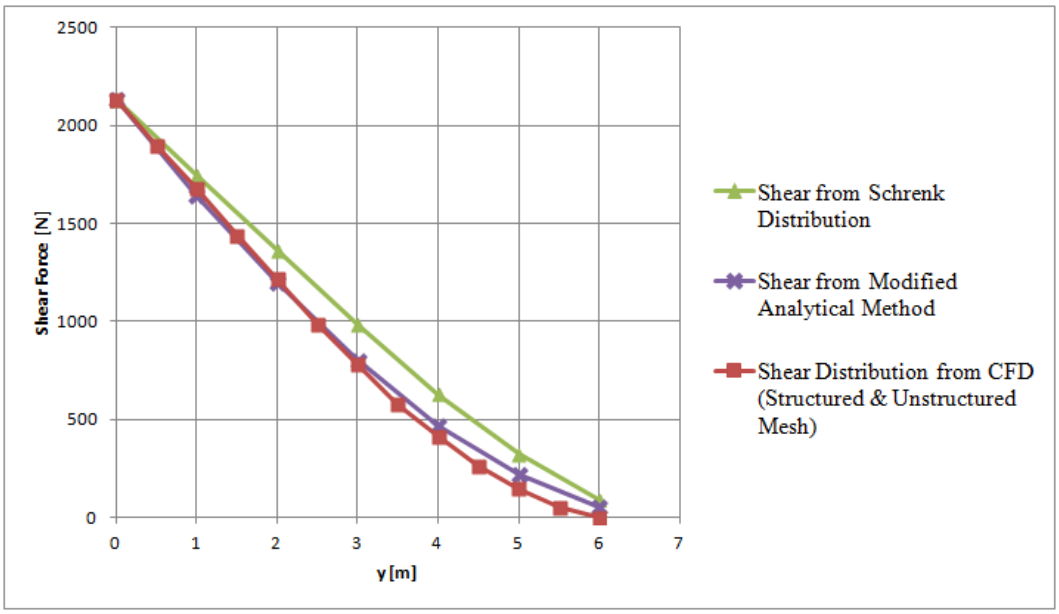

Figure 2-9: Comparison of Schrenk Method, Modified Analytical Method and CFD Results, Wing Twist=6 deg, AoA=10 deg

It is clearly seen from Figure 2-9 that the modified analytical method responds to wing twist in a desired fashion and produces more accurate results for lift distribution over the wings with twist angles.

The last verification is performed for the airload distribution over the wing with control surface deflections. The wing has an aileron from y=3 meters to the wingtip. The pressure distribution over the wing with aileron deflected 10 degrees is generated with CFD analysis and shown in Figure 2-10.

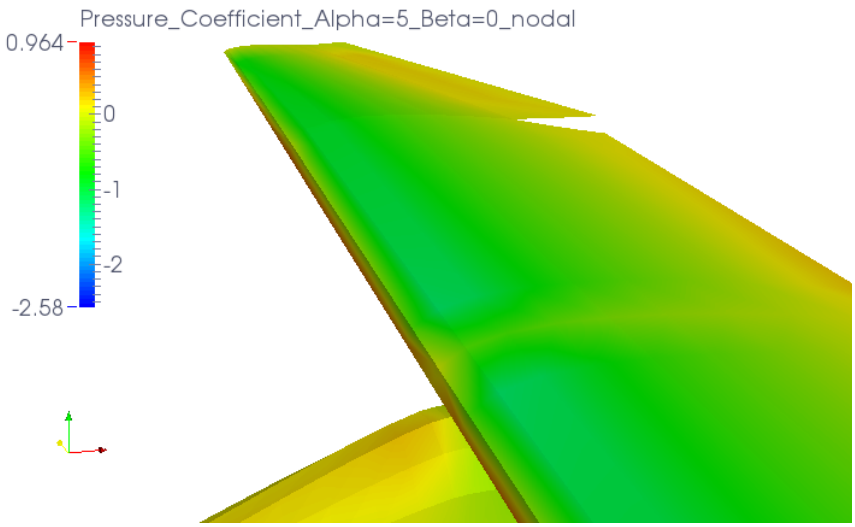

Figure 2-10: CFD results of the Aircraft with 10 degrees Aileron Deflection

Shear distribution from these methods are compared in Figure 2-11.

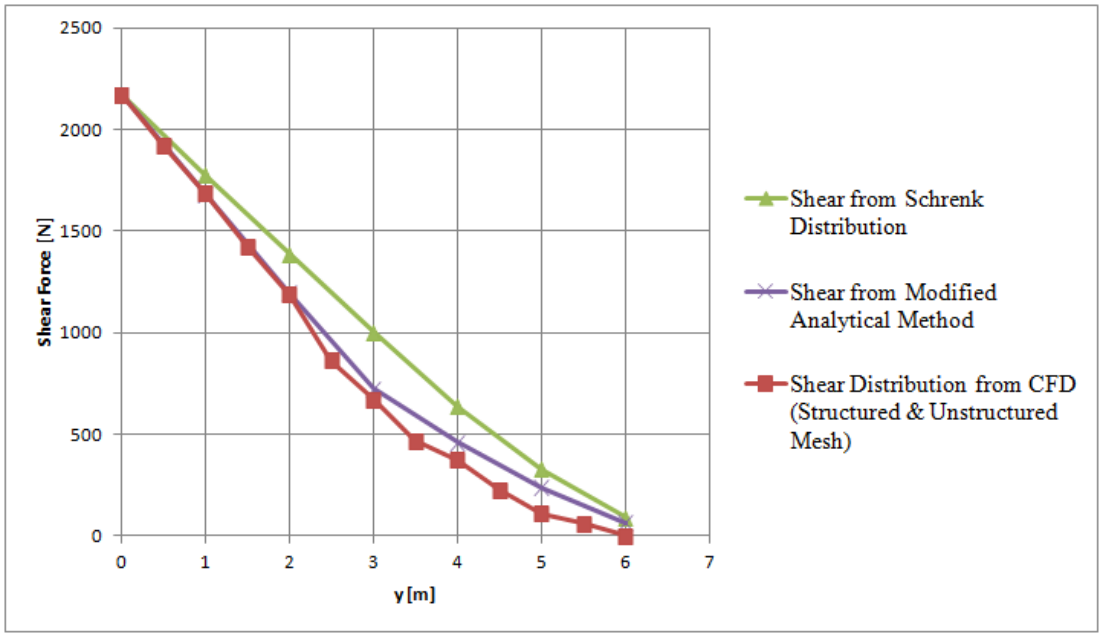

Figure 2-11: Comparison of Schrenk Method, Modified Analytical Method and CFD Results, Aileron Deflection=10 deg, AoA=10 deg

Since the approximation of control surface deflection is loosely made as a thin airfoil with camber line, the modified analytical method differs from the CFD results slightly. However, it is still more accurate than the Schrenk Method, which completely fails to take control surface deflections into account.

Similar to spanwise lift distribution, the chordwise distribution also has to be verified.

As mentioned in the introduction and literature review, there are some empirical approximations to the chordwise lift distribution. For symmetrical airfoils center of pressure is assumed to be at 25 percent of the chord [10], whereas for cambered airfoils center of pressure is believed to lie around 34 percent of the chord [12] for a typical angle of attack. Unfortunately these assumptions fail to take the center of pressure movement into account, especially for cambered airfoils, which is significant.

The method to be used in this study, however, is an analytical method which uses airfoil parameters. It is based on the calculation of center of pressure according to the formula given in equation 2-10 [37].

$$x_{cp} = (x_{ac} + \frac{c_{m_{ac}}}{c_l}) \tag{2. 10}$$

The comparison between the CFD results, Raymer's approximation [12], Howe's approximation [10] and analytical method which is formulated in Eq. 2.10 and based on the airfoil characteristics is given in Figure 2-12.

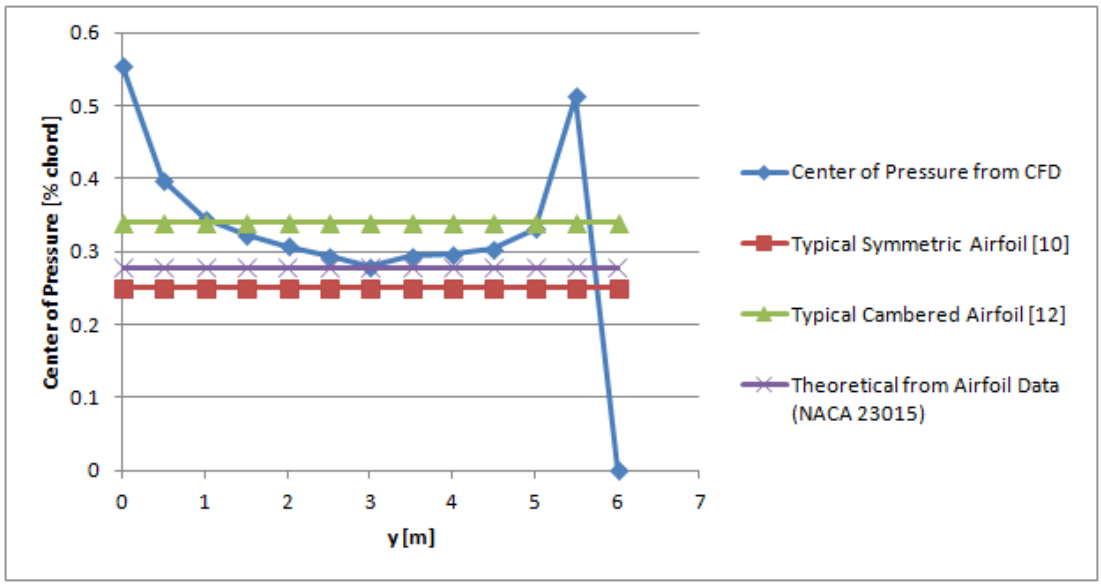

Figure 2-12: Location of Center of Pressure obtained from CFD and Analytical Methods.

As expected, analytical method produces the most accurate data for the airfoil section without wingtip and root effects, as seen in the station located at y=3 m, middle of the half wing. However, since it uses 2D airfoil characteristics, it is not quite accurate at wingtip or wing root. Despite its failure to take 3D wing effects into accounts, in this study, it is decided to use the analytical method, since it is based on more detailed calculation involving angle of attack, airfoil characteristics, etc.

2.4 Aircraft Mass Model

Aircraft weight and balance activities are quite interconnected with loads group in an aircraft design project. The reason is that the aircraft weights (Empty Weight, Maximum Take-off Weight, etc.), system weights, crew and payload weights, aircraft mass states and aircraft mass – inertia distribution are all major load analysis input.

Structural and system layout of the aircraft is given in Figure 2-13. Its system layout is simplified to represent the pilot, the fuel tank (shown with red color) and the engine (shown with blue color).

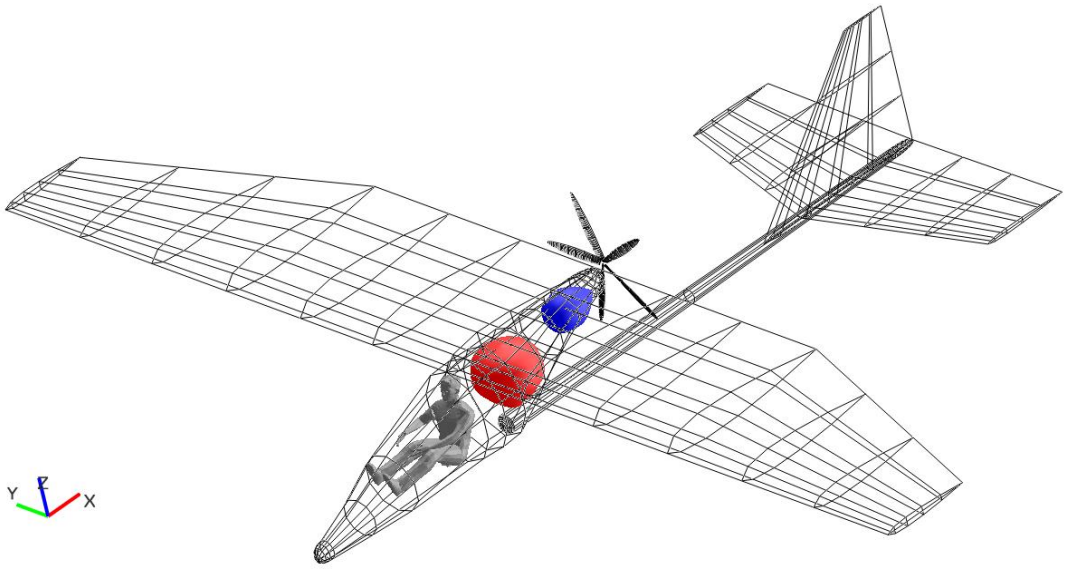

Figure 2-13: Structural and System Layout of the Aircraft

Weight breakdown of the aircraft is tabulated in Table 2-5. The x values are measured with respect to aircraft axis system as given in Figure 2-2.

Table 2-5: Weight Breakdown of the Aircraft

STRUCTURES		
WING & AILERONS		
	Mass [kg]	X [m]
Skin:	23.24 kg	0.9 m
Spars:	8.12 kg	0.9 m

Table 2-5 (Continued)

Stiffeners:	1.50 kg	0.2 m
Ribs:	2.89 kg	0.9 m
Ailerons:	2.45 kg	1.5 m
WING TOTAL:	38.2 kg	0.9 m
FRONT FUSELAGE		
Skin:	6.23 kg	0.25 m
Stiffeners:	3.20 kg	0.5 m
Frames:	1.40 kg	0.2 m
Wing / Engine Attach.:	2.05 kg	1.2 m
FRONT FUSELAGE TOTAL:	12.88	0.45 m
REAR FUSELAGE		
Skin:	2.88 kg	3.1 m
Stiffeners:	2.76 kg	3.5 m
Frames:	0.28 kg	3.4 m
Tail Attach.:	0.5 kg	5.1 m
REAR FUSELAGE TOTAL:	6.42 kg	3.44 m
HORIZONTAL TAIL & ELEVATOR		
Skin:	4.67 kg	5.2 m
Spars:	1.90 kg	5.3 m
Stiffeners:	0.50 kg	5.1 m
Ribs:	0.38 kg	5.5 m
Elevator.	1.17 kg	5.8 m

Table 2-5 (Continued)

HORIZONTAL TAIL TOTAL:	8.62 kg	5.31 m
VERTICAL TAIL & RUDDER		
Skin:	1.61 kg	5.4 m
Spars:	0.71 kg	5.5 m
Stiffeners:	0.19 kg	5.2 m
Ribs:	0.28 kg	5.5 m
Rudder:	0.58 kg	5.7 m
VERTICAL TAIL TOTAL:	3.37 kg	5.47 m
OTHER STRUCTURAL		
Fasteners:	3.5 kg	1.5 m
Paint:	3 kg	1.1 m
OTHER TOTAL:	6.5 kg	1.31 m
STRUCTURE TOTAL:	75.99 kg	1.78 m
SYSTEMS AND MISC. ITEMS		
Engine:	16 kg	1.8 m
Propeller:	6.5 kg	2.2 m
Fuel system:	0.5 kg	1.2 m
Ballistic Rescue System:	10 kg	0.5 m
Avionics:	3 kg	-1 m
Cockpit Furnishing:	3 kg	-0.5 m
Flight Control System:	1.5 kg	0.5 m
Canopy:	5 kg	-0.5 m

Table 2-5 (Continued)

Fire Extinguisher:	2 kg	-1 m
Other Systems:	1 kg	0.5 m
SYSTEMS TOTAL:	48.5 kg	0.84 m
AIRCRAFT EMPTY WEIGHT:	124.5 kg	1.41 m
Crew Weight:	100 kg	-0.5 m
Fuel Weight:	50 kg	0.75 m
Payload Weight:	20 kg	0.25 m
MAXIMUM TAKE-OFF WEIGHT:	294.5 kg	0.57 m

Mass model of the aircraft is simply the mass and inertia distribution of the aircraft, which is the main input for inertial loads. This distribution can be either continuous or discrete, depending on the solution methods. In industrial practice, discrete mass and inertia points, called as lumped masses, are calculated along the aircraft components and used for both static and dynamic load analysis. They are connected to the structure via multi-point constraint RB3 elements in case of NASTRAN analysis.

It is quite straightforward to obtain a lumped mass model, or discrete mass distribution using the structural and system layout. The lumped mass points are shown in Figure 2-14.

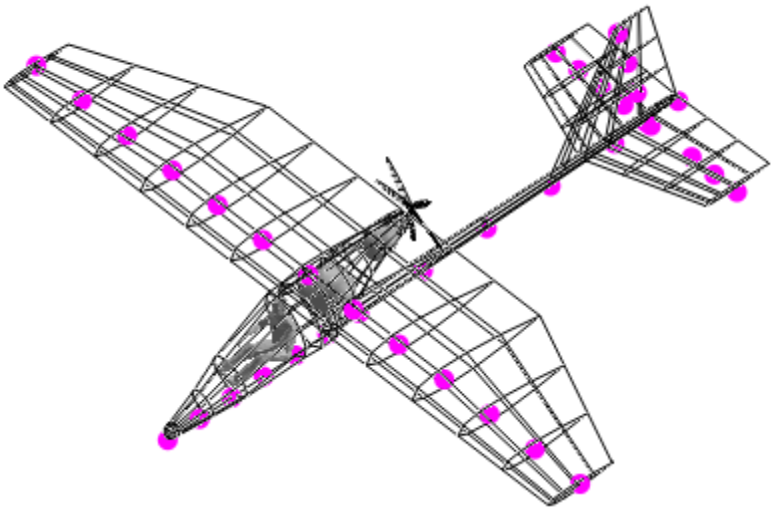

Figure 2-14: Lumped Mass Points on the Aircraft Structure

The distributed structure and system mass values at those station points (which are measured with respect to aircraft axis system as given in Figure 2-2) are calculated and tabulated in Table 2-6.

Table 2-6: Structure and System Mass Distribution at Station Points

Station	x [m]	y [m]	z [m]	Structure Mass [kg]	Systems Mass [kg]
FF1	-2	0	-0.9	0.709	2.1
FF2	-1	0	-0.75	2.127	8.6
FF3	0	0	-0.5	4.254	4.6
FF4	0.5	0	-0.5	2.836	5.1
FF5	1	0	-0.25	2.836	4.6
FF6	2	0	-0.1	1.418	22.6
RF1	0.5	0	-0.9	1.268286	0.04

Table 2-6 (Continued)

RF2	1	0	-0.9	1.213143	0.03
RF3	2	0	-0.9	1.158	0.03
RF4	3	0	-0.9	1.102857	0.03
RF5	4	0	-0.9	1.047714	0.03
RF6	5	0	-0.9	0.992571	0.03
RF7	6	0	-0.9	0.937429	0.03
WR1	0.5	0	0	3.06125	0.02
WR2	0.5	1	0	3.7525	0.02
WR3	0.5	2	0	3.7525	0.02
WR4	0.5	3	0	3.3575	0.02
WR5	0.5	4	0	2.46875	0.04
WR6	0.5	5	0	1.975	0.04
WR7	0.5	6	0	1.3825	0.04
WL1	0.5	0	0	3.18	0.02
WL2	0.5	-1	0	3.7725	0.02
WL3	0.5	-2	0	3.67375	0.02
WL4	0.5	-3	0	3.3775	0.02
WL5	0.5	-4	0	2.50875	0.04
WL6	0.5	-5	0	2.015	0.04
WL7	0.5	-6	0	1.4225	0.04
HR1	5.3	0	-1	1.488	0.02
HR2	5.3	0.5	-1	1.24	0.02

Table 2-6 (Continued)

HR3	5.3	1	-1	0.992	0.02
HR4	5.3	1.5	-1	0.744	0.04
HR5	5.3	2	-1	0.496	0.01
HR1	5.3	0	-1	1.488	0.02
HR2	5.3	-0.5	-1	1.24	0.02
HR3	5.3	-1	-1	0.992	0.02
HR4	5.3	-1.5	-1	0.744	0.04
HR5	5.3	-2	-1	0.496	0.01
VT1	5.5	0	-1	1.6345	0.01
VT2	5.5	0	-0.5	1.28425	0.02
VT3	5.5	0	0	1.05075	0.02
VT4	5.5	0	0.5	0.7005	0.01

The structure and system mass distribution along main aircraft components such as front fuselage or wing can be visualized in Figure 2-15 and 2-16.

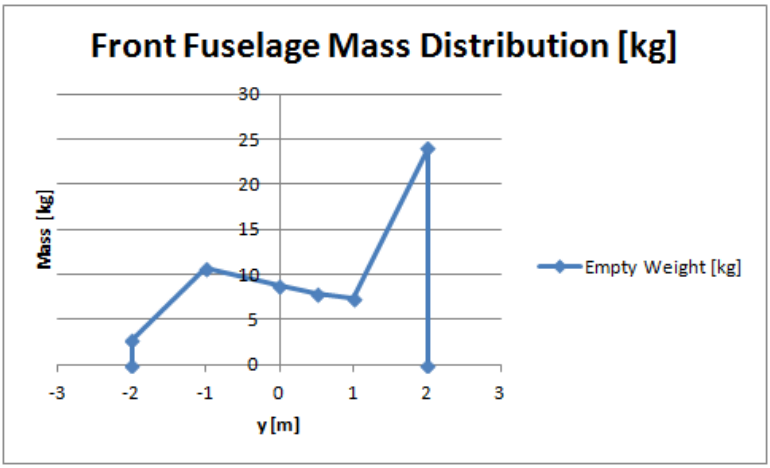

Figure 2-15: Front Fuselage Mass Distribution

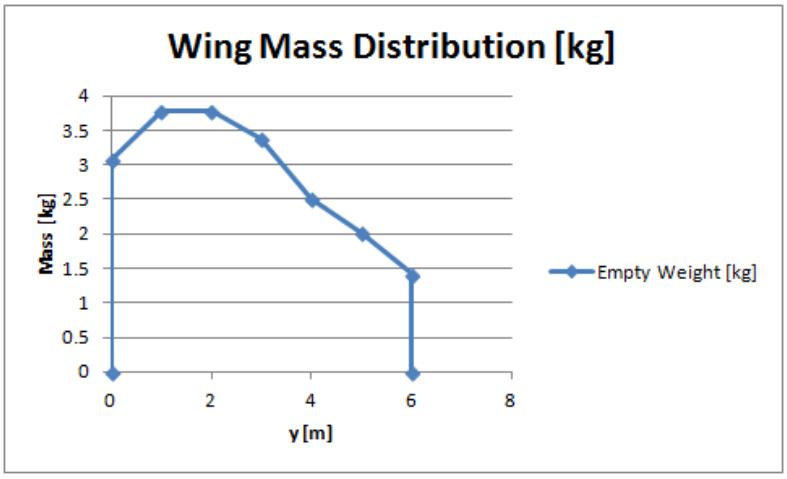

Figure 2-16: Wing Mass Distribution

The load factor, angular velocities and angular accelerations at each lumped mass point are multiplied by mass and inertia properties to calculate the inertial loads acting on the structures.

2.5 Aircraft Structural Model

With the basic structural layout of the aircraft being designed, the structural model of the aircraft can be generated using the initial sizing data of the structural components. The structural model consists of sectional stiffness values, which are mainly bending and torsional stiffness. This model, as mentioned in previous chapter, is called stick model or beam model of the aircraft. The beam model of the aircraft is illustrated in Figure 2-17.

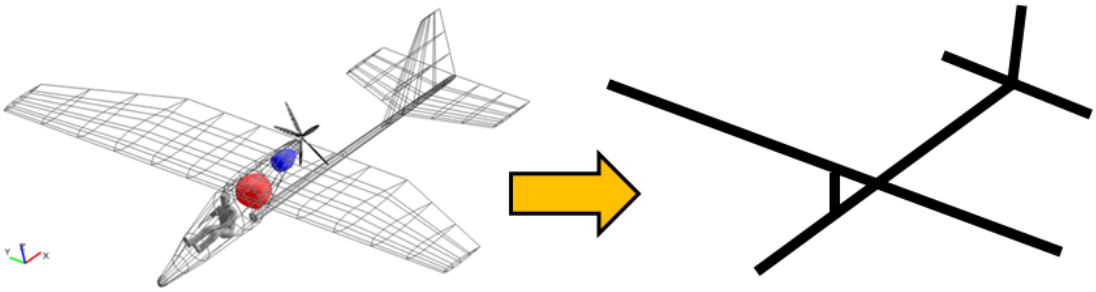

Figure 2-17: Beam Model Representation of the Aircraft Structural Model

The idealized structural model is prepared by the calculation of the second moments of inerti at the station points along the components. For instance, the wing structure can be idealized as shown in Figure 2-18:

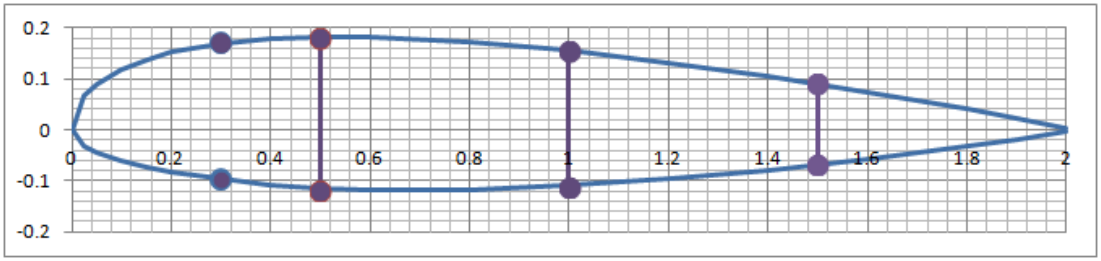

Figure 2-18: Wing Structural Layout

Using preliminary sizing data such as skin thicknesses, spar cap dimensions, spar web thicknesses and other design parameters, the second moments of inertia are calculated at each section, in order to evaluate sectional bending and torsional stiffness. For instance, at wing root, moments of inertia are calculated using equation 2-11.

$$I_{xx_{section}} = I_{xx_{skin}} + I_{xx_{stiffeners}} + I_{xx_{spar\ caps}} + I_{xx_{spar\ webs}} \quad (2.\ 11)$$

The contribution of wing skin to total moment of inertia is neglected since the aircraft has a very thin skin which is likely to buckle and lose its stiffness under bending loads. Hence the bending moment of inertia is simply calculated by taking spar caps, spar webs and stiffeners into account. Table 2-7 gives the moment of inertia values of each element of the wing root cross-section.

Table 2-7: Moment of Inertia Calculation of the Wing Section

Element	y [m]	y2 [m2]	Area [m2]	Ix'x'	Ixx
Stiffener 1	0.16	0.0256	0.00002256	-	5.78E-07
Stiffener 2	-0.1	0.01	0.00002256	-	2.26E-07
Spar Cap 1	0.16	0.0256	0.00004512	-	1.16E-06
Spar Cap 2	-0.12	0.0144	0.00004512	-	6.50E-07
Spar Cap 3	0.14	0.0196	0.00004512	-	8.84E-07
Spar Cap 4	-0.12	0.0144	0.00004512	-	6.50E-07
Spar Cap 5	0.072	0.005184	0.00004512	-	2.34E-07
Spar Cap 6	-0.095	0.009025	0.00004512	-	4.07E-07
Spar Web 1	-	-	-	5.74E-08	5.74E-08
Spar Web 2	-	-	-	5.74E-08	5.74E-08
Spar Web 3	-	-	-	5.74E-08	5.74E-08
				TOTAL	4.96E-06

Torsional moment of inertia is simply calculated by using the simple formula given in Equation 2-12.

$$J_{section} = \frac{4tA^2}{S} \tag{2. 12}$$

where A is the area of the closed thin walled rectangular section, t is the wall thickness and S is the perimeter.

Similar calculation is performed for all sections. Table 2-8 gives the stiffness distribution along the components at each station. Note that the first two letters in station codes represents the corresponding aircraft components, such as RF for rear fuselage, WR for right wing, HL for left horizontal tail and VT for vertical tail.

Table 2-8: Sectional Moment of Inertia Values

Station	x [m]	y [m]	z [m]	Iyy, Izz [m4]	Jxx [m4]
RF1	0.5	0	-0.9	6.91E-06	1.38E-05
RF2	1	0	-0.9	5.09E-06	1.02E-05
RF3	2	0	-0.9	4.19E-06	8.37E-06
RF4	3	0	-0.9	3.64E-06	7.28E-06
RF5	4	0	-0.9	3.09E-06	6.19E-06
RF6	5	0	-0.9	2.18E-06	4.37E-06
RF7	6	0	-0.9	3.64E-07	7.28E-07
Station	x [m]	y [m]	z [m]	Ixx [m4]	Jyy [m4]
WR1	0.5	0	0	4.96E-06	3.41E-05
WR2	0.5	1	0	4.56E-06	3.24E-05
WR3	0.5	2	0	4.26E-06	3.13E-05

Table 2-8 (Continued)

WR4	0.5	3	0	3.92E-06	2.69E-05
WR5	0.5	4	0	2.23E-06	1.93E-05
WR6	0.5	5	0	1.09E-06	9.50E-06
WR7	0.5	6	0	2.97E-07	4.05E-06
WL1	0.5	0	0	4.96E-06	3.41E-05
WL2	0.5	-1	0	4.56E-06	3.24E-05
WL3	0.5	-2	0	4.26E-06	3.13E-05
WL4	0.5	-3	0	3.92E-06	2.69E-05
WL5	0.5	-4	0	2.23E-06	1.93E-05
WL6	0.5	-5	0	1.09E-06	9.50E-06
WL7	0.5	-6	0	2.97E-07	4.05E-06
HR1	5.3	0	-1	7.89E-07	5.83E-06
HR2	5.3	0.5	-1	6.18E-07	5.15E-06
HR3	5.3	1	-1	4.50E-07	4.19E-06
HR4	5.3	1.5	-1	2.53E-07	2.24E-06
HR5	5.3	2	-1	5.52E-08	3.90E-07
HL1	5.3	0	-1	7.89E-07	5.83E-06
HL2	5.3	-0.5	-1	6.18E-07	5.15E-06
HL3	5.3	-1	-1	4.50E-07	4.19E-06
HL4	5.3	-1.5	-1	2.53E-07	2.24E-06
HL5	5.3	-2	-1	5.52E-08	3.90E-07
Station	x [m]	y [m]	z [m]	Ixx [m4]	Jzz [m4]

Table 2-8 (Continued)

VT1	5.5	0	-1	1.08E-06	7.84E-06
VT2	5.5	0	-0.5	7.90E-06	5.53E-06
VT3	5.5	0	0	3.46E-06	2.18E-06
VT4	5.5	0	0.5	1.19E-07	8.09E-07

This simplified structural model can also be used for the preliminary structural analysis and optimization [42].

CHAPTER 3

LOAD CASES

3.1 Requirements

In order to generate the load cases at which the load calculations are performed, the requirements have to be established. The requirements for the aircraft analyzed in this study are mainly taken from certification specifications. There are no additional project requirements that necessitate flight or ground conditions other than those specified in the regulations.

The aircraft designed for this study complies with ultralight specifications both domestically and internationally. It is decided to use the Turkish certification and airworthiness regulations for ultralight aircraft, which are quite similar to international specifications. Domestic and international specifications are also prepared in conjunction with each other, with similar paragraphs. For instance, roll maneuver conditions are specified in TR-UL 349, CS-22.349, CS-VLA.349, CS-23.349, FAR-23.349, CS-25.349 and FAR-25.359, in the same paragraph with similar requirements.

3.2 Configurations and Mass States

The aircraft studied in this thesis does not have any high lift devices, spoilers or retractable landing gear; hence it has only one configuration.

Aircraft weights are calculated in Chapter 2 and summarized in Table 3-1.

Table 3-1: Aircraft Weights

Mass State	Payload
Empty Weight	124.5 kg
Fuel Capacity	50 kg
Payload Weight	20 kg
Crew Weight	70 – 100 kg
MTOW	294.5 kg

Mass states are tabulated in Table 3-2.

Table 3-2: Mass States

Mass State	Crew	Fuel	Payload	Mass [kg]	CG [m]
MS01	70 kg	0	0	194.49	0.72749
MS02	70 kg	0	20 kg	214.49	0.682966
MS03	70 kg	25 kg	0	219.49	0.730054
MS04	70 kg	25 kg	20 kg	239.49	0.689964
MS05	70 kg	50 kg	0	244.49	0.732093
MS06	70 kg	50 kg	20 kg	264.49	0.695639
MS07	100 kg	0	0	224.49	0.563453
MS08	100 kg	0	20 kg	244.49	0.537811

Table 3-2 (Continued)

MS09	100 kg	25 kg	0	249.49	0.582145
MS10	100 kg	25 kg	20 kg	269.49	0.557496
MS11	100 kg	50 kg	0	274.49	0.597433
MS12	100 kg	50 kg	20 kg	294.49	0.573838

It is possible to prepare a weight – CG envelope of the aircraft, and include those mass states in the envelope, as given in Figure 3-1.

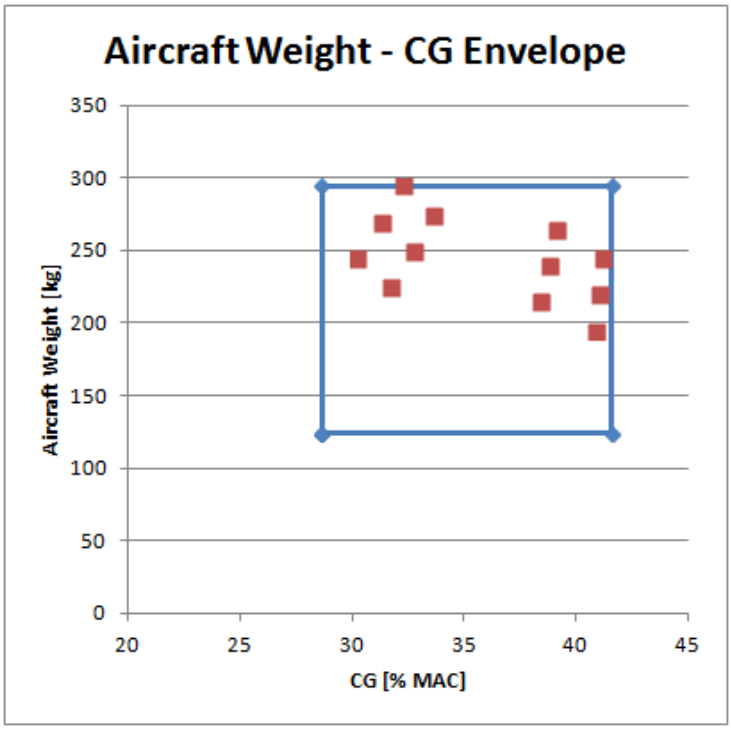

Figure 3-1: Aircraft Weight - CG Envelope with Mass States

3.3 Airspeeds and Altitudes

Design airspeeds of the aircraft are calculated according to both project and certification requirements. Certification requirements for airspeeds are detailed in Paragraph 335 of TR-UL specifications.

Calculation of those airspeeds can be performed as follows:

Stall Speed, V_S: This speed depends on the aerodynamic and mass properties of the aircraft and calculated to be 12 m/s.

Design Maneuvering Speed, V_A: This speed is basically $V_S*(n)^{1/2}$, where n is the maximum load factor and 4 for the aircraft in this thesis study. Hence V_A is calculated to be 24 m/s.

Gust Speed, V_B: According to TR-UL-335, gust speed can be decided by the designer, however, it needs not be less than $0.9V_H$ or V_A, whichever is greater. Therefore it is calculated to be 31.5 m/s, which is $0.9V_H$.

Cruise Speed V_C: It can be taken as V_H, since there is no constraint according to ultralight specifications.

Maximum Speed VH: It is chosen that he aircraft has a maximum level speed of 35 m/s.

Dive Speed VD: TR-UL-335 states that the dive speed need not be less than $1.2V_H$ of $1.5V_A$, whichever is greater. Hence, the dive speed is calculated to be 42 m/s, which is $1.2V_H$.

The design airspeeds for the aircraft are summarized in Table 3-3.

Table 3-3: Aircraft Design Airspeeds

Airspeed	Description	Velocity (Equivalent Airspeed, EAS)
V_S	Stall Speed	12 m/s (44 km/h)
V_A	Design Maneuvering Speed	24 m/s (88 km/h)
V_B	Gust Speed	32 m/s (113 km/h)
V_C	Cruise Speed	35 m/s (126 km/h)
V_H	Maximum Speed	35 m/s (126 km/h)
V_D	Dive Speed	42 m/s (151 km/h)

Maximum altitude of the aircraft is limited by the oxygen requirements for the pilot, since there is no pressurization and oxygen system in the aircraft. It is generally accepted that the maximum altitude for aircraft operation without supplemental oxygen is around 13000 feet [43].

3.4 Load Factors

Limit load factors of the aircraft are defined to be +4 g / -2 g by project requirements. These load factor limits are also dictated to be the minimum requirements for TR-UL certification specifications.

Gust load factors are also defined in TR-UL, and similar to CS-23 and CS-25 specifications. The gust load factor increments are calculated according to Equation 3-1.

$$n = 1 + \frac{k\frac{1}{2}\rho_0 v_\infty u_g c_{L_\alpha}}{\frac{mg}{S}} \tag{3. 1}$$

where k is the gust alleviation factor, u_g is the gust speed, v_∞ is the aircraft speed, c_{L_α} is the lift curve slope of the aircraft, g is the gravitational acceleration, m is the mass of the aircraft, ρ_0 is the density of air at sea level and S is the wing area. The gust alleviation factor is calculated according to TR-UL by using Equation 3-2.

$$k = \frac{0.88\mu}{5.3 + \mu} \tag{3. 2}$$

The value of μ is also calculated according to TR-UL and its formula is given in Equation 3-3.

$$J_{section} = \frac{2\frac{m}{S}}{\rho_0 c c_{L_\alpha}} \tag{3. 3}$$

where c is the mean geometric chord of the wing.

Using the airspeeds derived in the previous section, the load factor limits and the gust formula, it is possible to prepare a V-n diagrams at different altitudes as given in Figure 3-2 and 3-3.

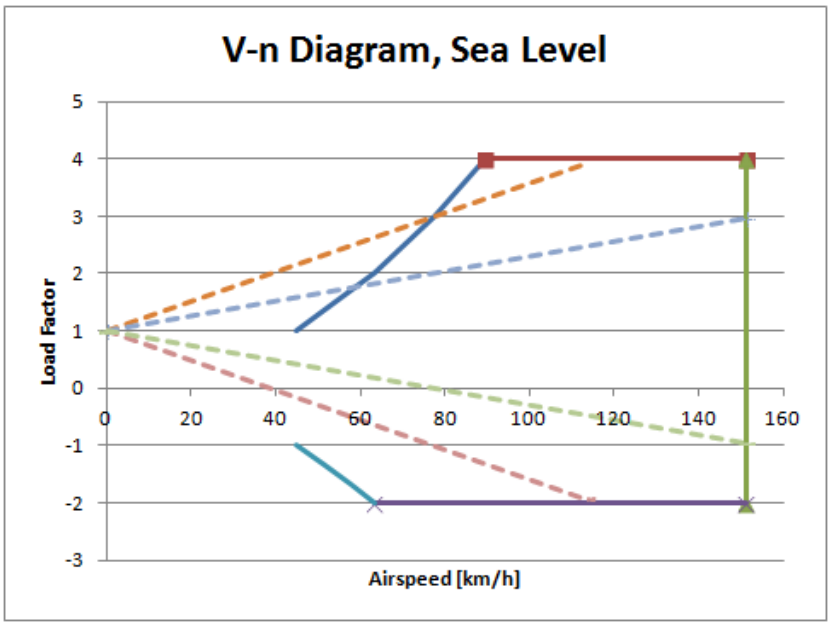

Figure 3-2: V-n Diagram of the Aircraft with Gust Lines at Sea Level

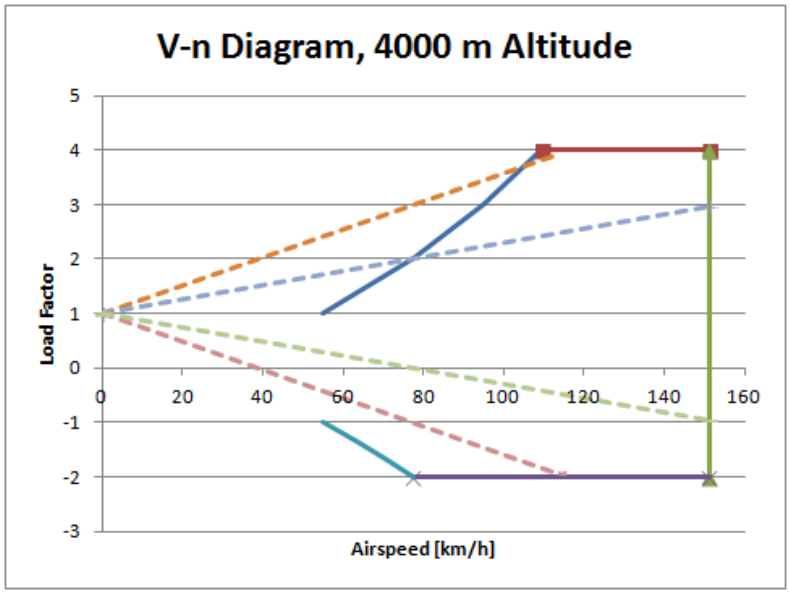

Figure 3-3: V-n Diagram of the Aircraft with Gust Lines at 4000 m Altitude

The dashed lines plotted in the V-n diagram are the gust lines which are specified in specifications. Gust lines represent the load factor increment resulting from vertical

positive and negative gusts of 15 m/s and 7.5 m/s speeds, as stated in the corresponding paragraphs of certification specifications, such as TR-UL 333.

3.5 Flight Conditions and Maneuvers

Similar to large aircraft (CS-25, FAR-25) and light aircrafts (CS-23, FAR-23), the flight conditions such as maneuvers and gusts are detailed in the certification specifications which the aircraft of this study is designed to comply. Flight loads are covered between Paragraph 321 – Paragraph 471 of the airworthiness and certification regulations.

3.5.1 Symmetrical Maneuvers

Symmetrical maneuvers are covered in TR-UL-331 as with other international regulation. It dictates that the symmetrical maneuvers to be performed for the airspeeds and load factors (both maneuver and gust) which are defined in subsequent paragraphs. TR-UL-331 also allows excluding the angular acceleration effects in the calculation of loads during symmetrical maneuvers, hence allowing them to be analyzed as balanced maneuvers.

Therefore, the loads are required to be analyzed at V_A and V_D at maximum and minimum load factors. Also static gust conditions must be analyzed at V_B with gust speeds of 7.5 m/s at V_D and 15 m/s, according to Paragraph 341.

Pitching cases, on the other hand, are specified for the analysis of loads on the horizontal tails, as stated in Paragraph 423.

The symmetrical flight conditions, required to be analyzed for the aircraft studied in this work, is listed in Table 3-4.

Table 3-4: Symmetrical Design Conditions for the Ultralight Aircraft

Symmetrical Flight Condition	TR-UL Paragraph
Maximum N_Z at V_A	331
Minimum N_Z at V_A	331
Maximum N_Z at V_D	331
Minimum N_Z at V_D	331
Upward 15 m/s Gust at V_B	341, 425
Downward 15 m/s Gust at V_B	341, 425
Upward 7.5 m/s Gust at V_D	341, 425
Downward 7.5 m/s Gust at V_D	341, 425
Pitching with Max. Up Elevator at V_A	423
Pitching with Max. Down Elevator at V_A	423
Pitching with 1/3 Up Elevator at V_D	423
Pitching with 1/3 Down Elevator at V_D	423

3.5.2 Unsymmetrical Maneuvers

Unsymmetrical maneuvers are regulated in Paragraph 347 of those regulations. Requirements for rolling maneuver are specified in Paragraph 349 whereas the yawing conditions are specified in Paragraph 351.

According to TR-UL 349 (and TR-UL 455 which is being referred), the aircraft must be designed for the loads at 2/3 of the maximum load factor combined with either full aileron deflection at V_A or 1/3 aileron deflection at V_D.

For the yawing conditions, TR-UL 351 states that the conditions in Paragraph 441 must be considered. Those conditions are, similar to rolling maneuvers, full rudder deflection at V_A or 1/3 rudder deflection at V_D.

In addition to yawing, TR-UL 443 also specifies the lateral gust conditions similar to vertical gusts, for the analysis of vertical tail. They can also be taken into account for the aircraft loads calculation.

All unsymmetrical conditions that the ultralight aircraft needs to be analyzed are listed in Table 3-5.

Table 3-5: Unsymmetrical Flight Conditions for the Ultralight Aircraft

Unsymmetrical Flight Condition	TR-UL Paragraph
Right Roll with Max. Aileron at V_A at 2.66 g	349, 455
Left Roll with Max. Aileron at V_A at 2.66 g	349, 455
Right Roll with 1/3 Aileron at V_D at 2.66 g	349, 455
Left Roll with 1/3 Aileron at V_D at 2.66 g	349, 455
Right Yaw with Max. Rudder at V_A	351, 441
Left Yaw with Max. Rudder at V_A	351, 441
Right Yaw with 1/3 Rudder at V_D	351, 441
Left Yaw with 1/3 Rudder at V_D	351, 441
Right 15 m/s Gust at V_B	443
Left 15 m/s Gust at V_B	443
Right 7.5 m/s Gust at V_D	443
Left 7.5 m/s Gust at V_D	443

3.6 Ground Conditions

In the certification specifications and regulations, the conditions are specified for the ultralight aircraft for landing, taxiing and ground handling although they are not as detailed as in FAR/CS-23 and FAR/CS-25. Since they require modeling of the landing gear and these loads are generally used for the sizing of local structure around landing gears and not for the aircraft in general, they are skipped in this study.

3.7 Load Cases Table

Load cases for the aircraft are generated by rational combination of the airspeeds, altitudes, mass states and flight and ground conditions that are derived in previous sections. After combining those parameters, a massive load case table is produced to summarize all load cases. It is included in the Appendix B. A portion of the load case table is given in Table 3-6.

Table 3-6: A Portion of Load Case Table

Load Case	Condition	Cert. Spec.	Mass State	Altitude [m]
LC001	Criuse with 1 g at VC	331	MS01	0
LC002	Maximum NZ at VA	331	MS01	0
LC003	Minimum NZ at VA	331	MS01	0
LC004	Maximum NZ at VD	331	MS01	0
LC005	Minimum NZ at VD	331	MS01	0
LC006	Upward 15 m/s Gust at VB	341, 425	MS01	0
LC007	Downward 15 m/s Gust at VB	341, 425	MS01	0
LC008	Upward 7.5 m/s Gust at VD	341, 425	MS01	0
LC009	Downward 7.5 m/s Gust at VD	341, 425	MS01	0
LC010	Pitching with Max. Up Elevator at VA	423	MS01	0

Table 3-6 (Continued)

LC011	Pitching with Max. Down Elevator at VA	423	MS01	0
LC012	Pitching with 1/3 Up Elevator at VD	423	MS01	0
LC013	Pitching with 1/3 Down Elevator at VD	423	MS01	0
LC014	Right Roll with Max. Aileron at 2.66 g at VA	349, 455	MS01	0
LC015	Left Roll with Max. Aileron at 2.66 g at VA	349, 455	MS01	0
LC016	Right Roll with 1/3 Aileron at 2.66 g at VD	349, 455	MS01	0
LC017	Left Roll with 1/3 Aileron at 2.66 g at VD	349, 455	MS01	0
LC018	Right Yaw with Max. Rudder at VA	351, 441	MS01	0
LC019	Left Yaw with Max. Rudder at VA	351, 441	MS01	0
LC020	Right Yaw with 1/3 Rudder at VD	351, 441	MS01	0
LC021	Left Yaw with 1/3 Rudder at VD	351, 441	MS01	0
LC022	Right 15 m/s Gust at VB	443	MS01	0
LC023	Left 15 m/s Gust at VB	443	MS01	0
LC024	Right 7.5 m/s Gust at VD	443	MS01	0
LC025	Left 7.5 m/s Gust at VD	443	MS01	0
LC026	Cruise with 1 g at VC	331	MS07	0
LC027	Maximum NZ at VA	331	MS07	0

Thousands of load cases can be created with all possible combinations of altitudes, mass states, airspeeds and flight conditions. For this study, however, it is enough to generate about 200 load cases to cover all of flight regime with major mass states and altitudes. Also these load cases are enough to comply with the certification and airworthiness specifications.

CHAPTER 4

AIRCRAFT LOADS CALCULATIONS

With the load cases created to cover all flight and ground conditions, mass states, altitudes, airspeeds, etc. with respect to project and certification requirements, the calculation of loads for each of these load cases can be performed.

A simple flowchart is prepared to detail the airload and inertial load calculation process and given in Figure 4-1.

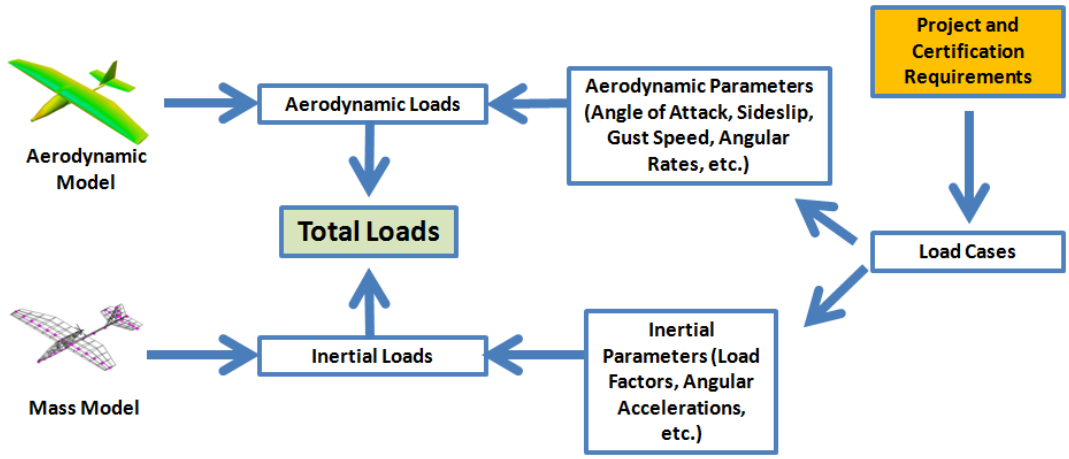

Figure 4-1: Load Calculation Process of Aerodynamic and Inertial Loads

An integration operation is generally the most straightforward way to calculate load distributions along the major aircraft structures, such as wings, fuselage and tail surfaces; as outlined in Figure 4-2.

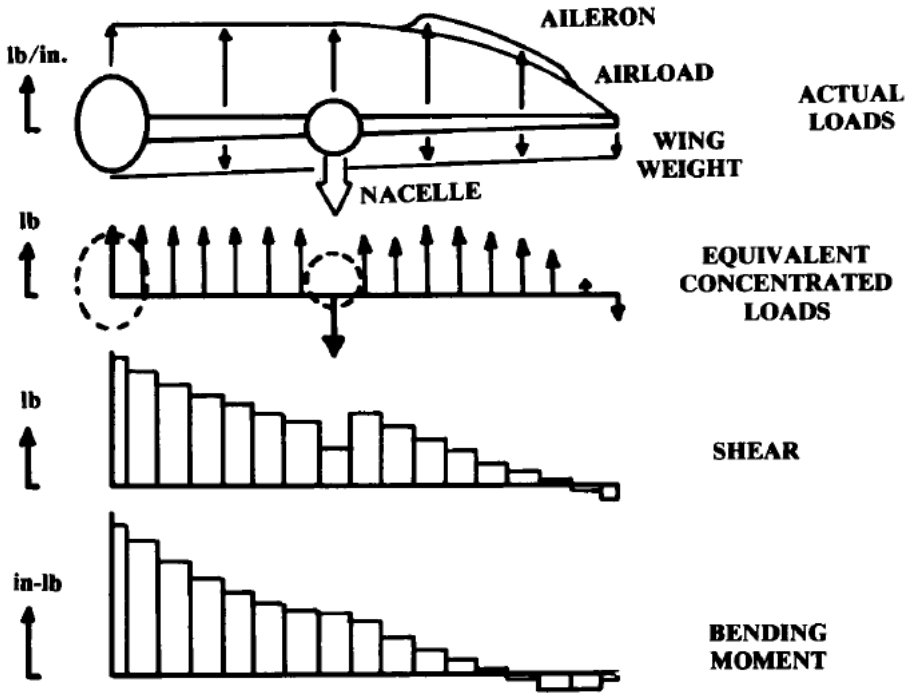

Figure 4-2: Integration of Airloads and Inertial Loads along the Aircraft [12]

In this study, a code is written to automate the calculation of aerodynamic and inertial loads on the aircraft and integrate these loads along the components.

For instance, the airload distribution, inertial load distribution and total loads distribution along the wing for load case LC79, which is a maximum NZ pull-up maneuver at dive speed at maximum take-off weight are calculated and given in Figure 4-3.

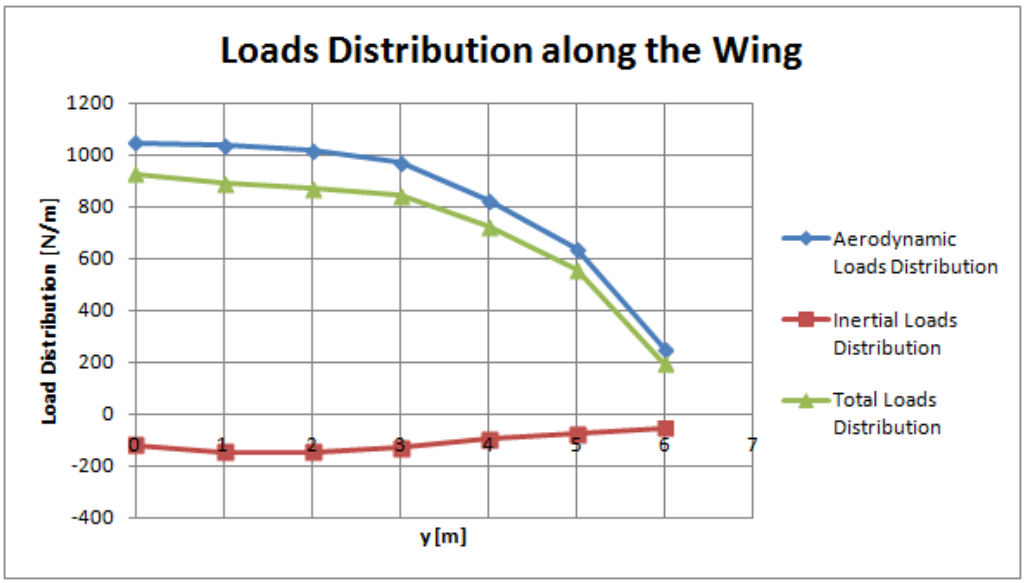

Figure 4-3: Loads Distributions along the Wing for LC79

After the calculation of aerodynamic, inertial and total load distributions along the wing, the distribution is integrated twice to obtain shear and bending moment diagrams, as given in Figures 4-4 and 4-5.

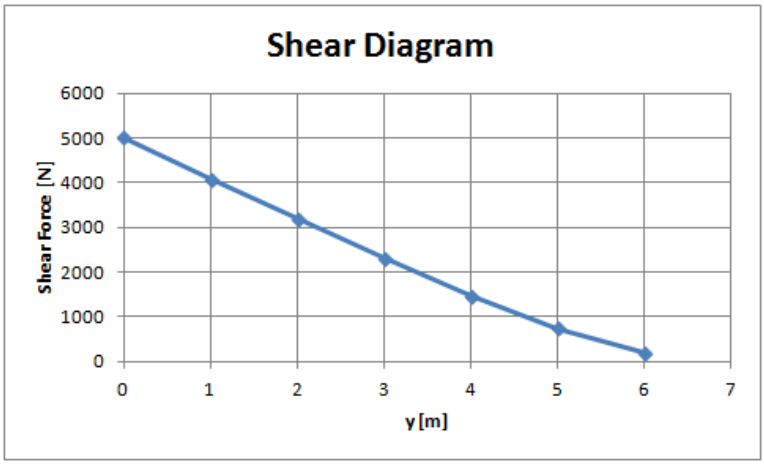

Figure 4-4: Shear Diagram along the Wing for LC79

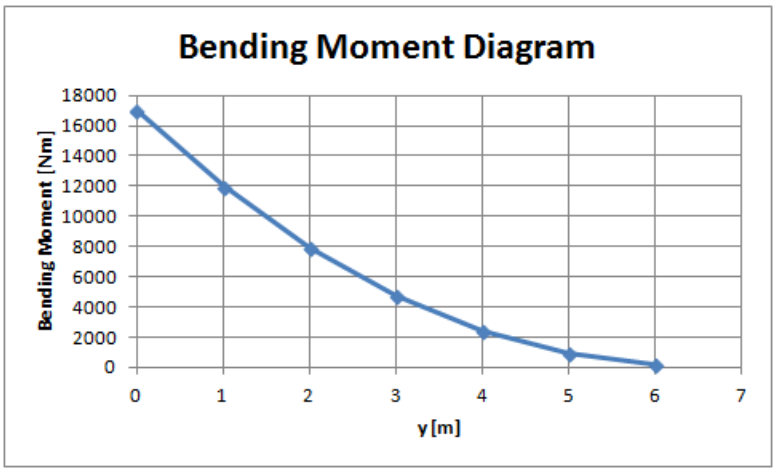

Figure 4-5: Bending Moment Diagram along the Wing for LC79

After the calculation of shear and moment distribution along the components, it becomes possible to evaluate structural deformations using the structural model. The bending deflections of the components are calculated by idealization of Euler-Bernoulli beam as given in Equations 4.1.

$$\frac{\partial^2}{\partial y^2}\left(EI(y)\frac{\partial^2 w(y)}{\partial y^2}\right) = q(y) \tag{4.1}$$

The torsional deflections of each section along the aircraft component are calculated similarly using Equation 4.2, which is torsional deflection of the beam formula.

$$\frac{\partial}{\partial y}\left(GJ(y)\frac{\partial \theta}{\partial y}\right) = T(y) \tag{4.2}$$

For the static aeroelastic analysis, the loads and deformations can be calculated at each section, then with the loads changing due to twisting effects and local angle of attacks, the deformations due to updated loads can be evaluated as a result of coupled aerodynamic and structural analysis. This coupling is illustrated in Figure 4-3.

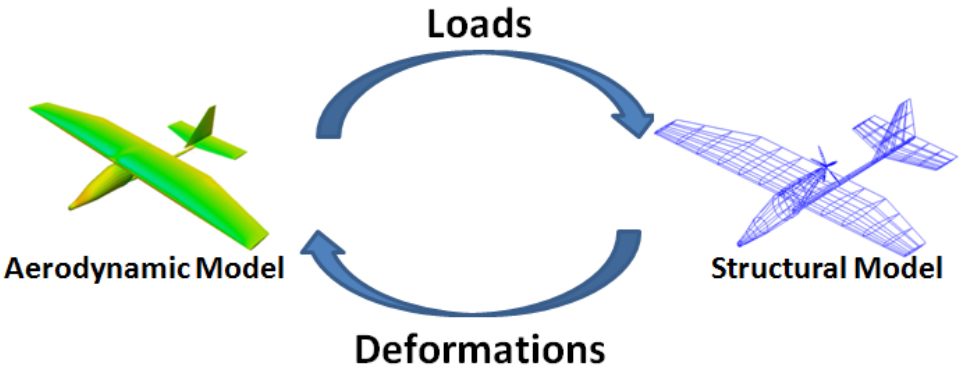

Figure 4-6: Static Aeroelastic Analysis as Coupled Aero-Structural Calculations

To comply with the aim of this study, the aerodynamic and structural models of the aircraft are simplified into analytical aerodynamic models and structural beam models. The static aeroelastic calculations are illustrated in Figure 4-4 after these simplifications and idealizations.

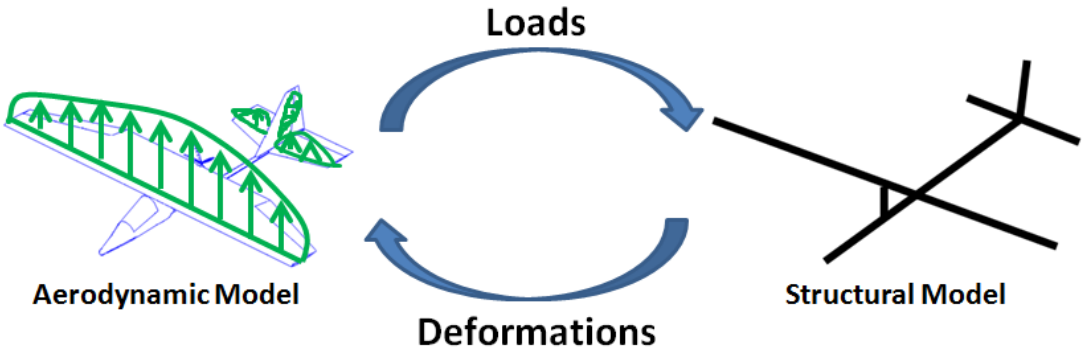

Figure 4-7: Static Aeroelastic Analysis with Simplified Models

Appendix C gives a more comprehensive flowchart for the flexible load analysis.

Also, the divergence speed can be obtained by analytical means for an airfoil section. Equation 4.2 gives the dynamic pressure at which divergence occurs on the wing section [4].

$$q_{div} = \frac{K_\theta}{ec^2 c_{l_\alpha}} \tag{4.3}$$

where K_θ is the torsional stiffness of the section, e is the chordwise location of elastic axis, c is the sectional chord and c_{l_α} is the lift curve slope at the section. K_θ value can be taken as sectional GJ for the sake of simplicity. In this study, the result obtained from this equation is also compared with the result from the iterative solution of aero-structural models at a given flight case.

The static aeroelastic analyses, however, are not needed to be performed with respect to certification and airworthiness regulations for ultralight aircraft. Nonetheless, they are calculated in this thesis study with most critical load cases, in order to investigate loads redistribution and divergence.

CHAPTER 5

LOADS POST-PROCESSING AND RESULTS

The results of the load analysis are mainly the load distribution along the components. These distributions can be visualized by the loads envelopes, mainly 1D loads envelopes. Loads envelopes are basically shear and moment diagrams that are used for both the selection of the critical load cases and the evaluation of critical loads. Especially during the preliminary design phase the load values from these diagrams are directly used for the structural analysis and sizing of main aircraft components. In the later stages in design, however, critical load cases are still selected from the envelopes, whereas the load values are taken from mainly 3D analyses according to critical load cases.

After the calculation of the loads, which are the loads with flexibility effects, on the aircraft, the post-process activities are performed in this chapter. These activities are generation of loads envelopes, selection of critical cases and evaluation of critical loads.

However, loads envelopes consist of two hundred loads cases. The legend for loads envelopes is prepared in Figure 5-1.

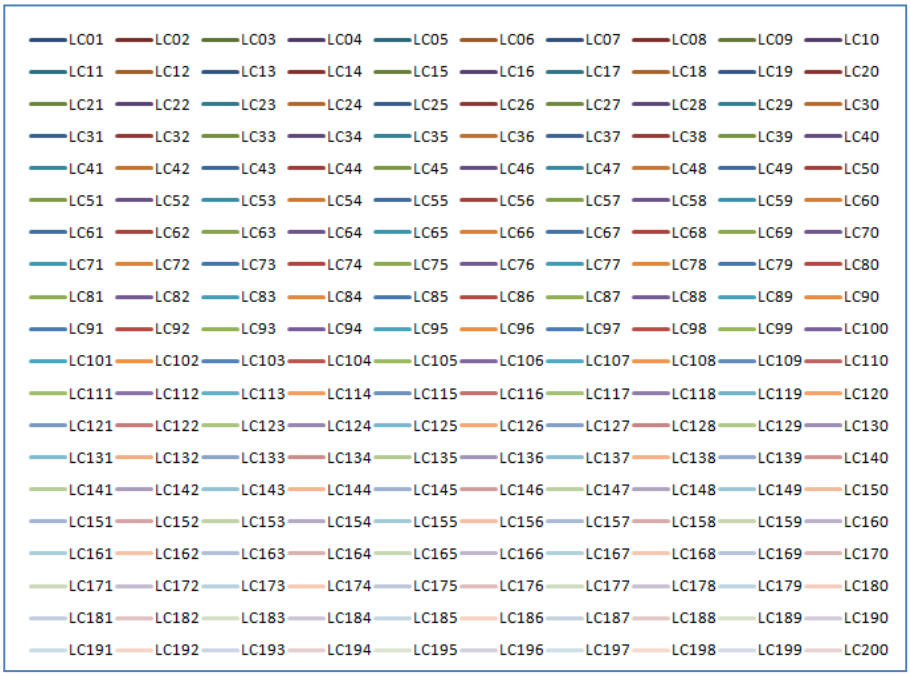

Figure 5-1: Load Case Colour Map for Loads Envelopes

5.1 Loads and Critical Cases for the Wing

The load envelopes for the wing are prepared and given in Figures 5-2, 5-3 and 5-4.

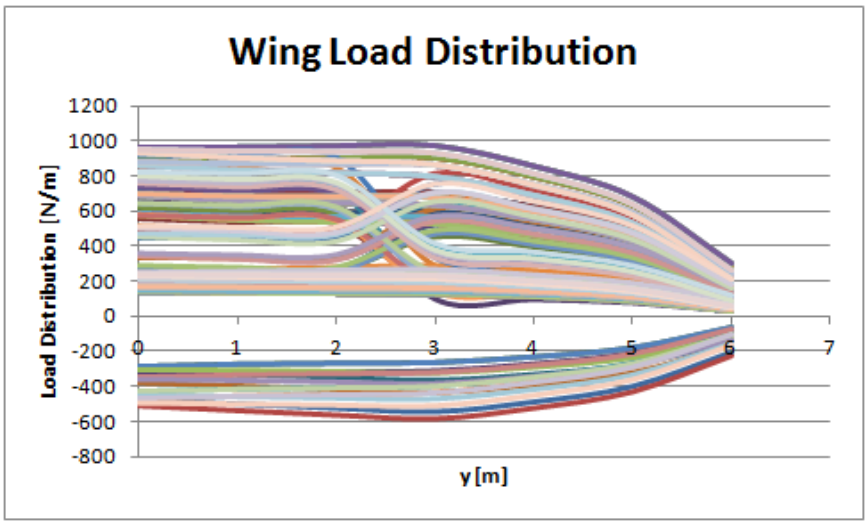

Figure 5-2: Wing Load Distribution

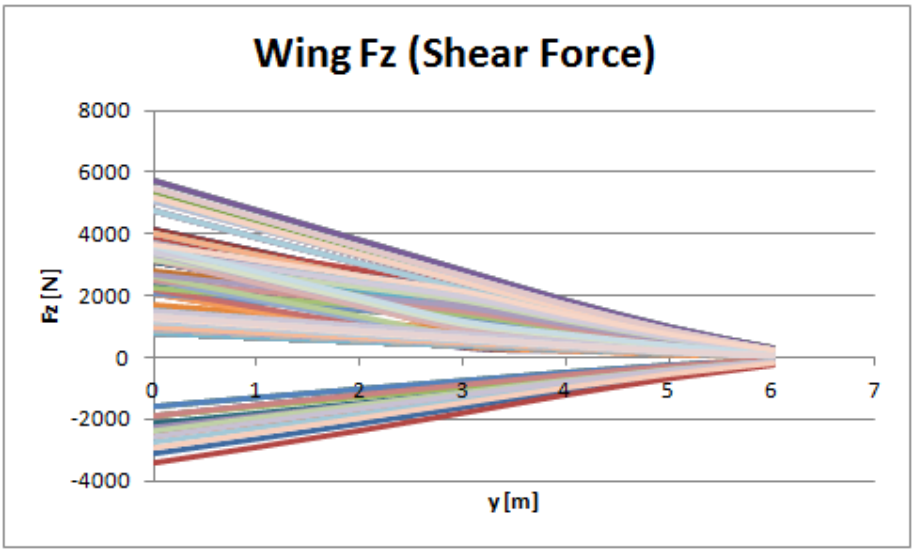

Figure 5-3: Wing Shear Force Distributiom

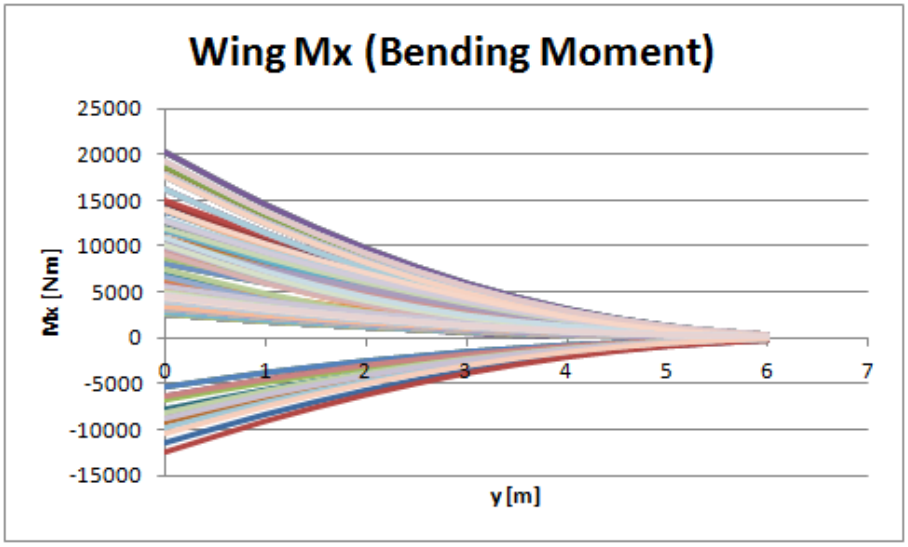

Figure 5-4: Wing Bending Moment

The load envelopes for the wing are examined and the critical loads for the wing are selected. The selection criteria is decided to be the wing root bending moment. These critical load cases are given in Table 5-1.

Table 5-1: Critical Load Cases for the Wing

Load Case	Case Description	Wing Root Bending Moment [Nm]
LC079	Maximum NZ at VD	20246.6
LC087	Pitching with 1/3 Up Elevator at VD	20246.6
LC080	Minimum NZ at VD	-12459.7
LC055	Minimum NZ at VD	-11521.4

Three cases are found critical for the wing, LC079, LC087, LC080 and LC055. Although the roll cases do not result in high force and moment values at the wing root, they become critical near the wing tip.

Wing torsional moments are also evaluated. The load envelope for wing torsion is prepared and given in Figure 5-5.

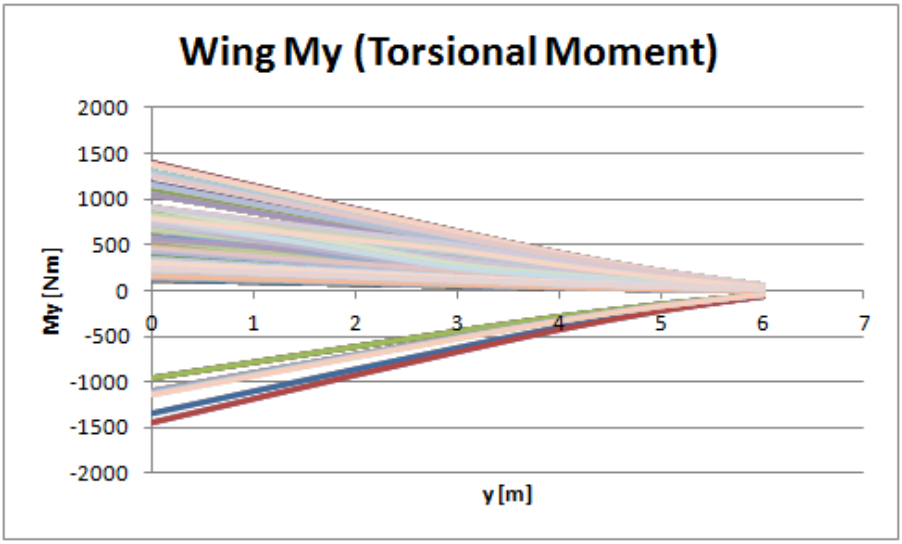

Figure 5-5: Wing Torsional Moment Distribution

The critical cases for wing torsion are given in Table 5-2.

Table 5-2: Critical Cases for the Wing Torsion

Load Case	Case Description	Torsion at Wing Root [Nm]
LC077	Maximum NZ at VA	1397.6
LC085	Pitching with Max. Up Elevator at VA	1397.6
LC080	Minimum NZ at VD	-1482.1
LC055	Minimum NZ at VD	-1381.4

2-D load envelopes for wing bending and torsional moment at wing root are also prepared and can be shown in Figure 5-6.

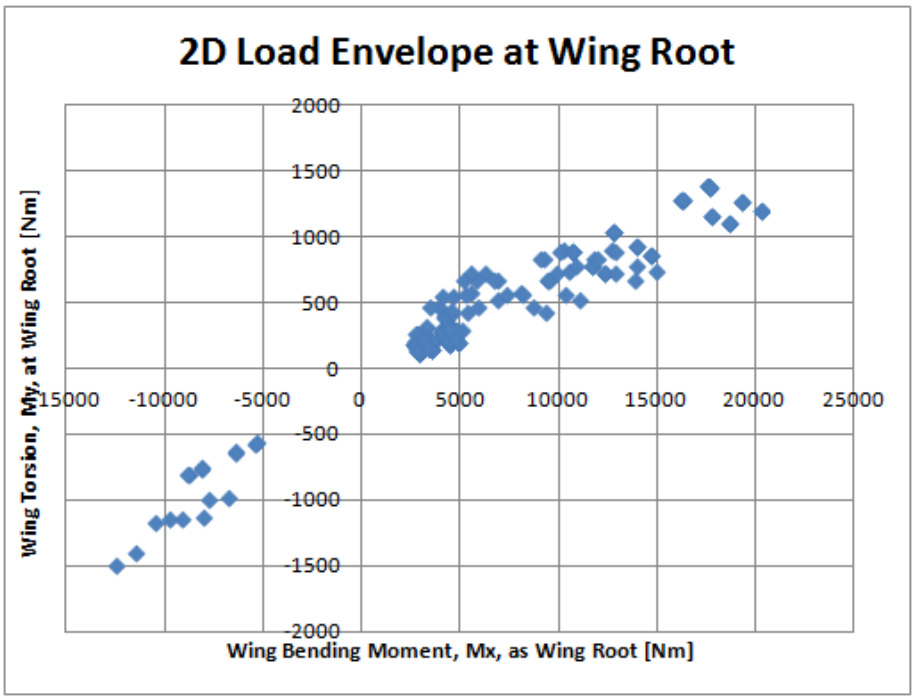

Figure 5-6: Wing Bending and Torsional Moment at Wing Root

The difference between maximum bending moment loads calculated with flexibility effects and with rigid aircraft assumption can be given in Figure 5-7.

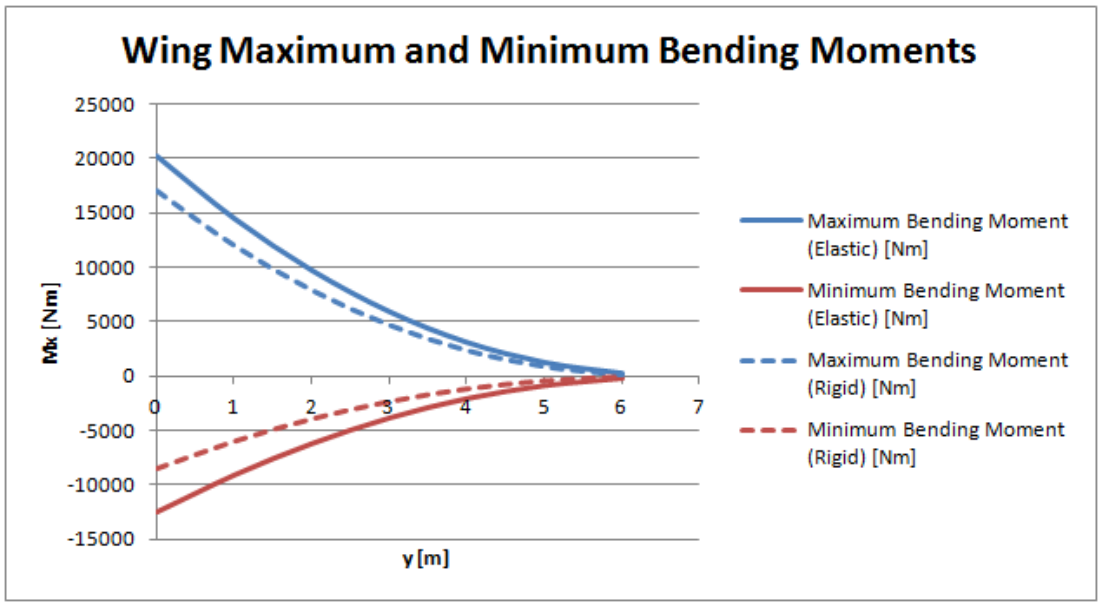

Figure 5-7: Comparison of Wind Bending Moment for Flexible and Rigid Analyses

5.2 Loads and Critical Cases for the Horizontal Tail

The load envelopes for horizontal tail are prepared and given in Figures 5-8, 5-9 and 5-10.

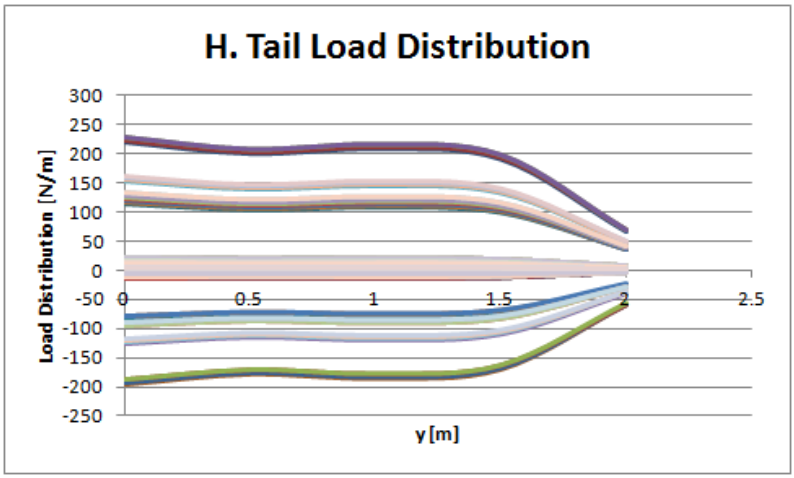

Figure 5-8: Horizontal Tail Load Distribution

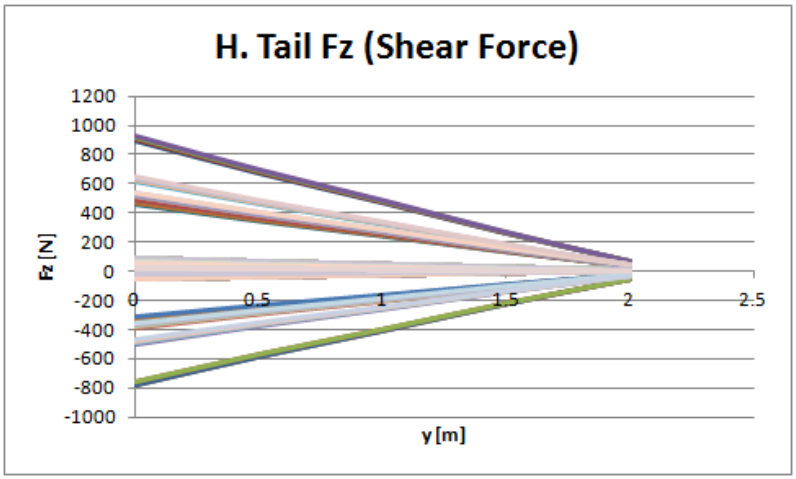

Figure 5-9: Horizontal Tail Shear Force Distribution

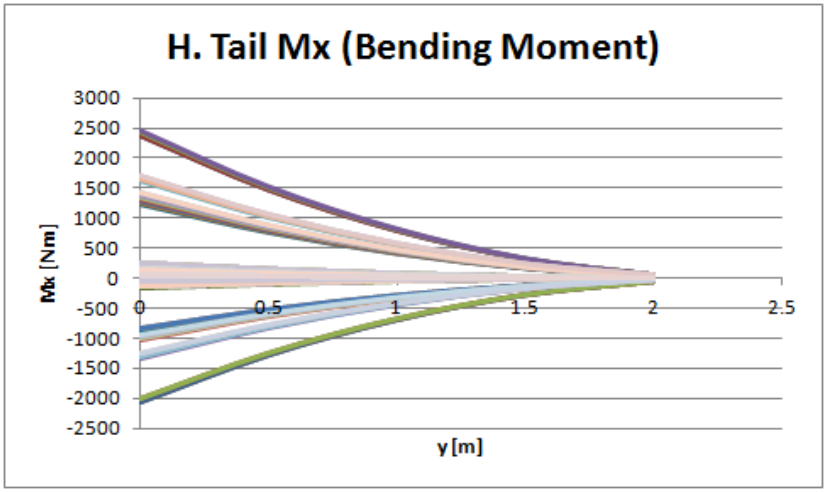

Figure 5-10: Horizontal Tail Bending Moment Distribution

The load envelopes for the horizontal tail are examined and the critical loads for the horizontal tail are selected. These critical load cases are given in Table 5-3.

Table 5-3: Critical Cases for the Horizontal Tail

Load Case	Case Description	Bending Moment at the Root [Nm]
LC088	Pitching with 1/3 Down Elevator at VD	2446.1
LC012	Pitching with 1/3 Up Elevator at VD	-2078.8
LC037	Pitching with 1/3 Up Elevator at VD	-2053.9

It is not surprising that the most critical cases for the horizontal tail are the pitching cases. Also, it should be noted that the mass states associated with these load cases are not only Maximum Take of Weight, but other mass states also become critical.

5.3 Loads and Critical Cases for the Vertical Tail

The load envelopes for vertical tail are prepared as in Figures 5-11, 5-12 and 5-13.

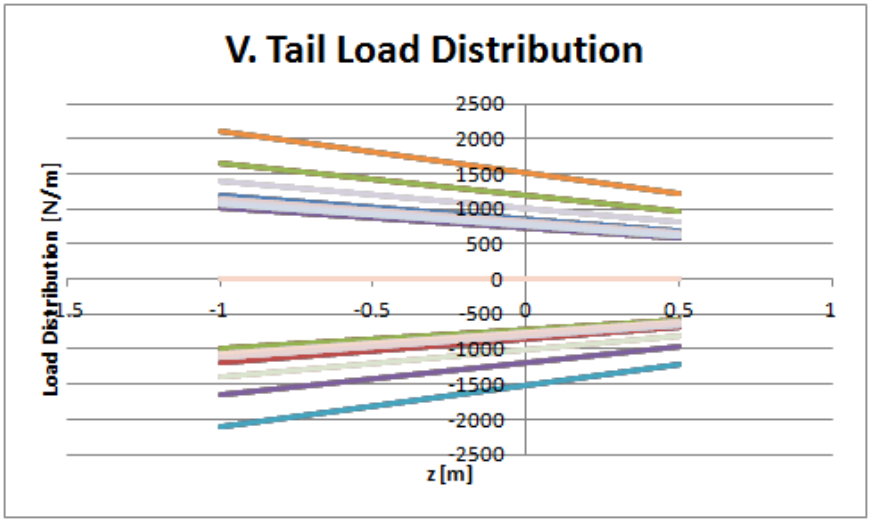

Figure 5-11: Vertical Tail Load Distribution

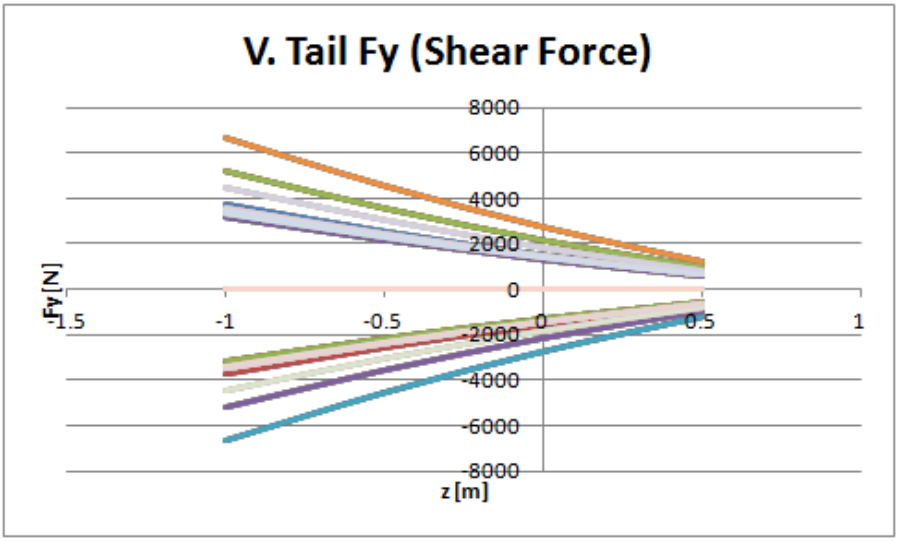

Figure 5-12: Vertical Tail Shear Force Distribution

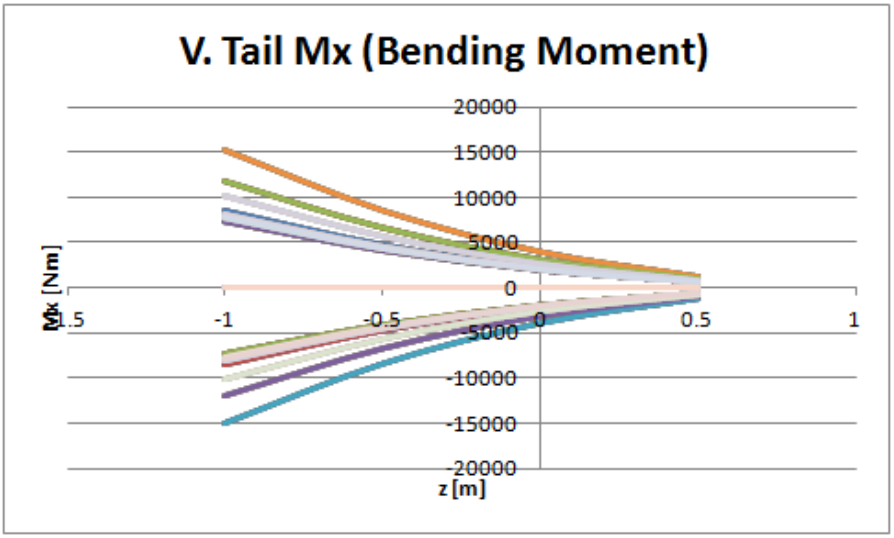

Figure 5-13: Vertical Tail Bending Moment Distribution

The load envelopes for the vertical tail are examined and the critical loads for the horizontal tail are selected. These critical load cases are given in Table 5-4.

Table 5-4: Critical Cases for the Vertical Tail

Load Case	Case Description	Bending Moment at the Root [Nm]
LC095	Right Yaw with 1/3 Rudder at VD	-15165.1
LC096	Left Yaw with 1/3 Rudder at VD	15165.1

Although the critical cases for the vertical tail are selected to be yawing cases, it should be noted that the lateral gust cases also produce high lateral forces on the vertical tail, and they are quite close to yawing cases. A comparison is made in below Table 5-5:

Table 5-5: Comparison of Gust and Yawing Cases

Load Case	Case Description	Fz at Root [N]	Mx at Root [Nm]
LC094	Left Yaw with Max. Rudder at VA	3211.5986	7317.4902
LC097	Right 15 m/s Gust at VA	3748.0874	8539.8574

Therefore, it can be discussed that the gust loads can be more dangerous in certain conditions.

5.4 Loads and Critical Cases for the Fuselage

The load envelopes for fuselage shear force distribution in Figure 5-14.

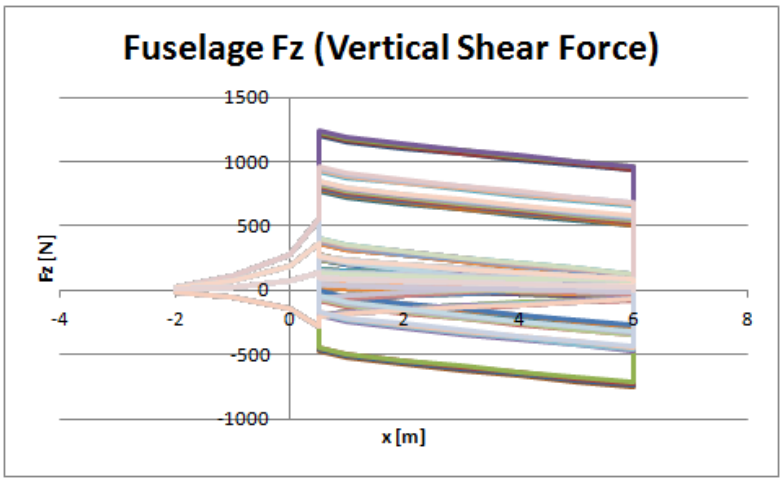

Figure 5-14: Fuselage Vertical Shear Force Distribution

Shear forces acting on the fuselage in y direction are given in Figure 5-15.

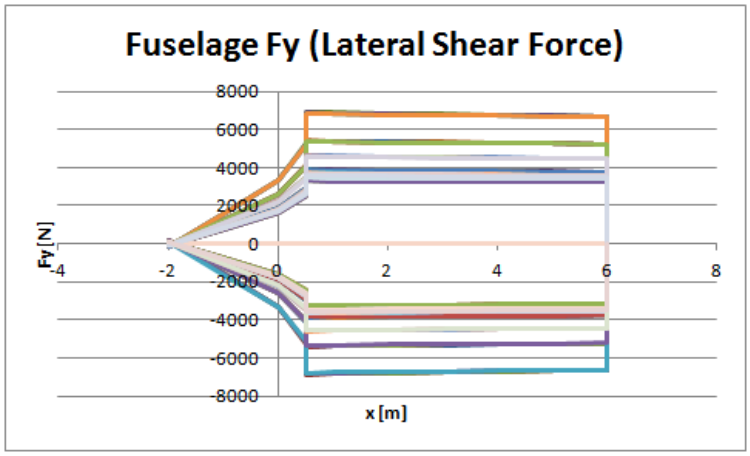

Figure 5-15: Fuselage Lateral Shear Force Distribution

Note that the inertial loads acting on the fuselage structure are much smaller compared to the loads coming from tail attachments. Therefore the critical cases for fuselage are identical to the critical cases for horizontal and vertical tail.

5.5 Deflection of the Wing under Critical Loads

Using the simplified structural model of the aircraft based on beam idealization, it becomes possible to calculate the deflections of lifting surfaces and the fuselage. The wing of the aircraft is investigated using one of the most critical load case evaluated above, which is the pull-up case at maximum take-off weight. The bending of the wing is calculated by using the simplified structural model of the wing as given in Figure 5-16.

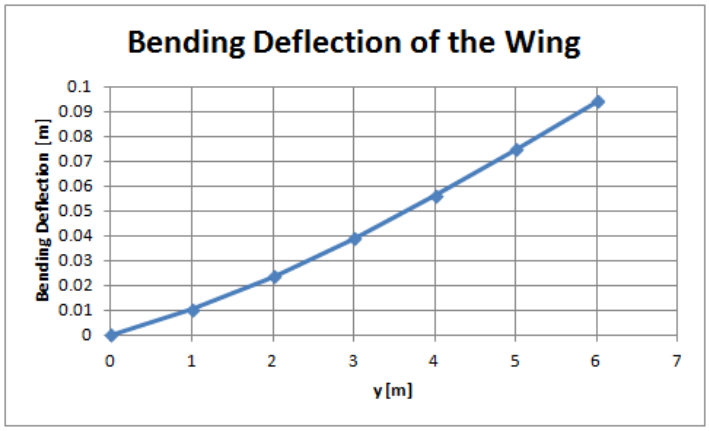

Figure 5-16: Bending Deflection of the Wing Under Critical Load Case

Vertical deflection of the wing is small enough and it does not result in significant loads redistribution. Tip deflection of the wing is around 0.1 meters.

Similarly, the torsional deflection of the wing is calculated for the critical case and given in Figure 5-17.

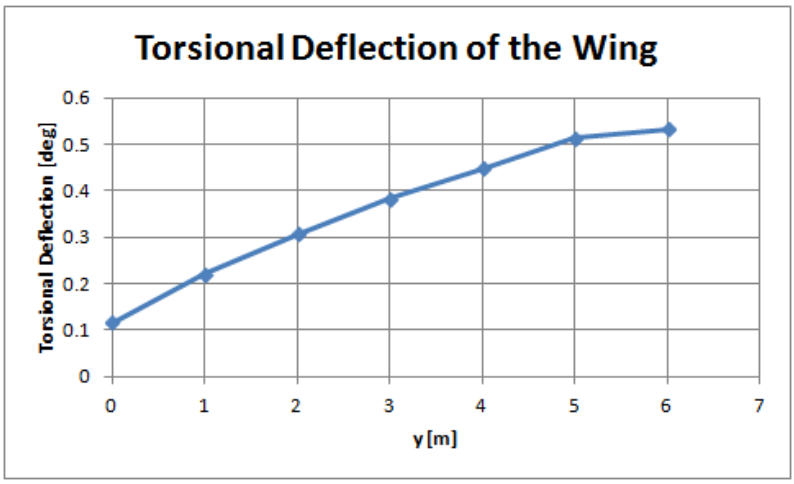

Figure 5-17: Torsional Deflection of the Wing Under Critical Load Case

5.6 Loads Redistribution

One of the static aeroelasticity phenomena, the load redistribution, is possible to be investigated as the loads and deflections on the wing are evaluated. By keeping the total lift constant, which is dictated by the definition of the load case, the load distributions over the rigid wing and elastic wing at load case LC079 are visualized in Figure 5-18.

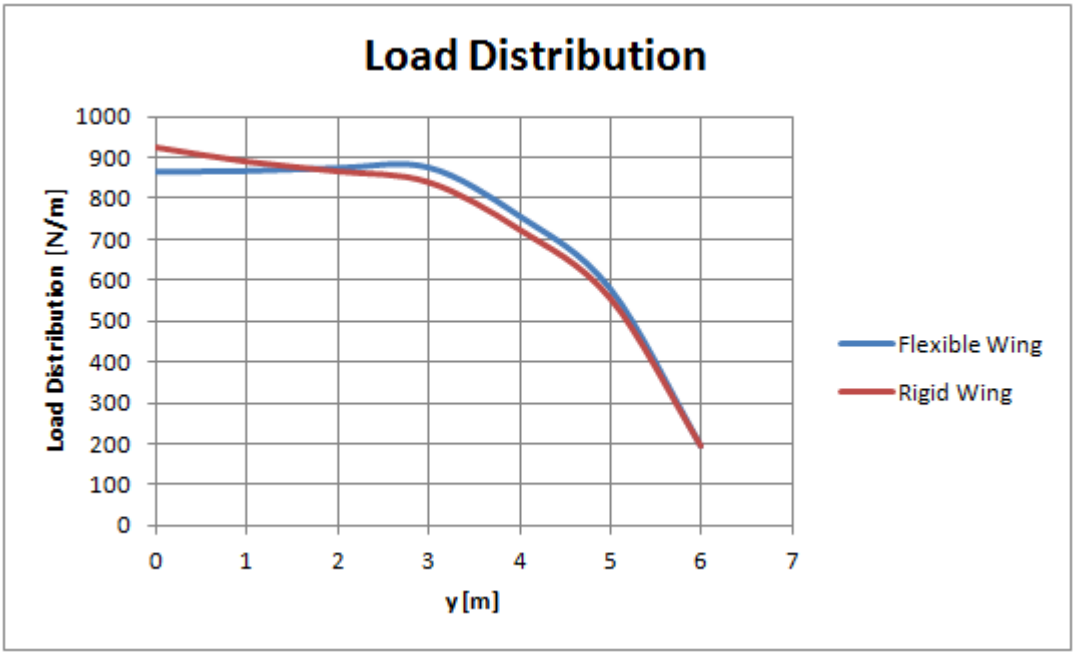

Figure 5-18: Comparison of Load Distributions over Flexible and Rigid Wing

It can be concluded that the torsional deflection at the most critical case can be considered as negligible, and the wing of the aircraft can be said to have significant stiffness, which is a good design feature.

5.7 Divergence Analysis of the Wing

With the calculation of torsional deflection of the wing using simplified structural model of the aircraft, simple static aeroelastic analysis can be performed as stated in Chapter 4. As mentioned previously, the divergence analysis is conducted by using iterative solution of deflection and airload re-distribution. The analytical formula for divergence is used for the comparison.

The torsional deflections of the wing sections are calculated using sectional torsional stiffness properties, which are then considered as changes in local angles of attack. These angle of attack increments are then used for the calculation of new lift and

moment values at corresponding sections. New torsional deflections are calculated similarly, in iterative manner, until convergence obtained. This analysis is done at several airspeeds to evaluate the divergence speed of the aircraft. The results are shown in Figure 5-19.

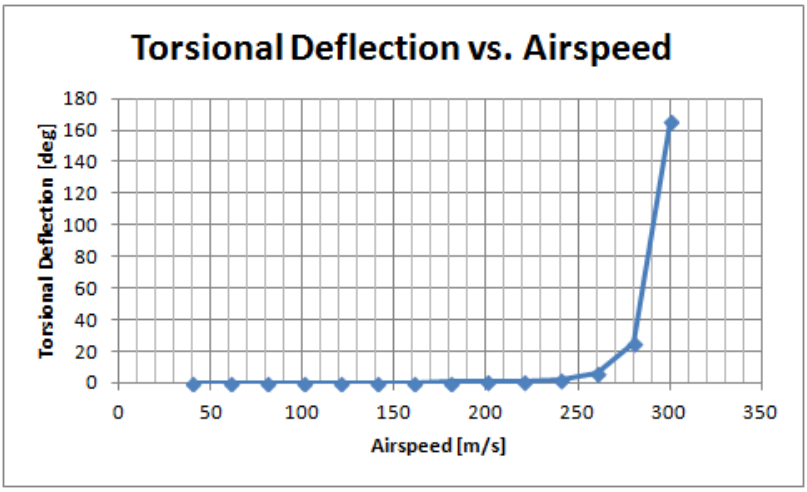

Figure 5-19: Torsional Deflection of the Wing at Various Airspeeds

As seen from Figure 5-14, the torsional deflections of the wing start to diverge at about 300 m/s. It can be compared to the analytical results obtained from the Equation 4.3, which gives an estimated divergence speed of 317 m/s. Figure 5-20 is prepared to show the comparison.

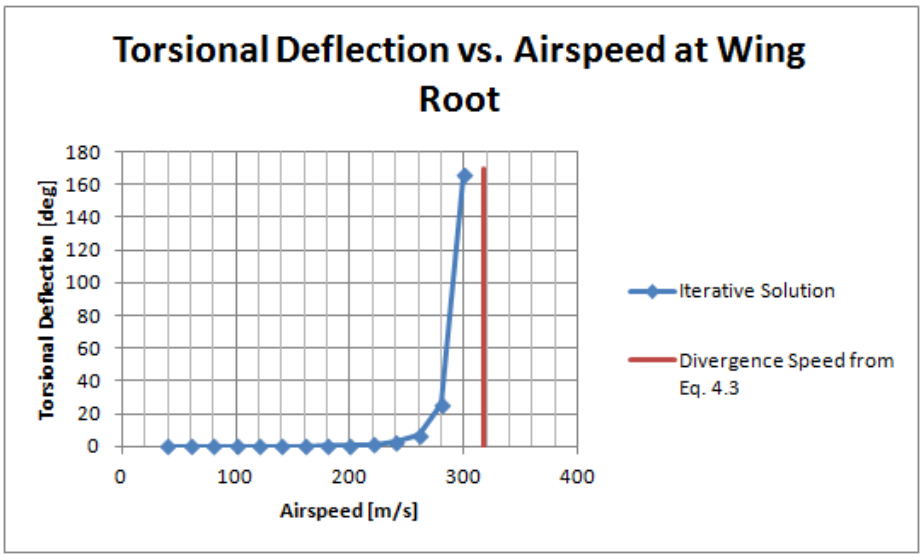

Figure 5-20: Torsional Deflection and Divergence Speed Comparison at Wing Root

The divergence analysis results obtained from the iterative solution of the loads and structural deflections are significantly close to the analytical formula which was given in Equation 4.3.

Also, divergence speed for other wing sections can be calculated and plotted in Figure 5-21.

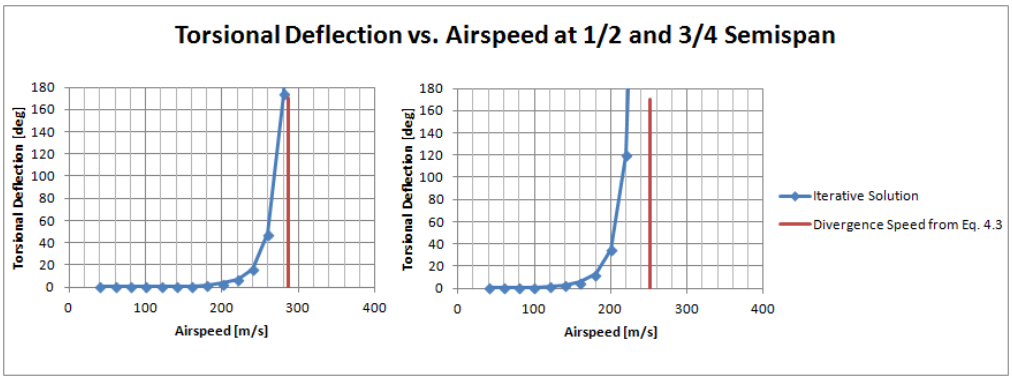

Figure 5-21: Torsional Deflection and Divergence Speed Comparison at Different Sections

Clearly, 317 m/s is an airspeed which in unattainable by an ultralight class aircraft. However, dive speed is more limited by flutter speed, rather than divergence speed, since divergence speed is generally much higher than flutter speed. The flutter speed analysis is a subject of dynamic aeroelasticity and beyond the scope of this thesis.

CHAPTER 6

CONCLUSIONS

In this thesis study, the aircraft load analysis procedure is detailed, the methods for simplification of loads input are discussed. Specifically, In the load analysis procedure, the use of simplified aerodynamic and structural models is emphasized.

After detailing load analysis, a simple ultralight class aircraft is selected to provide a case study for this thesis work. The type certificate of ultralight class aircraft is generally regulated by each country's civilian aviation authorities; for instance the aircraft in this thesis work falls into TR-UL category in Turkey.

In order to obtain the necessary input for the load analysis, the aerodynamic and structural model of the airplane is simplified, which is also a desired operation in early phases of design projects. Aerodynamic model is simplified by using a analytical formulation based on a modified version of the Schrenk Method. The Schrenk Method is an approximation for the calculation of airload distribution on lifting surfaces of aircraft. Unfortunately, the Schrenk method fails to take twist and control surface deflections into account. In this thesis work, the effects of twist and loads arising from deflected control surfaces are formulated to provide an analytical, simplified model for aerodynamic loads distribution. The simplified aerodynamic model is verified by methods of higher fidelity, such as CFD analyses. The structural model, on the other hand, is simplified to aircraft beam model by using structural

idealization methods. The structural idealizations are performed by the calculation of moments of inertia at each cross section along the aircraft components.

Although the design of the aircraft is not the within the scope this work, its requirements, design specifications, geometry, structural layout, system installation and various design parameters are detailed since they all are required for the preparation of models. In the present study the emphasis is given on the preparation of loads input for the aircraft.

After the simplified aerodynamic, inertial and structural models are prepared, the load cases for analyses are generated. The generation of load cases involves the determination of aircraft configurations, mass states, airspeeds, altitudes, flight and ground conditions. A total of 200 load cases are created, which is enough to cover the requirements set by the regulations for the aircraft under ultralight classification.

With the load cases being generated to cover all of flight regime of the aircraft, the calculation of loads are performed for each case in an automated process. The calculation is performed in a straightforward approach by integration of loads along the aircraft components using the analytical formulae derived in the simplification of aerodynamic model.

After the calculation of loads, load envelopes are prepared and most critical load cases are selected. The load envelopes are generated to visualize the load distributions along the primary aircraft components. Those envelopes enabled the selection of critical load cases as well as the evaluation of the critical loads acting on the aircraft structure during flight.

Deflection of wing is investigated under critical loads by using simplified structural model of the aircraft. The pressure redistribution is calculated. Divergence analysis is also performed by iterative solution of structural deflection and airload redistribution. The result from divergence analysis is compared with analytical formula for

divergence speed. It is found that the divergence speeds obtained from analytical formula and iterative solution are close.

6.1 Recommendations of Future Work

Although all flight conditions specified by the corresponding airworthiness and certification regulations are covered in the load analysis, there is still room for more improvement for maneuver analysis. Integration of a flight mechanics model of the aircraft into the analysis makes it possible to perform maneuver simulations with time-history analysis. Especially for the unsteady pitching, rolling and yawing maneuvers, maneuver simulation is quite important.

In addition to flight loads, a dynamic structural model of the aircraft can be constructed with landing gears modeled, in order to perform ground load analysis as well. It enables the precise calculation of ground loads, which are also specified in airworthiness and certification specifications.

With the structural model of the aircraft constructed, static and dynamic aeroelastic analysis can be done. Especially for the dynamic gust cases, it becomes important to corporate aeroelastic analysis into load analysis. As the beam model of the aircraft is available, it is straightforward to calculate the structural modes and natural frequencies. Also, within aeroelastic analyses, it becomes possible to evaluate the flutter speed of the aircraft, which is a critical parameter for flight safety.

REFERENCES

[1] Roskam, J., Airplane War Stories An Account of the Professional Life and Work of Dr. Jan Roskam, Airplane Designer and Teacher, Darcorporation, 2002.

[2] Anderson, J. D., Aircraft Performance and Design, McGrawHill, 1999.

[3] Lomax, T., Structural Loads Analysis for Commercial Aircraft: Theory and Practice, AIAA Education Series, 1996.

[4] Wright, J. and J. Cooper , Introduction to Aircraft Aeroelasticity and Loads, McGraw Hill, 2007.

[5] Hodges, D.H. and Pierce, G.A., Introduction to Structural Dynamics and Aeroelasticity, Cambridge University Press, 2002.

[6] *Europa Aviation Safety Agency, Certification Specifications for Large Aeroplanes, CS-25, Amendment 3, 2007.*

[7] *Federal Aviation Administration, Airworthiness Standards: Transport Category Airplanes, FAR-25.*

[8] Niu, M. C. Y., Airframe Stress Analysis and Sizing, Adaso/Adastra Engineering Center, 2011.

[9] Kier, Thiemo and Looye, Gertjan and Hofstee, Jeroen (2005) Development of Aircraft Flight Loads Analysis Models with Uncertainties for Pre-Design Studies, *International Forum on Aroelasticity and Structural Dynamics* Munich, 2005.

[10] Howe D, Aircraft Loading and Structural layout, AIAA Education Series, 2004.

[11] MIL-A-8861B, Military Specification: Airplane Strength and Rigidity Flight Loads (7 FEB 1986).

[12] Raymer D., Aircraft Design: A Conceptual Approach. American Institute of Aeronautics and Astronautics, 1989.

[13] Schrenk, O., 1940; "A Simple Approximation Method for Obtaining the Spanwise Lift Distribution", Technical Memorandums, National Advisory Committee for Aeronautics, Washington, EUA.

[14] Sivells, James C. An improved approximate method for calculating lift distributions due to twist, National Advisory Committee for Aeronautics, 1951.

[15] Multhopp, H., Methods for Calculating the Lift Distribution of Wings (Subsonic Lifting-Surface Theory). R.& M. 2884. January, 1950.

[16] Blackwell, J.A., A Finite-Step Method for Calculation of Theoretical Load Distributions for Arbitrary Lifting Surface Arrangement at Subsonic Speeds, National Aeronautics and Space Administration, 1969.

[17] Alam, M.; Budd, C.; Hill, A., Study Group report: An Interpolation Tool for Aircraft Surface Pressure Data. Airbus & University of Bath, England, 2006.

[18] Ünay, E., Kahraman, E. Gürak, D., Uçak Rüzgar Tüneli Aerodinamik Verilerinin Sonlu Elemanlar Modeline Dağıtılması, *V. Savunma Teknolojileri Kongresi*, Ankara, Türkiye, 2010.

[19] Jenkins, J., DeAngelis, V., A Summary of Numerous Strain-Gage Load Calibrations on Aircraft Wings and Tails in a Technological Format, NASA Dryden Flight Research Center; Edwards, CA United States, 1997

[20] Taylor, J., The Investigation of Air Loads in Flight from Measurements of Strain in the Structure, National Aeronautical Establishment Library, London, 1950.

[21] JSSG-2006, Department of Defense Joint Service Specification Guide: Aircraft Structures (30 OCT 1998).

[22] Ünay, E., Kiper, T., Işıkdoğan, Ö., Gürak, D. Methods for Evaluation of Aircraft Mass Distribution, 28th International Congress of the Aeronautical Sciences, Brisbane, Australia, 2012.

[23] Reschke, C., Integrated Flight Loads Modelling and Analysis for Flexible Transport Aircraft, Ph.D. thesis, University of Stuttgart, Sturrgart, Germany, July 2006.

[24] Baluch, H.A., van Tooren M., Multidisciplinary Design of Flexible Aircraft, Proceedings of the 15th ISPE International Conference on Concurrent Engineering, 2008.

[25] I. Tuzcu. Dynamics and Control of Flexible Aircraft. PhD Thesis, Virginia Polytechnic Institute and State University, Blacksburg, Virginia, December 2001.

[26] Li N. X. Modeling of Flexible Aircraft for 3D Motion-Based Flight Simulators, M.Sc. Thesis, University of Toronto, 2010.

[27] Waszak, M. R., Modeling and Model Simplification of Aeroelastic Vehicles: An Overview, National Aeronautics and Space Administration, 2013.

[28] Bruhn, E. F., Analysis and Design of Flight Vehicle Structures, Tri-State Offset Company, 1965..

[29] Neubauer M, Gunther G. Aircraft Loads. *Aging Aircraft Fleets: Structural and Other Subsystem Aspects*, Sofia, Bulgaria, Paper No: 9, pp 9-1 - 9-11, 2000.

[30] *Europa Aviation Safety Agency, Certification Specifications for Normal, Utility, Aerobatic, and Commuter Category Aeroplanes, CS-23, Amendment 3, 2012*.

[31] Niu, M. C. Y., Airframe Structural Design: Practical Design Information and Data on Aircraft Structures, Adaso/Adastra Engineering Center, 2006.

[32] Cavagna L., De Gaspari A., Ricci S., Riccobene L., Travaglini L.: Neocass: an Open Source Environment for the Aeroelastic Analysis at Conceptual Design Level, Proceedings of 28th Congress of the International Council of the Aeronautical Sciences (ICAS 2012), Brisbane, Australia, 23-28 Sept. 2012.

[33] Luber W., Fullhas K. Design Loads for Future Fighter Aircraft IMAC-XXI: Conference & Exposition on Structural Dynamics - Innovative Measurement Technologies, Orlando, Kissimmee , FL, Paper No: 8, 2003.

[34] NATO RTO Design Loads for Future Aircraft. Journal Name, Vol. 1, No. 1, pp 1-11, 2001.

[35] Ünay, E., Gürak, D., Özerciyes, V., Uzunoğlu, A., Kestek, H., Çıkrıkcı, D. Tool Development for Aircraft Loads Post-Processing, Proceedings of 28th Congress of the International Council of the Aeronautical Sciences (ICAS 2012), Brisbane, Australia, 23-28 Sept. 2012.

[36] M. Guillaume, A. Gehri, P. Stephani, J. Vos, G. Mandanis, Fluid structure interaction simulation on the F/A-18 vertical tail, in: AIAA 20110-4613, 40th Fluid Dynamics Conference and Exhibit, 2010.

[37] Roskam J., Airplane Flight Dynamics and Automatic Flight Controls, DARcorporation, 2003.

[38] *Federal Aviation Administration, "Title 14: Aeronautics and Space, Part 103 - Ultralight Vehicles", Retrieved 2014-12-20*

[39] *Sivil Havacılık Genel Müdürlüğü, SHT-HHA-S Hafif Hava Araçlarının Sertifikasyonu Talimatı, Retrieved 2014-12-10*

[40] Limbach Flugmotoren Coorp. ”http://www.limflug.de”, Last update 1999

[41] Yechout, T.R., Introduction to Aircraft Flight Mechanics, AIAA education series, American Institute of Aeronautics & Astronautics, 2003.

[42] Maalawi, K. Y., Negm, H. M., El Sheikh, M. M., Aerodynamic/Structural Optimization of a Training Aircraft Wing, 13th International Conference on Aerospace Sciences & Aviation Technology (ASAT- 13), Cairo, Egypt, 2009.

[43] *Civil Aviation Authority, CAP 393, Air Navigation: The Order and the Regulations, Retrieved May 2014*.

APPENDIX A

CODE FOR INTEGRATION OF CFD RESULTS

The code for processing the pressure distribution from CFD results for load analysis is given in this appendix.

```
REAL ELEMENT(10000,7)
REAL NODE(10000,3)
REAL S(100000), NX(100000), NY(100000), NZ(100000)
REAL CP(100000,180)
REAL FX(100000,180), FY(100000,180), FZ(100000,180)
REAL CENTER(100000,3)
REAL FST(100000,3, 180), STF(10000), STW(10000), STV(10000)
REAL MST(100000,3, 180)
CHARACTER*120 DUM
REAL LENGTH, WINGSPAN, XMIN, XMAX
REAL  VERTSPAN
INTEGER NVSTATION, nres, NFSTATION, NWSTATION
!!!!PARAMETERS
nres=1
LENGTH=8
VERTSPAN=1.
XMIN=-2.
XMAX=6
VERTXMIN=4
VERTXMAX=6
VERTZMIN=0
VERTZMAX=1.5
WINGSPAN=12.
WINGXMIN=-0.1
WINGXMAX=2.1
WINGZMIN=-0.0
WINGZMAX=1
NFSTATION=10
NWSTATION=6
NVSTATION=10
```

```
!!!!READING STATIONS
OPEN(1,FILE="STATIONS.DAT")
READ(1,*)NFSTATION
DO I=1,NFSTATION
READ(1,*)STF(I)
ENDDO
STF(NFSTATION+1)=LENGTH
READ(1,*)NWSTATION
DO I=1,NWSTATION
READ(1,*)STW(I)
ENDDO
STW(NWSTATION+1)=WINGSPAN/2
READ(1,*)NVSTATION
DO I=1,NVSTATION
READ(1,*)STV(I)
ENDDO
STV(NVSTATION+1)=-1*VERTSPAN
CLOSE(1)
!!!!READING LOADS
OPEN(1,FILE="INPUT.DAT")
DO I=1,5
READ(1,*)DUM
ENDDO
READ(1,*)NPANELWAKE
READ(1,*)DUM
READ(1,*)NPANEL
READ(1,*)DUM
READ(1,*)NNODE
READ(1,*)DUM
READ(1,*)AIRSPEED
DO I=1,49
READ(1,*)DUM
ENDDO
!!!!!S
DO I=1,NPANEL
READ(1,*)S(I)
ENDDO
DO I=1,NPANELWAKE-NPANEL
READ(1,*)DUM
ENDDO
!!!!!FF
READ(1,*)DUM
DO I=1,NPANELWAKE
READ(1,*)DUM
ENDDO
!!!NORMAL
READ(1,*)DUM
DO I=1,NPANEL
READ(1,*)NX(I), NY(I), NZ(I)
ENDDO
DO I=1,NPANELWAKE-NPANEL
READ(1,*)DUM
```

```
ENDDO
!!!LVECTOR
READ(1,*)DUM
DO I=1,NPANELWAKE
READ(1,*)DUM
ENDDO
!!!PVECTOR
READ(1,*)DUM
DO I=1,NPANELWAKE
READ(1,*)DUM
ENDDO
!!!CENTERPOINTS
READ(1,*)DUM
DO I=1,NPANEL
READ(1,*)(CENTER(I,J),J=1,3)
ENDDO
DO I=1,NPANELWAKE-NPANEL
READ(1,*)DUM
ENDDO
!!!CP
READ(1,*)DUM
DO I=1,NPANEL
READ(1,*)(CP(I,j),j=1,nres)
ENDDO
CLOSE(1)
!!!!
!!!!CALCULATING FORCES
do j=1,nres!!!
FZTOT=0
STOT=0
DO I=1,NPANEL
FX(I,j)=-1*NX(I)*S(I)*CP(I,j)*1/2*1.225*AIRSPEED**2
FY(I,j)=-1*NY(I)*S(I)*CP(I,j)*1/2*1.225*AIRSPEED**2
FZ(I,j)=-1*NZ(I)*S(I)*CP(I,j)*1/2*1.225*AIRSPEED**2
TOTALFZ=TOTALFZ+FZ(I,j)
ENDDO
PRINT*,TOTALFZ
!!!!
!!!
!!!!
!!!!INTEGRATING  FUSELAGE
DO IS=1,NFSTATION
FST(IS,1,j)=0
FST(IS,2,j)=0
FST(IS,3,j)=0
DO IP=1,NPANEL
IF(CENTER(IP,1).GE.XMIN.AND.CENTER(IP,1).LT.XMAX)THEN
IF(CENTER(IP,1).GE.STF(IS).AND.CENTER(IP,1).LT.STF(IS+1))THEN
FST(IS,1,j)=FST(IS,1,j)+FX(IP,j)
FST(IS,2,j)=FST(IS,2,j)+FY(IP,j)
FST(IS,3,j)=FST(IS,3,j)+FZ(IP,j)
ENDIF
```

```
      ENDIF
      ENDDO
      ENDDO
      enddo
      !!!!OUTPUT FUSELAGE
      OPEN(1,FILE="FUS-fy.DAT")
      DO I=1,NFSTATION
      WRITE(1,100)STF(I), (FST(I,2,j), j=1,nres)
      ENDDO
      CLOSE(1)
      OPEN(1,FILE="FUS-fz.DAT")
      DO I=1,NFSTATION
      WRITE(1,100)STF(I), (FST(I,3,j),J=1,NRES)
      ENDDO
      CLOSE(1)
      !!!!
      !!!!
      !!!!
      do j=1,nres
      !!!!INTEGRATING  RIGHT WING
      DO IS=1,NWSTATION
      FST(IS,1,j)=0
      FST(IS,2,j)=0
      FST(IS,3,j)=0
      MST(IS,2,j)=0
      DO IP=1,NPANEL
      IF(CENTER(IP,1).GE.WINGXMIN.AND.CENTER(IP,1).LT.WINGXMAX
     >  .AND.CENTER(IP,3).GE.WINGZMIN.AND.CENTER(IP,3).LT.WINGZMAX)THEN
      IF(CENTER(IP,2).GE.STW(IS).AND.CENTER(IP,2).LT.STW(IS+1))THEN
      FST(IS,1,j)=FST(IS,1,j)+FX(IP,j)
      FST(IS,2,j)=FST(IS,2,j)+FY(IP,j)
      FST(IS,3,j)=FST(IS,3,j)+FZ(IP,j)
      MST(IS,2,j)=MST(IS,2,j)+FZ(IP,j)*CENTER(IP,1)*NZ(IP)
      ENDIF
      ENDIF
      ENDDO
      ENDDO
      enddo
      !!!!OUTPUT RIGHT WING
      OPEN(1,FILE="WING_RIGHT.DAT")
      DO I=1,NWSTATION
      WRITE(1,100)STW(I), (FST(I,3,j),J=1,NRES)
      ENDDO
      CLOSE(1)
      OPEN(1,FILE="WING_RIGHT_MY.DAT")
      DO I=1,NWSTATION
      WRITE(1,100)STW(I), (MST(I,2,j),J=1,NRES)
      ENDDO
      CLOSE(1)
      do j=1,nres
      !!!!INTEGRATING LEFT WING
      DO IS=1,NWSTATION
```

```
      FST(IS,1,j)=0
      FST(IS,2,j)=0
      FST(IS,3,j)=0
      MST(IS,2,j)=0
      DO IP=1,NPANEL
      IF(CENTER(IP,1).GE.WINGXMIN.AND.CENTER(IP,1).LT.WINGXMAX
     >  .AND.CENTER(IP,3).GE.WINGZMIN.AND.CENTER(IP,3).LT.WINGZMAX)THEN
      IF(-CENTER(IP,2).GE.STW(IS).AND.-CENTER(IP,2).LT.STW(IS+1))THEN
      FST(IS,1,j)=FST(IS,1,j)+FX(IP,j)
      FST(IS,2,j)=FST(IS,2,j)+FY(IP,j)
      FST(IS,3,j)=FST(IS,3,j)+FZ(IP,j)
      MST(IS,2,j)=MST(IS,2,j)+FZ(IP,j)*CENTER(IP,1)
      ENDIF
      ENDIF
      ENDDO
      ENDDO
       enddo
      !!!!OUTPUT LEFT WING
      OPEN(1,FILE="WING_LEFT.DAT")
      DO I=1,NWSTATION
      WRITE(1,100)-STW(I), (FST(I,3,j),J=1,NRES)
      ENDDO
      CLOSE(1)
      OPEN(1,FILE="WING_LEFT_MY.DAT")
      DO I=1,NWSTATION
      WRITE(1,100)-STW(I), (MST(I,2,j),J=1,NRES)
      ENDDO
      CLOSE(1)
      do j=1,nres        !
      !!!!
      !!!!  !!!!
      !!!!INTEGRATING  VERTICALTAIL
      DO IS=1,NVSTATION
      FST(IS,1,j)=0
      FST(IS,2,j)=0
      FST(IS,3,j)=0
      DO IP=1,NPANEL
      IF(CENTER(IP,1).GE.VERTXMIN.AND.CENTER(IP,1).LT.VERTXMAX
     >  .AND.CENTER(IP,3).GE.VERTZMIN.AND.CENTER(IP,3).LT.VERTZMAX)THEN
      IF(CENTER(IP,3).lt.STV(IS).AND.CENTER(IP,3).ge.STV(IS+1))THEN
      FST(IS,1,j)=FST(IS,1,j)+FX(IP,j)
      FST(IS,2,j)=FST(IS,2,j)+FY(IP,j)
      FST(IS,3,j)=FST(IS,3,j)+FZ(IP,j)
      ENDIF
      ENDIF
      ENDDO
      ENDDO
      enddo
      !!!!OUTPUT VERTICALTAIL
      OPEN(1,FILE="VERT.DAT")
      DO I=1,NVSTATION
      WRITE(1,100)STV(I),(FST(I,2,j),J=1,NRES)
```

```
      ENDDO
      CLOSE(1)
100   format(121e18.6)
      !!!!
      !!!!
      !!!!
      !!!FINISHING
      PRINT*,"DONE"
      READ*,DUM
      STOP
      END
```

APPENDIX B

COMPLETE LIST OF LOAD CASES

The complete table of load cases is included in this appendix.

Table B-1: Complete List of Load Cases

Load Case	Condition	Cert. Spec.	Mass State	Altitude [m]
LC001	Criuse with 1 g at VC	331	MS01	0
LC002	Maximum NZ at VA	331	MS01	0
LC003	Minimum NZ at VA	331	MS01	0
LC004	Maximum NZ at VD	331	MS01	0
LC005	Minimum NZ at VD	331	MS01	0
LC006	Upward 15 m/s Gust at VB	341, 425	MS01	0
LC007	Downward 15 m/s Gust at VB	341, 425	MS01	0
LC008	Upward 7.5 m/s Gust at VD	341, 425	MS01	0
LC009	Downward 7.5 m/s Gust at VD	341, 425	MS01	0
LC010	Pitching with Max. Up Elevator at VA	423	MS01	0
LC011	Pitching with Max. Down Elevator at VA	423	MS01	0
LC012	Pitching with 1/3 Up Elevator at VD	423	MS01	0
LC013	Pitching with 1/3 Down Elevator at VD	423	MS01	0
LC014	Right Roll with Max. Aileron at 2.66 g at VA	349, 455	MS01	0
LC015	Left Roll with Max. Aileron at 2.66 g at VA	349, 455	MS01	0
LC016	Right Roll with 1/3 Aileron at 2.66 g at VD	349, 455	MS01	0
LC017	Left Roll with 1/3 Aileron at 2.66 g at VD	349, 455	MS01	0
LC018	Right Yaw with Max. Rudder at VA	351, 441	MS01	0

Table B-1 (Continued)

LC019	Left Yaw with Max. Rudder at VA	351, 441	MS01	0
LC020	Right Yaw with 1/3 Rudder at VD	351, 441	MS01	0
LC021	Left Yaw with 1/3 Rudder at VD	351, 441	MS01	0
LC022	Right 15 m/s Gust at VB	443	MS01	0
LC023	Left 15 m/s Gust at VB	443	MS01	0
LC024	Right 7.5 m/s Gust at VD	443	MS01	0
LC025	Left 7.5 m/s Gust at VD	443	MS01	0
LC026	Criuse with 1 g at VC	331	MS07	0
LC027	Maximum NZ at VA	331	MS07	0
LC028	Minimum NZ at VA	331	MS07	0
LC029	Maximum NZ at VD	331	MS07	0
LC030	Minimum NZ at VD	331	MS07	0
LC031	Upward 15 m/s Gust at VB	341, 425	MS07	0
LC032	Downward 15 m/s Gust at VB	341, 425	MS07	0
LC033	Upward 7.5 m/s Gust at VD	341, 425	MS07	0
LC034	Downward 7.5 m/s Gust at VD	341, 425	MS07	0
LC035	Pitching with Max. Up Elevator at VA	423	MS07	0
LC036	Pitching with Max. Down Elevator at VA	423	MS07	0
LC037	Pitching with 1/3 Up Elevator at VD	423	MS07	0
LC038	Pitching with 1/3 Down Elevator at VD	423	MS07	0
LC039	Right Roll with Max. Aileron at 2.66 g at VA	349, 455	MS07	0
LC040	Left Roll with Max. Aileron at 2.66 g at VA	349, 455	MS07	0
LC041	Right Roll with 1/3 Aileron at 2.66 g at VD	349, 455	MS07	0
LC042	Left Roll with 1/3 Aileron at 2.66 g at VD	349, 455	MS07	0
LC043	Right Yaw with Max. Rudder at VA	351, 441	MS07	0
LC044	Left Yaw with Max. Rudder at VA	351, 441	MS07	0
LC045	Right Yaw with 1/3 Rudder at VD	351, 441	MS07	0
LC046	Left Yaw with 1/3 Rudder at VD	351, 441	MS07	0
LC047	Right 15 m/s Gust at VB	443	MS07	0
LC048	Left 15 m/s Gust at VB	443	MS07	0
LC049	Right 7.5 m/s Gust at VD	443	MS07	0
LC050	Left 7.5 m/s Gust at VD	443	MS07	0
LC051	Criuse with 1 g at VC	331	MS11	0
LC052	Maximum NZ at VA	331	MS11	0
LC053	Minimum NZ at VA	331	MS11	0
LC054	Maximum NZ at VD	331	MS11	0
LC055	Minimum NZ at VD	331	MS11	0
LC056	Upward 15 m/s Gust at VB	341, 425	MS11	0

Table B-1 (Continued)(

LC057	Downward 15 m/s Gust at VB	341, 425	MS11	0
LC058	Upward 7.5 m/s Gust at VD	341, 425	MS11	0
LC059	Downward 7.5 m/s Gust at VD	341, 425	MS11	0
LC060	Pitching with Max. Up Elevator at VA	423	MS11	0
LC061	Pitching with Max. Down Elevator at VA	423	MS11	0
LC062	Pitching with 1/3 Up Elevator at VD	423	MS11	0
LC063	Pitching with 1/3 Down Elevator at VD	423	MS11	0
LC064	Right Roll with Max. Aileron at 2.66 g at VA	349, 455	MS11	0
LC065	Left Roll with Max. Aileron at 2.66 g at VA	349, 455	MS11	0
LC066	Right Roll with 1/3 Aileron at 2.66 g at VD	349, 455	MS11	0
LC067	Left Roll with 1/3 Aileron at 2.66 g at VD	349, 455	MS11	0
LC068	Right Yaw with Max. Rudder at VA	351, 441	MS11	0
LC069	Left Yaw with Max. Rudder at VA	351, 441	MS11	0
LC070	Right Yaw with 1/3 Rudder at VD	351, 441	MS11	0
LC071	Left Yaw with 1/3 Rudder at VD	351, 441	MS11	0
LC072	Right 15 m/s Gust at VB	443	MS11	0
LC073	Left 15 m/s Gust at VB	443	MS11	0
LC074	Right 7.5 m/s Gust at VD	443	MS11	0
LC075	Left 7.5 m/s Gust at VD	443	MS11	0
LC076	Cruise with 1 g at VC	331	MS12	0
LC077	Maximum NZ at VA	331	MS12	0
LC078	Minimum NZ at VA	331	MS12	0
LC079	Maximum NZ at VD	331	MS12	0
LC080	Minimum NZ at VD	331	MS12	0
LC081	Upward 15 m/s Gust at VB	341, 425	MS12	0
LC082	Downward 15 m/s Gust at VB	341, 425	MS12	0
LC083	Upward 7.5 m/s Gust at VD	341, 425	MS12	0
LC084	Downward 7.5 m/s Gust at VD	341, 425	MS12	0
LC085	Pitching with Max. Up Elevator at VA	423	MS12	0
LC086	Pitching with Max. Down Elevator at VA	423	MS12	0
LC087	Pitching with 1/3 Up Elevator at VD	423	MS12	0
LC088	Pitching with 1/3 Down Elevator at VD	423	MS12	0
LC089	Right Roll with Max. Aileron at 2.66 g at VA	349, 455	MS12	0
LC090	Left Roll with Max. Aileron at 2.66 g at VA	349, 455	MS12	0
LC091	Right Roll with 1/3 Aileron at 2.66 g at VD	349, 455	MS12	0
LC092	Left Roll with 1/3 Aileron at 2.66 g at VD	349, 455	MS12	0
LC093	Right Yaw with Max. Rudder at VA	351, 441	MS12	0
LC094	Left Yaw with Max. Rudder at VA	351, 441	MS12	0

Table B-1 (Continued)

LC095	Right Yaw with 1/3 Rudder at VD	351, 441	MS12	0
LC096	Left Yaw with 1/3 Rudder at VD	351, 441	MS12	0
LC097	Right 15 m/s Gust at VB	443	MS12	0
LC098	Left 15 m/s Gust at VB	443	MS12	0
LC099	Right 7.5 m/s Gust at VD	443	MS12	0
LC100	Left 7.5 m/s Gust at VD	443	MS12	0
LC101	Criuse with 1 g at VC	331	MS01	4000
LC102	Maximum NZ at VA	331	MS01	4000
LC103	Minimum NZ at VA	331	MS01	4000
LC104	Maximum NZ at VD	331	MS01	4000
LC105	Minimum NZ at VD	331	MS01	4000
LC106	Upward 15 m/s Gust at VB	341, 425	MS01	4000
LC107	Downward 15 m/s Gust at VB	341, 425	MS01	4000
LC108	Upward 7.5 m/s Gust at VD	341, 425	MS01	4000
LC109	Downward 7.5 m/s Gust at VD	341, 425	MS01	4000
LC110	Pitching with Max. Up Elevator at VA	423	MS01	4000
LC111	Pitching with Max. Down Elevator at VA	423	MS01	4000
LC112	Pitching with 1/3 Up Elevator at VD	423	MS01	4000
LC113	Pitching with 1/3 Down Elevator at VD	423	MS01	4000
LC114	Right Roll with Max. Aileron at 2.66 g at VA	349, 455	MS01	4000
LC115	Left Roll with Max. Aileron at 2.66 g at VA	349, 455	MS01	4000
LC116	Right Roll with 1/3 Aileron at 2.66 g at VD	349, 455	MS01	4000
LC117	Left Roll with 1/3 Aileron at 2.66 g at VD	349, 455	MS01	4000
LC118	Right Yaw with Max. Rudder at VA	351, 441	MS01	4000
LC119	Left Yaw with Max. Rudder at VA	351, 441	MS01	4000
LC120	Right Yaw with 1/3 Rudder at VD	351, 441	MS01	4000
LC121	Left Yaw with 1/3 Rudder at VD	351, 441	MS01	4000
LC122	Right 15 m/s Gust at VB	443	MS01	4000
LC123	Left 15 m/s Gust at VB	443	MS01	4000
LC124	Right 7.5 m/s Gust at VD	443	MS01	4000
LC125	Left 7.5 m/s Gust at VD	443	MS01	4000
LC126	Criuse with 1 g at VC	331	MS07	4000
LC127	Maximum NZ at VA	331	MS07	4000
LC128	Minimum NZ at VA	331	MS07	4000
LC129	Maximum NZ at VD	331	MS07	4000
LC130	Minimum NZ at VD	331	MS07	4000
LC131	Upward 15 m/s Gust at VB	341, 425	MS07	4000
LC132	Downward 15 m/s Gust at VB	341, 425	MS07	4000

Table B-1 (Continued)

LC133	Upward 7.5 m/s Gust at VD	341, 425	MS07	4000
LC134	Downward 7.5 m/s Gust at VD	341, 425	MS07	4000
LC135	Pitching with Max. Up Elevator at VA	423	MS07	4000
LC136	Pitching with Max. Down Elevator at VA	423	MS07	4000
LC137	Pitching with 1/3 Up Elevator at VD	423	MS07	4000
LC138	Pitching with 1/3 Down Elevator at VD	423	MS07	4000
LC139	Right Roll with Max. Aileron at 2.66 g at VA	349, 455	MS07	4000
LC140	Left Roll with Max. Aileron at 2.66 g at VA	349, 455	MS07	4000
LC141	Right Roll with 1/3 Aileron at 2.66 g at VD	349, 455	MS07	4000
LC142	Left Roll with 1/3 Aileron at 2.66 g at VD	349, 455	MS07	4000
LC143	Right Yaw with Max. Rudder at VA	351, 441	MS07	4000
LC144	Left Yaw with Max. Rudder at VA	351, 441	MS07	4000
LC145	Right Yaw with 1/3 Rudder at VD	351, 441	MS07	4000
LC146	Left Yaw with 1/3 Rudder at VD	351, 441	MS07	4000
LC147	Right 15 m/s Gust at VB	443	MS07	4000
LC148	Left 15 m/s Gust at VB	443	MS07	4000
LC149	Right 7.5 m/s Gust at VD	443	MS07	4000
LC150	Left 7.5 m/s Gust at VD	443	MS07	4000
LC151	Criuse with 1 g at VC	331	MS11	4000
LC152	Maximum NZ at VA	331	MS11	4000
LC153	Minimum NZ at VA	331	MS11	4000
LC154	Maximum NZ at VD	331	MS11	4000
LC155	Minimum NZ at VD	331	MS11	4000
LC156	Upward 15 m/s Gust at VB	341, 425	MS11	4000
LC157	Downward 15 m/s Gust at VB	341, 425	MS11	4000
LC158	Upward 7.5 m/s Gust at VD	341, 425	MS11	4000
LC159	Downward 7.5 m/s Gust at VD	341, 425	MS11	4000
LC160	Pitching with Max. Up Elevator at VA	423	MS11	4000
LC161	Pitching with Max. Down Elevator at VA	423	MS11	4000
LC162	Pitching with 1/3 Up Elevator at VD	423	MS11	4000
LC163	Pitching with 1/3 Down Elevator at VD	423	MS11	4000
LC164	Right Roll with Max. Aileron at 2.66 g at VA	349, 455	MS11	4000
LC165	Left Roll with Max. Aileron at 2.66 g at VA	349, 455	MS11	4000
LC166	Right Roll with 1/3 Aileron at 2.66 g at VD	349, 455	MS11	4000
LC167	Left Roll with 1/3 Aileron at 2.66 g at VD	349, 455	MS11	4000
LC168	Right Yaw with Max. Rudder at VA	351, 441	MS11	4000
LC169	Left Yaw with Max. Rudder at VA	351, 441	MS11	4000
LC170	Right Yaw with 1/3 Rudder at VD	351, 441	MS11	4000

Table B-1 (Continued)

LC171	Left Yaw with 1/3 Rudder at VD	351, 441	MS11	4000
LC172	Right 15 m/s Gust at VB	443	MS11	4000
LC173	Left 15 m/s Gust at VB	443	MS11	4000
LC174	Right 7.5 m/s Gust at VD	443	MS11	4000
LC175	Left 7.5 m/s Gust at VD	443	MS11	4000
LC176	Criuse with 1 g at VC	331	MS12	4000
LC177	Maximum NZ at VA	331	MS12	4000
LC178	Minimum NZ at VA	331	MS12	4000
LC179	Maximum NZ at VD	331	MS12	4000
LC180	Minimum NZ at VD	331	MS12	4000
LC181	Upward 15 m/s Gust at VB	341, 425	MS12	4000
LC182	Downward 15 m/s Gust at VB	341, 425	MS12	4000
LC183	Upward 7.5 m/s Gust at VD	341, 425	MS12	4000
LC184	Downward 7.5 m/s Gust at VD	341, 425	MS12	4000
LC185	Pitching with Max. Up Elevator at VA	423	MS12	4000
LC186	Pitching with Max. Down Elevator at VA	423	MS12	4000
LC187	Pitching with 1/3 Up Elevator at VD	423	MS12	4000
LC188	Pitching with 1/3 Down Elevator at VD	423	MS12	4000
LC189	Right Roll with Max. Aileron at 2.66 g at VA	349, 455	MS12	4000
LC190	Left Roll with Max. Aileron at 2.66 g at VA	349, 455	MS12	4000
LC191	Right Roll with 1/3 Aileron at 2.66 g at VD	349, 455	MS12	4000
LC192	Left Roll with 1/3 Aileron at 2.66 g at VD	349, 455	MS12	4000
LC193	Right Yaw with Max. Rudder at VA	351, 441	MS12	4000
LC194	Left Yaw with Max. Rudder at VA	351, 441	MS12	4000
LC195	Right Yaw with 1/3 Rudder at VD	351, 441	MS12	4000
LC196	Left Yaw with 1/3 Rudder at VD	351, 441	MS12	4000
LC197	Right 15 m/s Gust at VB	443	MS12	4000
LC198	Left 15 m/s Gust at VB	443	MS12	4000
LC199	Right 7.5 m/s Gust at VD	443	MS12	4000
LC200	Left 7.5 m/s Gust at VD	443	MS12	4000

APPENDIX C

WING LOADS CALCULATION FLOWCHART

This appendix gives a simple flowchart for wing loads calculation.

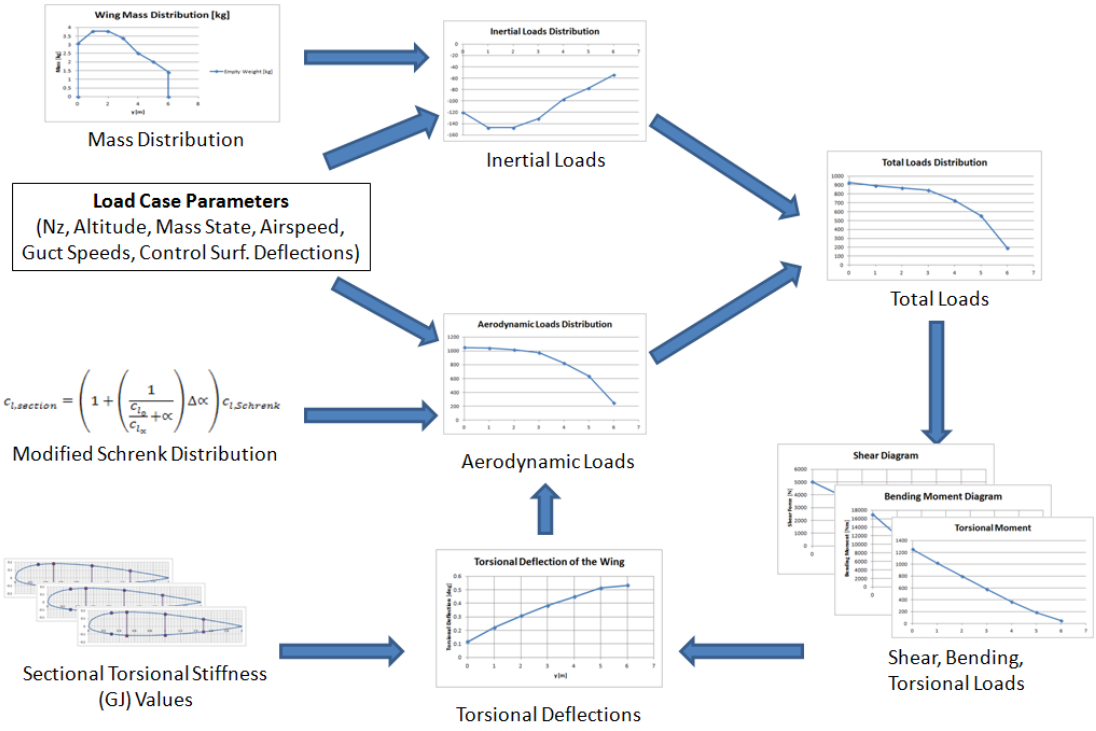

Figure 22: Flowchart of Wing Loads Calculation